Water Vapor Interference in the UV Absorption Measurement of Atmospheric Ozone

by

Kevin Locke Wilson

B.S. University of North Carolina at Asheville, 1997

A thesis submitted to the

Faculty of the Graduate School of the

University of Colorado in partial fulfillment

Of the requirement fro the degree of

Doctor of Philosophy

Department of Chemistry and Biochemistry

2005

This thesis entitled:
Water Vapor Interference in the UV Absorption
Measurement of Atmospheric Ozone
written by Kevin Locke Wilson
has been approved for the
Department of Chemistry and Biochemistry

_____
John W. Birks

_____
Kathy L. Rowlen

Date_____

The final copy of this thesis has been examined by the signatories, and we find that both the content and the form meet acceptable presentation standards of scholarly work in the above mentioned discipline.

Wilson, Kevin Locke (Ph.D., Chemistry)

Water Vapor Interference in the UV Absorption Measurement of Atmospheric Ozone

Thesis directed by Professor John W. Birks

Abstract

In this thesis work, a significant and sometimes large water vapor interference inherent to many and possibly all UV-based, commercially available ozone monitors was positively identified for the first time. Depending upon the instrument's recent atmospheric history and calibration method, ozone monitors can give erroneous results both immediately and hours later, and as a consequence possibly affect the apparent compliance of municipalities with EPA ozone regulations. Deviations from true ozone concentrations result from modulations in the water vapor concentration within the cell between I and I_o measurements as a result of the ozone scrubber (usually hopcalite or a similar material) acting as a water vapor reservoir, alternately drying or humidifying the air stream flowing through the absorbance cell. The mechanism of this indirect interference, as water itself does not directly absorb 254 nm light, is elucidated: the interference is caused by changes in the transmission efficiency of light through the UV absorption cell as a result of adsorption of water molecules to the cell surface.

The magnitude and sign of the water vapor interference varies for ozone monitors produced by different manufacturers, which is explainable in terms of differing cell wall compositions. Depending upon the composition of the absorbance cell surface, the reflectivity of the cell wall itself, and the relative humidity inside the absorbance cell, a variety of light interactions occur as a result of multiple

interactions of non-collimated UV-light with the cell surface. This complex set of interactions includes reflection, refraction, and total internal reflection (TIR). Simple modeling of the light paths in the absorption cells of the TEI and 2B Technologies ozone monitors qualitatively explains the opposite sign of the water vapor interference in instruments produced by these two manufacturers.

Consistent with the proposed mechanism, a number of factors were found to reduce or eliminate the water vapor interference. These include heating the absorption cell, changing the composition of the absorption cell, and reducing the reservoir effect by decreasing the surface area of the ozone destruction catalyst. For the 2B Tech Ozone Monitor, a switch from a borosilicate glass to a quartz cell provided the greatest single improvement to the water interference with a 60% decrease, while heating the cell resulted in a 50% reduction to the interference. Decreasing the surface area of scrubber material to the minimum needed for complete ozone destruction resulted in a 33% reduction, while a different approach of utilizing various TiO_2 hollow-tube photoreactors for ozone destruction proved 100% successful at first but ineffective over time due to a loss in catalytic activity.

The use of a Nafion® tube to equilibrate the humidities of scrubbed and unscrubbed air prior to the absorbance cell proved successful in reducing the humidity interference to an insignificant level (±2 ppbv for rapid cycling between 0% and 90% relative humidity). To date, Nafion® tubes, for elimination of the water vapor interference, have been installed in more than fifty 2B Tech Ozone Monitors with no reported adverse effects over time such as loss of ability to equilibrate water vapor, decreased sensitivity to ozone or large shifts in the instrument zero.

Furthermore, the National Oceanic and Atmospheric Administration Climate Monitoring and Diagnostics Laboratory (NOAA/CMDL) currently utilizes these Nafion® modified 2B Technology Ozone Monitors on a fleet of light aircraft which obtain vertical profiles of ozone on a weekly basis at numerous sites in the U.S. The complete elimination of the water vapor interference presented in this thesis is critical, not only in making valid ozone measurements on balloons and aircraft where rapid changes in humidity are encountered on time scales of seconds or less, but also in ambient monitoring sites across the globe where large humidity variations often occur as a result of weather fronts and/or calibration methods which can potentially affect the results of ozone monitoring for compliance with environmental standards such as the U.S. Clean Air Act.

Acknowledgments

I would like to thank the many people (family, friends, and instructors) who helped me reach this point of accomplishment. To my parents who encouraged me to ask questions and be curious about the world around me, I thank you. You provided not only wonderful examples of hard work and the value of an education, but also influential memories of seeing each of you late at night laboring over your college studies after you thought I had fallen asleep. You were not only my first teachers, but also the first to challenge me not to take the easy path.

To the numerous teachers who influenced me over the years, I thank you: Jim Goode who challenged me to open my mind to other ways of thinking about and viewing my place in the world; Ann Simpson for transferring her extremely high standards and expectations to me and for providing the conditions to discover that I *actually* enjoy expository writing; S. Dexter Squibb for his friendship, scholarship, and mischievous twinkle in his eye - he is the reason I and so many others are chemists today; Debra VanEngelen for imparting her fondness of Analytical Chemistry and for helping make my first research experience a positive one; John Stevens for transferring a portion of his incredible energy to me through our research interactions and for his pushing me to apply to graduate school; John Birks for his sheer love of thinking about science. I feel lucky to have had him as an advisor. He not only provided an extremely positive example of a research scientist to myself and others, but also proved himself to be a friend, and excellent example of what it means to be a respectable person in the world.

To my lab-mates (Brian Lerner, Kristen Schulz, Christine Karbiwnyk, and Jim Boulter), thanks for the fun, support, and fond memories throughout the years. My experience in the lab was greatly enhanced through our interactions and I look forward to having all of you as colleagues in the years ahead. I also wish to sincerely thank Brandy Gamblin, without whom I may have never gotten through undergrad and certainly would have never undertaken graduate school. Her friendship over the years has proven invaluable to me and I thank her for all her support.

Lastly, but not least, I want to thank my wife, Jacqueline Donnelly, without whose love and support this thesis would not be possible. Her unwavering

confidence in me through the ups and downs of completing my thesis strengthened my ability to get through it all and succeed in the end. I cannot thank her enough for her patience and understanding, for her bearing our geographical separation through this process, nor for all those times that she encouraged and confirmed her love and caring for me. Thank you again for allowing me the time and space to complete this thesis and for all the little things you did along the way to assist and show your support. I love you very much and am honored to have you as my partner!

Thank you all,
K.L.W.

Table of Contents

Table of Contents (cont.)

Tables

Figures

Figures (cont.)

Figures (cont.)

Figures (cont.)

Figures (cont.)

Figures (cont.)

Chapter 1
Introduction

1.1 The Ozone Molecule

First discovered by Christian Schobein in the late 1830s, ozone (O_3) is the tri-atomic form of molecular oxygen. It is a colorless, toxic, unstable gas, with a distinctive sharp odor, which condenses to a dark blue liquid at -112 °C. Ozone is normally manufactured by passing an electrical discharge through O_2 gas or air. As a result of its extreme reactivity, ozone is capable of oxidizing organic compounds and is used industrially as a bleaching agent (Roncero et al., 2003). Ozone is also employed in the sterilization of air, drinking water, and surfaces due to its antibacterial properties (Schalekamp, 1979; Ohmi et al., 1992). Ozone exists in both the Earth's upper atmosphere and at ground level and is often considered either "good" or "bad", depending on its relative proximity to plant and animal life.

1.2 "Good" Ozone

"Good ozone", which protects the biosphere from ultraviolet radiation in the wavelength region between ≈ 230-320 nm, occurs naturally in the stratosphere (15 to 50 km above the Earth's surface) and its concentration is regulated through natural photochemical reactions involving O_2. When diatomic oxygen in the stratosphere absorbs ultraviolet radiation with wavelengths less than 242 nm, it breaks apart into two oxygen atoms (Equation 1). These oxygen atoms combine with O_2 molecules, in the presence of a third molecule (M), to form ozone (Equation 2), thus resulting in the net formation of two ozone molecules from three oxygen molecules (Equation 3).

$$O_2 \xrightarrow{h\upsilon} 2O \quad (1)$$

$$2\left[O + O_2 \xrightarrow{M} O_3\right] \quad (2)$$

$$3O_2 \longrightarrow 2O_3 \quad (3)$$

An ozone molecule can also absorb ultraviolet radiation with wavelengths as long as ≈ 320 nm causing the molecule to decompose into O_2 molecules and oxygen atoms (Equation 4). This oxygen atom may again repeat the reaction shown in Equation 2, or it may react with an ozone molecule to form two oxygen molecules as shown in Equation 5. Thus, the net destruction of ozone (Equation 6) is essentially the opposite of the net production shown in Equation 3 (Chapman, 1930).

$$O_3 \xrightarrow{h\upsilon} O_2 + O \quad (4)$$

$$O + O_3 \longrightarrow O_2 + O_2 \quad (5)$$

$$2O_3 \longrightarrow 3O_2 \quad (6)$$

As a result of the relative photodissociation rates of ozone (Equation 4) and oxygen (Equation 1), the relative availability of the required light energies at different altitudes, and the transport of ozone into the troposphere at lower altitudes, ozone concentration reaches a localized maximum of up to 10 to 20 ppmv in an area 20 to 30 km above sea level at mid latitudes (Turco, 1997a). This region of higher ozone concentrations, commonly referred to as the ozone layer (Figure 1.1), is where ozone aids oxygen molecules in shielding the Earth's surface from most of the sun's

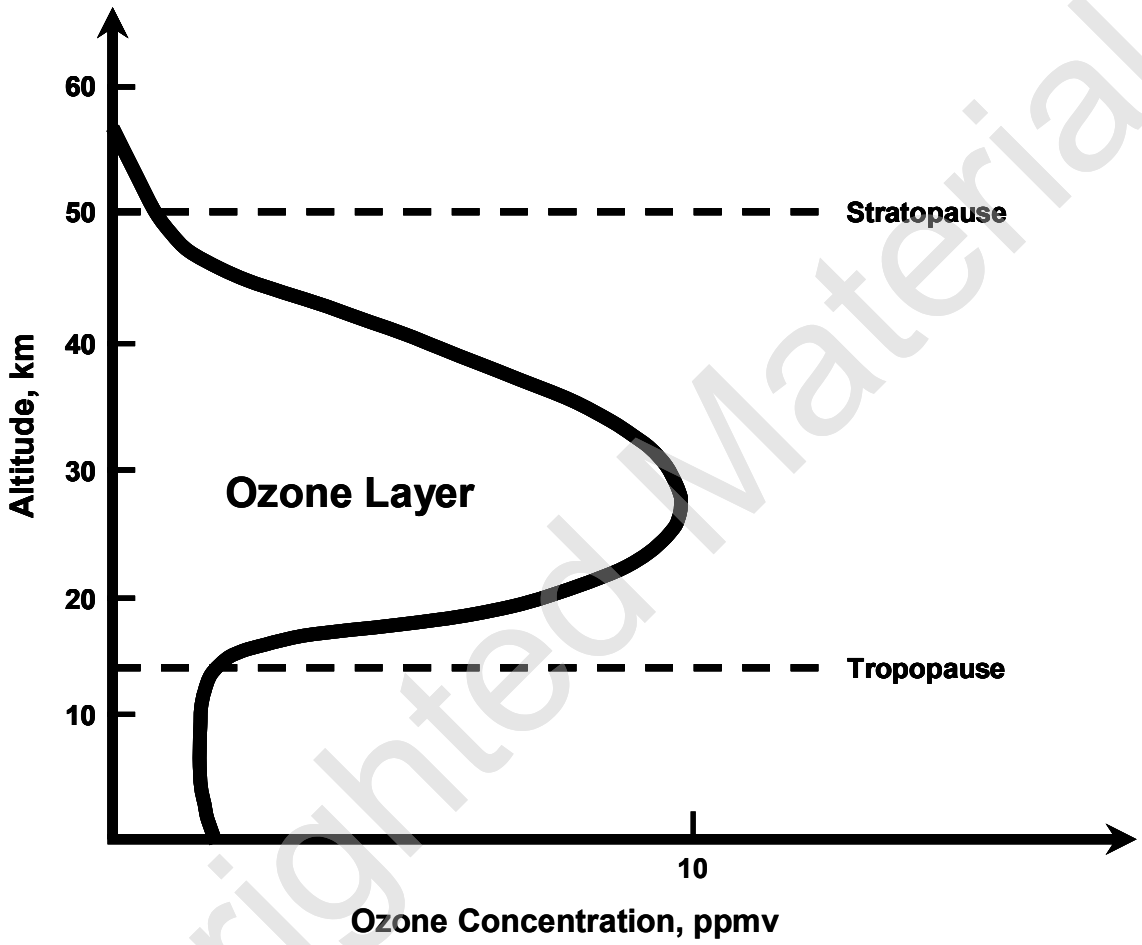

Fig. 1.1. The vertical distribution of ozone in the Earth's atmosphere. Adapted from Turco (1997a).

harmful ultraviolet (UV) radiation. As described above, diatomic oxygen absorbs only the highest energy ultraviolet radiation from the sun (wavelengths $\leq$ 242 nm), whereas ozone absorbs throughout the region of $\approx$ 200-320 nm, covering the UV-B radiation range from 280 to 320 nm which is most damaging to our DNA (Middlebrook and Tolbert, 1996). Ozone is the only atmospheric species having the ability to efficiently absorb UV-B radiation. Thus, stratospheric ozone prevents highly energetic radiation from reaching the Earth's surface, providing protection to all terrestrial life.

1.3 "Bad" Ozone

Conversely, "bad ozone", also known as tropospheric or ground-level ozone, is detrimental to both plant and animal life due to its oxidation of biological tissue. Ground-level ozone is responsible for 500 million dollars in reduced crop production in the United States each year (U.S. EPA, 2003) through its interference with a plant's capacity to produce and store food, thereby increasing its vulnerability to disease, insects, other pollutants, and harsh weather (New York Public Library, 1995; U.S. EPA, 1999a). In humans, elevated ozone levels impair lung function and cause irritation to the respiratory tract by damaging the bronchioles and alveoli, leading to permanent damage with repeated exposure (U.S. EPA, 2003). Even at lower concentrations, breathing ozone for sustained periods can initiate a variety of health issues including chest pain, coughing, nausea, throat irritation, and congestion, while exacerbating existing cases of bronchitis, heart disease, emphysema, and asthma (U.S. EPA, 1999b). Furthermore, ozone exposure in adults may hasten the normal

aging process of lung tissue, while recurring short-term ozone exposure in children may lead to diminished lung function later in adulthood (U.S. EPA, 1999a; U.S. EPA, 2003).

1.4 Tropospheric Ozone Formation

Tropospheric ozone is formed from the photochemical reaction of NO and hydrocarbons, and for this reason is referred to as a secondary pollutant since there are no significant direct, man-made (anthropogenic) emissions of ozone into the troposphere. Although there are cases, such as the remote ridge tops of the Smokey Mountain National Park (Neufeld, 1992; National Park Service, 2004), where oxides of nitrogen in the form of peroxyacetylnitrate (PAN) and other pollutants, are transported many miles downwind to rural areas where natural (biogenic) hydrocarbon emissions exist, ozone is most commonly formed in the polluted air of urban areas (Birks, 1998). The highest concentrations of the primary pollutants, NO and anthropogenic hydrocarbons, occur in densely populated urban areas as emissions from the combustion reactions present in industrial processes and vehicular traffic. Nitric oxide, formed only in the elevated temperatures found in these combustion reactions (Equation 7),

$$N_2 + O_2 \xrightarrow{\Delta} 2NO \qquad (7)$$

catalytically reacts in the presence of sunlight with non-combusted hydrocarbons, such as alkanes (RCH_3) to yield ozone through the following set of reactions (Birks, 1998):

$$RCH_3 + OH \longrightarrow H_2O + RCH_2 \quad (8)$$

$$RCH_2 + O_2 \xrightarrow{M} RCH_2O_2 \quad (9)$$

$$RCH_2O_2 + NO \longrightarrow NO_2 + RCH_2O \quad (10)$$

$$RCH_2O + O_2 \longrightarrow RCHO + HO_2 \quad (11)$$

$$HO_2 + NO \longrightarrow OH + NO_2 \quad (12)$$

$$2\left[NO_2 \xrightarrow{h\upsilon} NO + O \right] \quad (13)$$

$$2\left[O + O_2 \xrightarrow{M} O_3 \right] \quad (14)$$

$$RCH_3 + 4O_2 \longrightarrow RCHO + H_2O + 2O_3 \quad (15)$$

As a result of its dependence upon both emission of primary pollutants and time for subsequent photochemistry to occur, ozone concentrations usually peak in the afternoons of the sunnier, summer months (Figure 1.2). Normal background levels of ozone are usually less than 30 ppbv, but ozone concentrations can rise to levels over 300-500 ppbv as a direct result of photochemical smog in areas with no emissions control (Finlayson-Pitts and Pitts, 2000a).

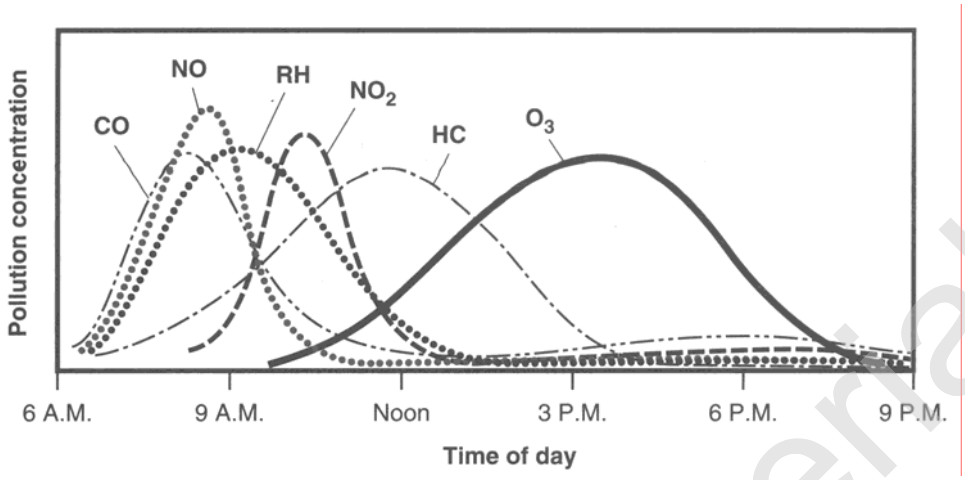

Fig. 1.2. Time dependent nature of chemical components of photochemical smog: Carbon monoxide (CO), nitric oxide (NO), reactive hydrocarbons (RH), nitrogen dioxide (NO_2), hydrocarbon by-products (HC), and ozone (O_3). Adapted from Turco (1997b).

1.5 Ozone Regulation, Monitoring History and Practices

The Clean Air Act of 1970 began the process of national, legislative control of air pollutants in the U.S. From this beginning, ozone has proven the most troublesome pollutant to bring into compliance with air quality standards, as its formation is tied at the localized, regional level, to the complex interaction of the primary pollutants that lead to its formation. The Clean Air Act Amendments of 1990 (U.S. EPA, 2004; U.S. EPA, 2005) require the U.S. Environmental Protection Agency (EPA), states, and cities to implement programs to further reduce emissions of ozone precursors from sources such as cars, fuels, industrial facilities, power plants, and consumer/commercial products. As a result of the Clean Air Act, hundreds of SLAMS (State and Local Monitoring Stations) are required to monitor the levels of primary pollutants such as hydrocarbons and NO as well as the secondary pollutant, ozone, in their geographic region (U.S. EPA, 1998). The EPA

characterizes ozone levels in "noncompliance" when levels exceed the National Ambient Air Quality Standard of 120 ppbv over an hour or exceed an 80 ppbv average over 8 hours (U.S. EPA, 2004; U.S. EPA, 2005). As shown in *Figures 1.3 and 1.4*, millions of Americans live in areas where the national ozone health standards are either routinely exceeded or soon will be exceeded. The health implications illustrated by these charts reveal the necessity of measuring ozone concentrations both now and in the future.

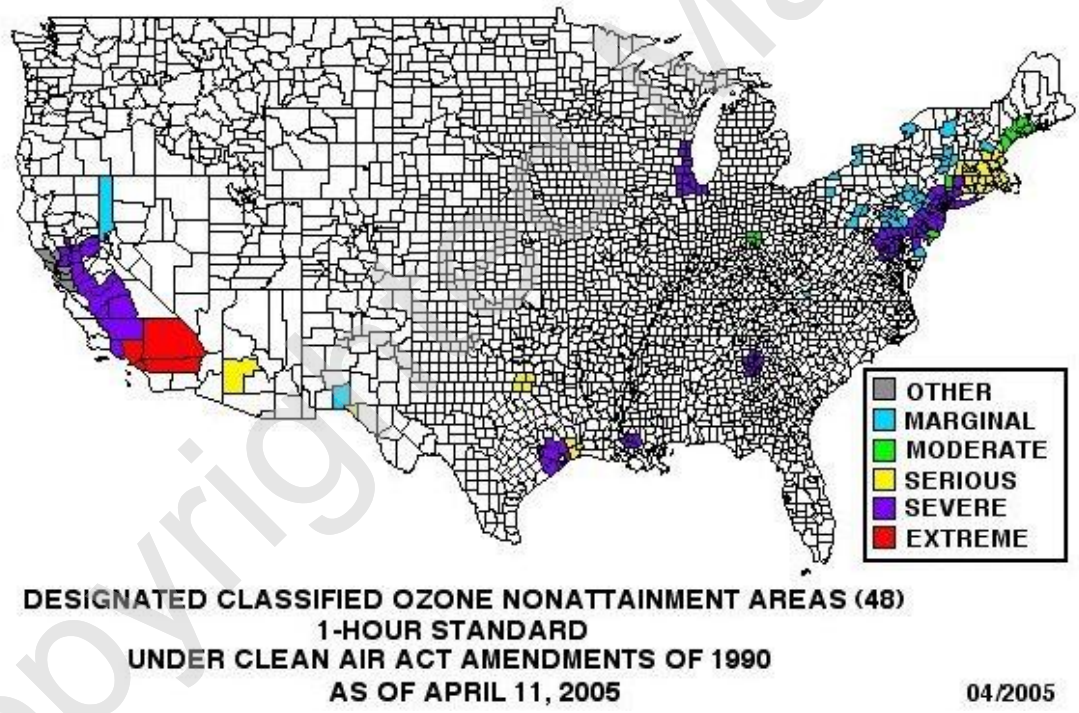

Fig. 1.3. Current non-attainment of 1-hour ozone standards. Ozone classifications are defined by the ozone concentration and prescribed attainment dates allowed under the Clean Air Act: *Extreme* - above 280 ppbv / June, 2024, *Severe 17* – between 190 & up to 280 ppbv / June, 2021, *Severe 15* – between 180 & up to 190 ppbv / June, 2019, *Serious* – between 160 & up to 180 ppbv / June, 2013, *Moderate* - between 138 & up to 160 ppbv / June, 2010, *Marginal* - between 121 & up to 138 ppbv / June, 2007, *Other* – San Francisco. Adapted from A.S.L. & Associates (2005a).

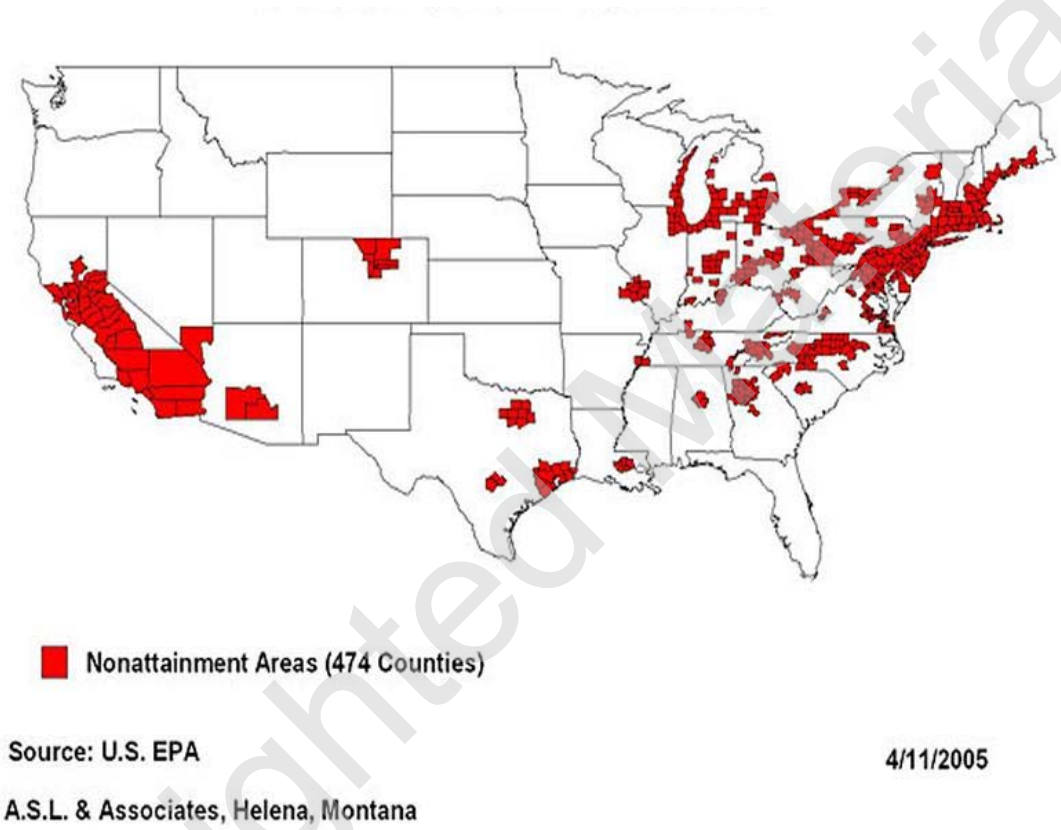

Fig. 1.4. Non-attainment areas by county as of 11th April 2005 of EPA 8-hour ozone standard. Adapted from A.S.L. & Associates (2005b).

1.6 Ozone Monitoring: Remote Sensing Techniques and Instrumentation

Ozone monitoring can be discussed with respect to two broad categories: remote sensing and *in situ* measurements. The various types of instrumentation utilized in both remote sensing (Dobson and related spectrometers, LIDAR, and satellites) and in *in situ* (detectors installed near the Earth's surface and placed on various platforms such as rockets, airplanes, and kites and balloons) applications have benefits and disadvantages with respect to expense, accuracy, spatial requirements, and quantity and/or time resolution of ozone data desired by a researcher.

Hartley's work in 1881 represents the first instance of the remote sensing of ozone (Wayne, 1991). Through a combination of his spectroscopic knowledge of the UV absorption spectrum of ozone, ozone's visible spectrum measured by M.J. Chappius in 1880, and the full spectrum of sunlight measured in 1879 by A. Cornu, Hartley was able to infer the concentration maximum of ozone to be located high in the upper atmosphere (Turco, 1997c). It would take almost 50 years to determine the exact altitude of this ozone maximum.

Exploiting the direct UV absorption of ozone, G. M. B. Dobson developed the ozone spectrophotometer in 1924 and began continuous measurements of total column ozone in Arosa, Switzerland (Keesee, 2004a). Five years later, the Umkehr method, which relies on the intensities of reflected rather than direct UV light was combined with the Dobson spectrometer making it possible to also determine the vertical distribution of ozone. Since that time, ground based spectrometer stations have been measuring ozone levels continuously at various points around the globe. The benefits of this include the obvious long-term data collection of both the total

column and vertical distribution of ozone, but unfortunately these data are collected at only a few points relative to remote sensing by satellites discussed below. Furthermore, the Dobson spectrometers are strongly affected by aerosols, interfering pollutants, and the weather in the air column being measured and therefore must be located in remote areas at high elevation to diminish these interferences. For these reasons, Dobson spectrophotometers are primarily used only to help calibrate data obtained by other remote sensing methods such as satellites (Stephens, 1994).

Another ground-based instrument used to measure overhead ozone is the LIght Detection And Ranging (LIDAR) technique based upon absorption of laser light by ozone. First used in 1960 (Browell, 1989), LIDAR relies on a telescope to collect ultraviolet light, which is scattered by two laser beams, one of which is absorbed by ozone (308 nm) and the other not absorbed (351 nm). By comparing the intensity of the scattered light, an ozone profile is determined over an altitude range of 10 km to 50 km. Much like the Dobson spectrometer, LIDAR is limited by aerosols and the inability to measure through cloudy or foggy weather. Another limitation is LIDAR's cost and complexity, which restricts its use to only a few monitoring stations worldwide.

The final remote sensing device to be mentioned is the TOMS (Total Ozone Mapping Spectrometer), which has been aboard various satellites since 1978 (Keesee, 2004b; Finlayson-Pitts and Pitts, 2000b). TOMS determines ozone concentrations by comparing incident solar radiation with radiation reflected from Earth's atmosphere at six different UV wavelengths. The benefits of this technique include the ability to measure ozone in most types of weather, over even the most remote regions on Earth,

thus providing comprehensive ozone data. Limitations of TOMS include SO_2 interference from volcanic eruptions, attenuation due to back scattering of light from polar stratospheric clouds (PSCs) (Heath et al., 1975), and the extreme cost to launch and keep operational any satellite-based instrument. Although it is capable of measuring both total column ozone as well as ozone profiles, TOMS, much like the other remote sensing techniques mentioned above, proves inadequate for highly accurate ozone measurements at lower altitudes (Singer and Wentworth, 1957, McCormick 1984).

1.7 Ozone Monitoring: *in situ* Techniques and Instrumentation

To collect more precise data at lower altitudes, *in situ* techniques are required. These include an array of platforms such as rockets, airplanes, kites, and balloons, which can carry a wide range of ozone monitoring equipment including electrochemical, chemiluminescent, and UV-based ozone detectors. Rockets are occasionally used in measuring ozone profiles up to 75 km and are capable of being flown in all types of weather (Hilsenrath et al., 1980), but are limited by their short flight time, narrow geographic range, and cost. Aircraft are more functional due to their large payload capacities and are often used to fly multiple instruments capable of simultaneously gathering information about many atmospheric analytes in the troposphere, and in the stratosphere using highflying aircraft such as the ER2. For this reason, they are normally used for detailed studies of reaction and transport phenomena in a specific region. An airplane's usefulness is narrowed by concerns for pilot safety, the range and flight duration, relatively expensive operating costs, and

their inability to provide continuous measurements. For these reasons, balloons (Brewer, 1957; Mast and Saunders, 1962), and to a lesser extent kites (Balsley et al., 1994a,b) have primarily been used since the 1950's to provide a relatively inexpensive and widely dispersed ozone platform capable of carrying small instruments as high as 40 km while keeping them aloft for several days of continuous coverage.

The devices used to measure ozone from the various platforms described above are often called ozonesondes and derive their name from the nautical term "to sound," which means to make measurements. Types of ozonesondes include the following: electrochemical concentration cells (ECCs), laser *in situ* sensors, both gas and solid-phase chemiluminescent detectors, and UV-based spectrometers. It should be noted that each of these techniques also is suitable for ambient determination of ground-level ozone by simply placing it on a tower or bench top.

Laser *in situ* sensors measure absorption of laser light projected from a balloon and reflected back to a sensor by a mirror tethered below it (Stephens, 1994; Keesee, 2004b). Benefits of this technique include its ability to use multiple wavelengths capable of simultaneously measuring several analytes and the absence of an air pump, which can lead to errors in other *in situ* ozone monitors. Limitations include weather events such as fog, clouds, or rain, which can scatter the laser light, and wind, which can cause the hanging mirror to swing out of alignment with the balloon sensors. Other limitations relate to interfering compounds and aerosols, which can attenuate the light signal, and the high cost of the apparatus. This technique receives limited use compared to the other monitors described in later

pages.

Both gas and solid-phase chemiluminescent techniques rely upon the detection of light generated from the reaction of ozone with another compound to generate an excited state species capable of relaxing with emission of a photon. One type of gas-phase instrument is the common NO_x box utilized in reverse, with high levels of NO added instead of ozone. In this technique ozone reacts with NO at reduced pressure to form an O_2 molecule and an excited-state NO_2^* molecule (Fontijn, 1970).

$$NO + O_3 \longrightarrow NO_2^* + O_2 \tag{16}$$

$$NO_2^* \longrightarrow NO_2 + h\upsilon \tag{17}$$

Emission of light from NO_2^* provides the analytical signal. A more common gas-phase monitor involves ethylene or an ethylene derivative as the chemiluminescence reagent (Aimedieu and Barat, 1981; Gregory et al., 1983; Mehrabzadeh et al. 1983). Solid-phase techniques entail the use of chemiluminescent dyes such as Rhodamine-B (Hilsenrath et al., 1980) or derivatives of Coumarin, which are absorbed onto a surface where they react with ozone to emit light (Güsten et al., 1992; Güsten and Heinrich, 1996). Although highly sensitive, chemiluminescent techniques are not absolute methods and require the use of standards and extra preparation time to calibrate the instruments before their use. The solid-phase reagents require replacement before each set of measurements, making their repeated use time consuming, whereas generation and storage of reagents for the gas-phase instruments

require external equipment making their use cumbersome and unsuitable for small platforms such as balloons.

The ECC, the most commonly used ozonesonde, measures the current produced by chemical reactions with ozone and is based upon a technique developed by Komhyr in the late 1960's. Two half-cells, each with Pt electrodes immersed in different concentrations of KI solution, provide their own internal, driving electric potential. Air is bubbled through one half-cell where each ozone molecule causes two electrons to flow in an external circuit by forming free I_2 in the cathode solution which drives a subsequent oxidation / reduction reaction (Komhyr, 1969; Komhyr and Harris, 1971). Thus, the electrical current is directly related to the uptake of ozone in the cathode chamber. The ECC's simple design principle, small size, and low cost (≈ $400/instrument) makes the ECC suitable as a single-use release sonde. The accuracy of an ECC sonde, however, is only ± 10% (Barnes et al., 1985) due to interfering species such as NO_2 (positive offset) and SO_2 (negative offset) which are commonly found in polluted air (Finlayson-Pitts and Pitts, 1986), and from variations in the pumping speed due to either changing battery voltage, air temperature, or pressure changes.

Spectroscopy, which uses film, or more commonly electronic sensors sensitive to UV light, to measure wavelengths absorbed by ozone, relies upon the ozone molecule having an absorption maximum at 254 nm. This coincides with the principal emission of 253.7 nm from a low vapor pressure mercury lamp. As shown in *Figure 1.5*, ozone is determined from the attenuation of 254 nm light passing through an absorption cell. As a pump pulls air through the instrument, a solenoid

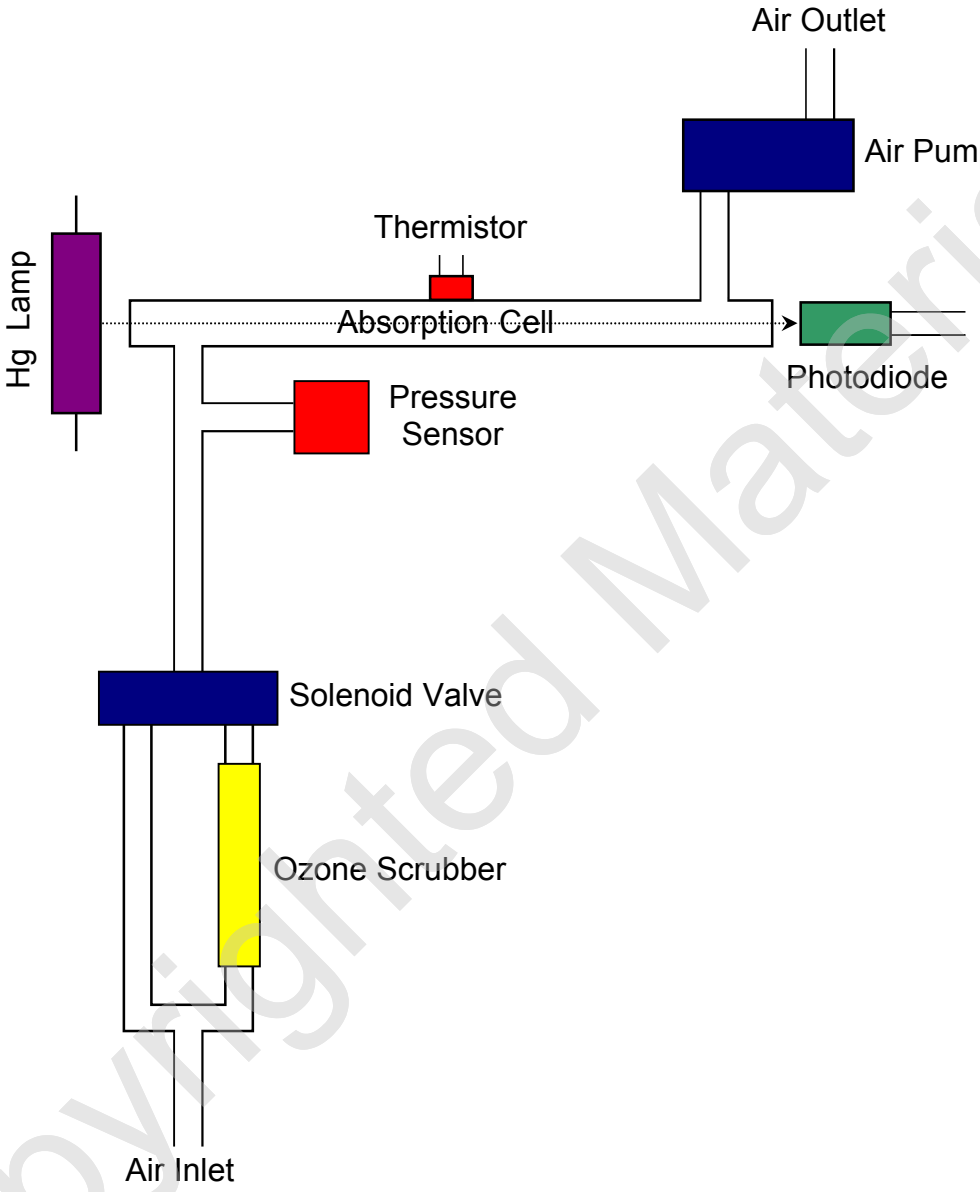

Fig 1.5. Schematic Drawing of UV-based Ozone Monitor.

switches between permitting air scrubbed of ozone or unscrubbed air to pass through the cell. The intensity of light in the cell is measured at the photodiode giving I_o for scrubbed air and I for the unscrubbed air. These light intensities are used in calculating ozone concentrations according to the Beer-Lambert law:

$$C_{O_3} = \frac{1}{\sigma l} \ln\left(\frac{I_o}{I}\right) \tag{18}$$

where l is the pathlength and σ is the absorption cross section or extinction coefficient for ozone at 254 nm (1.15×10^{-17} cm^2 $molecule^{-1}$). Because the absorbances measured are extremely small, equation (18) can be approximated by equation (19):

$$C_{O_3} = \frac{1}{\sigma l}\left(\frac{I_o - I}{I_o}\right) \tag{19}$$

Although minor corrections due to photodiode nonlinearity and instrument electronics may be required, the measurement of ozone based on UV absorbance is an absolute method, requiring no external calibration standard.

This method has few limitations for stationary measurements, is the desired EPA method, and is considered a primary standard (McElroy, 1979) for ambient monitoring of ozone due to its ease of use and high accuracy and precision (Bowman and Horak, 1972). The observed high precision and accuracy of this method are due to the maximum ozone absorbance being at least two orders of magnitude higher than the commonly found interfering species (Bowman and Horak, 1972). More importantly, water, which is highly variable in the troposphere (concentration range

of 0 to 4 %) and is often problematic in other atmospheric measurements, does not directly interfere with the absorbance measurements of ozone (Figure 1.6).

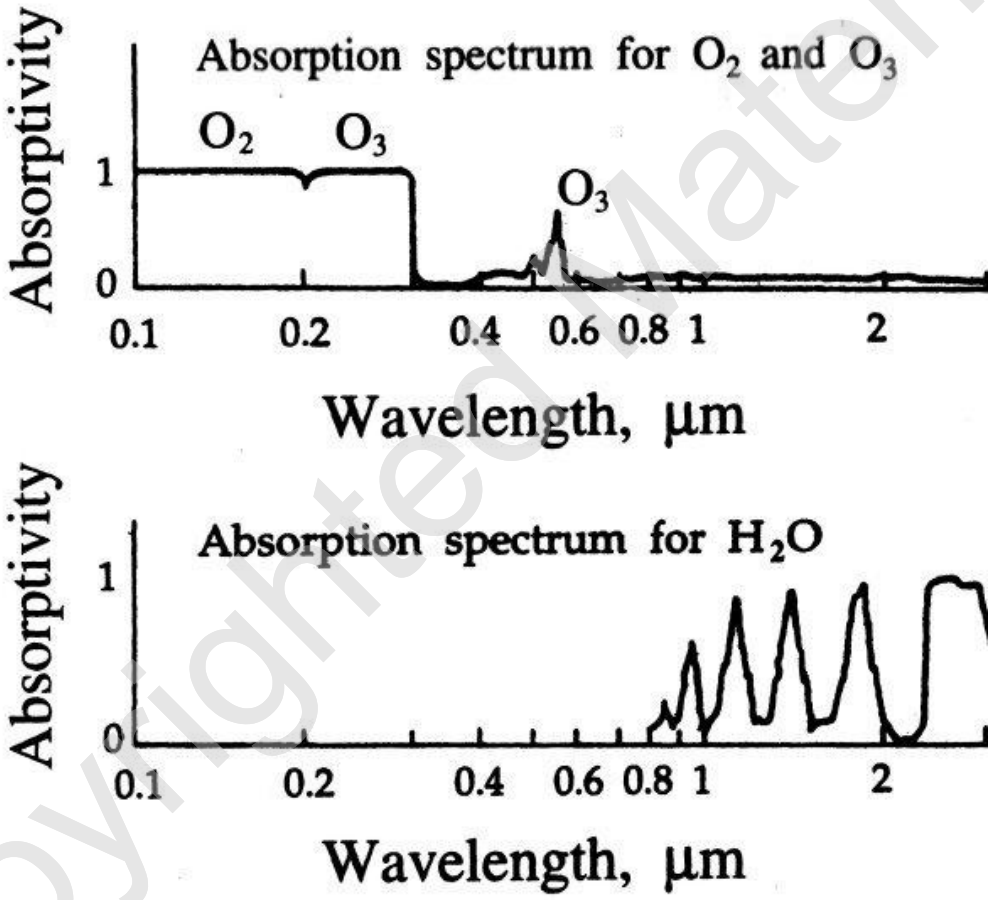

Fig. 1.6. Absorption Spectra of Ozone and Water. Adapted from Seinfeld and Pandis (1998).

1.8 Current UV-Based Ozone Photometers and Limitations

Major manufacturers of ozone photometers and their instruments, often employed in measuring ozone at SLAMS sites, include Thermo Environmental Inc. (Model 49 and 49C), Dasibi Environmental (Model 1003 and 1008), and Advanced Pollution Instrumentation, Inc. (Model 400). These instruments share the same basis of operation, described above, but are all limited in use to either powered ground or airplane-based operation as a result of their large size (58 cm x 43 cm x 22 cm for the Thermo Environmental Inc. instruments), mass (16 kg), and power consumption (150 watts).

It was with this limitation in mind that a lightweight, low-power, and miniaturized UV-based ozone monitor suitable for use in kite or balloon-based vertical profiling measurements was developed by our research group (Bognar and Birks, 1996). Although early bench top and field studies appeared promising, additional field work with this instrument led to the discovery of a humidity interference which called into question the accuracy of UV photometers in ambient monitoring. The primary goal of this thesis project was to develop an understanding of the cause of the water vapor interference, and to design improvements to our UV-based ozone monitor to remove this interference, making the ozone instrument suitable for both extended ground-based and vertical profile measurements of ozone without sacrificing its low power consumption, lightweight, and low-cost characteristics.

Chapter 1 – References

A.S.L. & Associates. "Nonattainment Areas for the 1-Hour Ozone Standard." Accessed 11 July 2005. < http://www.asl-associates.com/currenta.htm> (**2005a**).

A.S.L. & Associates. "Attainment and Nonattainment Areas in the U.S. 8-Hour Ozone Standard." Accessed 11 July 2005. <http://www.asl-associates.com/current8-hra.htm> (**2005b**).

Aimedieu, P and J. Barat. "Instrument to Measure Stratospheric Ozone with High Resolution." *Rev. Sci. Instrum.* 52 (**1981**): 432-437.

Balsley, B.B., J.W. Birks, M.L. Jensen, K.G. Knapp, J.B. Williams, and G.W. Tyrell. "Vertical Profiling of the Atmosphere Using High-Tech Kites." *Environ. Sci. Tech.* 28 (**1994a**): 422A-427A.

Balsley, B.B., J.W. Birks, M.L. Jensen, K.G. Knapp, J.B. Williams, and G.W. Tyrell. "Ozone Profiling Using Kites." *Nature* 369 (**1994b**): 23.

Barnes, R.A., A.R. Bandy and A.L. Torres. "Electrochemical Concentration Cell Ozonesonde Accuracy and Precision." *J. Geophys. Res.* 90 (**1985**). 7881-7887.

Birks, J.W. "Oxidant Formation in the Troposphere." *Perspectives in Environmental Chemistry*, Ed. D.L. Macalady. Oxford University Press: New York, **1998**. 233-256.

Bognar, J.A. and J. W. Birks. "Miniaturized Ultraviolet Ozonesonde for Atmospheric Measurements." *Anal. Chem.* 68 (**1996**): 3059-3062.

Bowman, L.D. and R.F. Horak. "A Continuous Ultraviolet Absorption Ozone Photometer." *Air Quality Instrumentation, Vol. 2*, Ed. J.W. Scales. Instrument Society of America: Research Triangle Park, N.C., **1972**.

Brewer, A.W. "Measuring Ozone in the Stratosphere." *New Scientist* 2 (**1957**): 32.

Browell, E.V. "Differential Absorption LIDAR Sensing of Ozone." *Proc. IEEE* 77 (**1989**): 419-432.

Chapman, S. "A Theory of Upper-Atmospheric Ozone." *Memoirs of the Royal Meteorological Society* 3 (**1930**): 103-125.

Finlayson-Pitts, B.J. and J.N. Pitts Jr. *Atmospheric Chemistry*. Wiley & Sons: New York, **1986**.

Finlayson-Pitts, B.J. and J.N. Pitts Jr. "Analytical Methods and Typical Atmospheric Concentrations for Gases and Particles." *Chemistry of Upper and Lower Atmosphere*. Academic Press: San Diego, C.A., **2000a**. 583.

Finlayson-Pitts, B.J. and J.N. Pitts Jr. "Scientific Basis for Control of Halogenated Organics." *Chemistry of Upper and Lower Atmosphere*. Academic Press: San Diego, C.A., **2000b**. 737.

Fontijn, A, A.J. Sabadell, R.J. Ronco. "Homogeneous Chemiluminescent Measurements of Nitric Oxide with Ozone: Implications for Continuous Selective Monitoring of Gaseous Air Pollutants." *Anal. Chem.* 42 (**1970**): 575-579.

Gregory, G.L., C.H. Hudgins and R.A. Edhal. "Laboratory Evaluation of an Airborne Ozone Instrument That Compensates for Altitude/Sensitivity Effects." *Environ. Sci. Tech.* 17 (**1983**): 100-103.

Güsten, H., G. Heinrich, R. Schmidt and U. Schurath. "A Novel Ozone Sensor for Direct Eddy Flux Measurements." *J. Atm. Chem.* 14 (**1992**): 73-84.

Güsten, H. and G. Heinrich. "On-line Measurements of Ozone Surface Fluxes: Part I. Methodology and Instrumentation." *Atmos. Environ*. 30 (**1996**): 897-909.

Heath, D.F., A.J. Krueger, H.A. Roeder and B.D. Henderson. "The Solar Backscattered Ultraviolet and Total Ozone Mapping Spectrometer (SBUV/TOMS) for NIMBUS G." *Opt. Eng.* 14 (**1984**): 323-331.

Hilsenrath, E. and P.T. Kirschner. "Recent Assessment of the Performance and Accuracy of a Chemiluminescent Rocket Sonde for Upper Atmospheric Ozone Measurements." *Rev. Sci. Instrum.* 51 (**1981**): 1381-1389.

Keesee, B. "History of the Ozone Layer." Accessed 10th July 2005. <http://www.albany.edu/faculty/rgk/atm101/o3histor.htm> (19th Aug, **2004a**).

Keesee, B. "Measured Ozone Depletion." Accessed 11th July 2005. <http://www.albany.edu/faculty/rgk/atm101/ozmeas.htm> (19th Aug, **2004b**).

Komhyr, W.D. "Electrochemical Concentration Cells for Gas Analysis." *Ann. Geophys*., 25 (**1969**): 203-210.

Komhyr, W.D and T. B. Harris. "Development of an ECC-Ozonesonde." *NOAA Tech. Rep. ERL 200-APCL 18ARL-149*. Washington: GPO, **1971**.

Mast, G.M. and H.E. Saunders. "Research and Development of the Instrumentation of Ozone Sensing." *Inst. Soc. Am. Trans.* 1 (**1962**): 325-328.

McCormick, M.P., T.J. Swissler, E. Hilsenrath, A.J. Krueger and M.T. Osborn. "Satellite and Correlative Measurements of Stratospheric Ozone: Comparison of Measurements Made by SAGE, ECC Balloons, Chemiluminescent, and Optical Rocketsondes." *J. Geophys, Res.* 89 (**1984**): 5315-5320.

McElroy, F.F. *Transfer Standards for Calibration of Air Monitoring Analyzers for Ozone - EPA-600/4-79-056*. Research Triangle Park, N.C.: U.S. EPA Environmental Monitoring and Support, **1979**.

Mehrabzadeh, A.A., R.J. O'Brien, T.M. Hard. "Optimization of Response of Chemiluminescence Analyzers." *Anal. Chem.* 55 (**1983**): 1660-1665.

Middlebrook, A.M. and M.A. Tolbert. Draft of *Understanding Global Changes: Earth Science and Human Impacts – Stratospheric Ozone Depletion*. UCAR: Boulder, CO, **1996**.

National Park Service – U.S. Department of Interior. "2001-2003 Average of the Annual 4th Highest Daily Maximum 8-hr Ozone Concentration." Accessed 10 July 2005. <http://www2.nature.nps.gov/air/Monitoring/exceed2.htm> (1st Nov. **2004**).

Neufeld, H.S., J.R. Renfro, W.D. Hacker, and D. Silsbee. "Ozone in Great Smoky Mountains National Park: Dynamics and Effects on Plants." *Proceedings of Air and Waste Management Association Symposium on Tropospheric Ozone and the Environment II - Effects, Modeling and Control, Atlanta, G.A.* Pittsburgh, PA: Air & Waste Management Association; **1992**. 594-617.

New York Public Library. "The Disappearing Ozone?" *Science Desk Reference*, Ed. P. Barnes-Svarney. Stonesong Press Inc.: New York, **1995**. 482-483.

Ohmi, T., T. Isagawa, T. Imaoka, and I. Suciyama. "Ozone Decomposition in Ultrapure Water and Continuous Ozone Sterilization for a Semiconductor Ultrapure Water System." *J. Electrochem. Soc.* 139 (**1992**): 3336-3345.

Roncero, M.B., M.A. Queral, J.F. Colom, T. Vidal. "Why Acid pH Increases the Selectivity of the Ozone Bleaching Processes." *Ozone–Sci. & Engin.* 25 (**2003**): 523-534.

Schalekamp, M. "A Comparison of Two Ozone Water-Treatment Plants –One with Low and the Other with Medium High Frequency." *Ozone–Sci. & Engin.* 1 (**1979**): 107-117.

Singer, S.F. and R.C. Wentworth. "A Method for the Determination of the Vertical Ozone Distribution from a Satellite." *J. Geophys. Res.* 62 (**1957**): 299-308.

Seinfeld, J. H., and S. N. Pandis. *Atmospheric Chemistry and Physics From Air Pollution to Climate Change*. John Wiley: New York, **1998**. 28.

Stephens, G.L. *Remote Sensing of the Lower Atmosphere*. Oxford University Press: New York, **1994**.

Turco, R.P. "The Stratospheric Ozone Layer." *Earth Under Siege*. Oxford University Press: New York, **1997a**. 411.

Turco, R.P. "Smog: The Urban Syndrome." *Earth Under Siege*. Oxford University Press: New York, **1997b**. 157.

Turco, R.P. "Smog: The Urban Syndrome." *Earth Under Siege*. Oxford University Press: New York, **1997c**. 23.

U.S. EPA Office of Air and Radiation. *Ozone and Your Health – EPA-452/F-99-003*. Washington, DC: US Environmental Protection Agency, **1999a**.

U.S. EPA Office of Air and Radiation. *Smog – Who Does It Hurt? – EPA-452/F-99-001*. Washington, DC: US Environmental Protection Agency, **1999b**.

U.S. EPA Office of Air and Radiation. *Ozone: Good Up High, Bad Nearby – EPA-451/K-03-001*. Washington, DC: US Environmental Protection Agency, **2003**.

U.S. EPA Office of Air and Radiation. "Clean Air Ozone Rules of 2004: Final Rule Designating and Classifying Areas Not Meeting the National Air Quality Standard for 8-Hour Ozone." Accessed 10 July 2005. <http://www.epa.gov/ozonedesignations/finrulefs.htm > (20th May **2005**).

U.S. EPA Office of Air Quality Planning and Standards. *Quality Assurance Handbook for Air pollution Measurement Systems - EPA-454/R-98-004*. Research Triangle Park, N.C.: U.S. Environmental Protection Agency, **1998**.

U.S. EPA Office of Air Quality Planning and Standards. *The Ozone Report: Measuring Progress Through 2003 – EPA-454/K-04-001*. Research Triangle Park, N.C.: U.S. Environmental Protection Agency, **2004**.

Chapter 2

Discovery of Water Vapor Interference in UV-Absorption-Based O_3 Detectors

2.1 Background to Discovery

In recent work at the University of Colorado, a miniaturized instrument for measurement of atmospheric ozone by UV absorption was constructed and field-tested (Bognar and Birks, 1996). John Birks and Donald David in the CIRES/Chemistry Instrument Design and Fabrication Facility (IDFF) redesigned this instrument for commercial sale through the University of Colorado. 2B Technologies, Inc. of Golden, Colorado subsequently licensed the technology where further improvements were made in conjunction with IDFF, and approximately 300 instruments have been manufactured and sold as of July 2005 as the 2B Technologies' *Model 202 Ozone Monitor*^{TM}. The 2B Tech Ozone Monitor has advantages of being small (9 cm × 22 cm × 28 cm), light weight (0.7 kg without case; 2.1 kg with case) and having a very low power requirement (4.0 watt) compared to other commercial instruments based on UV absorption, while achieving the same accuracy (±1 ppbv in the range 0-100 ppbv; 2% above 100 ppbv) and precision (0.5 – 1 ppbv). The instrument differs from previously commercialized instruments in that it is single beam (single absorption cell) rather than dual beam, has a shorter pathlength (15 cm vs. 30 cm for the TEI instrument), and uses photodiodes with built-in 254 nm dielectric band-pass filters in place of vacuum phototubes for detection. As shown in *Figure 2.1*, all of the other components such as solenoid valves, connecting tubing, and electronic circuit are miniature by comparison as well.

Fig. 2.1 Main components used in the 2B Technologies Ozone Monitor

Figure 2.2 is a photograph showing the relative sizes of the 2B Tech, Dasibi and TEI instruments. The 2B Tech Ozone Monitor was developed for applications where size, weight and power are highly restrictive and was developed specifically for vertical profiling work in the Birks group using kites (Balsley et al., 1994a,b; Knapp et al., 1998a,b), balloons (Knapp et al., 1998a,b; Helmig et al., 2002), powered parachutes (Schulz, 2003; 2004) and small airplanes (Schulz, 2003). Previous work made use of electrochemical ozone sondes. Electrochemical ozone sondes are lightweight (0.6 kg), low in power consumption (2 watt), and sufficiently inexpensive to be disposable (Komhyr and Harris, 1971). These instruments display similar accuracy and precision as UV absorbance instruments but are designed for short-term use (hours to days) and require the use of chemicals (iodine/sodium iodide) that cannot be transported onboard commercial aircraft. Perhaps the greatest drawback to the use of electrochemical ozone sondes is that they require approximately two hours of preparation time, during which they are exposed to high and low concentrations of ozone. Also, the half-cell solutions must be periodically replaced and conditioned with ozone. Basically, these instruments are designed for one-time measurements as release sondes.

Except for aircraft measurements during field missions lasting typically a few days to weeks, vertical profiles of ozone within the troposphere have seldom been measured. Vertical profiling using electrochemical ozonesondes have focused primarily on the stratosphere (Deshler and Hofmann, 1991, McPeters et al., 1999, Nardi et al., 1999, Schulz et al., 2001). In vertical profiling, atmospheric instruments must measure analyte mixing ratios in air having a wide range of

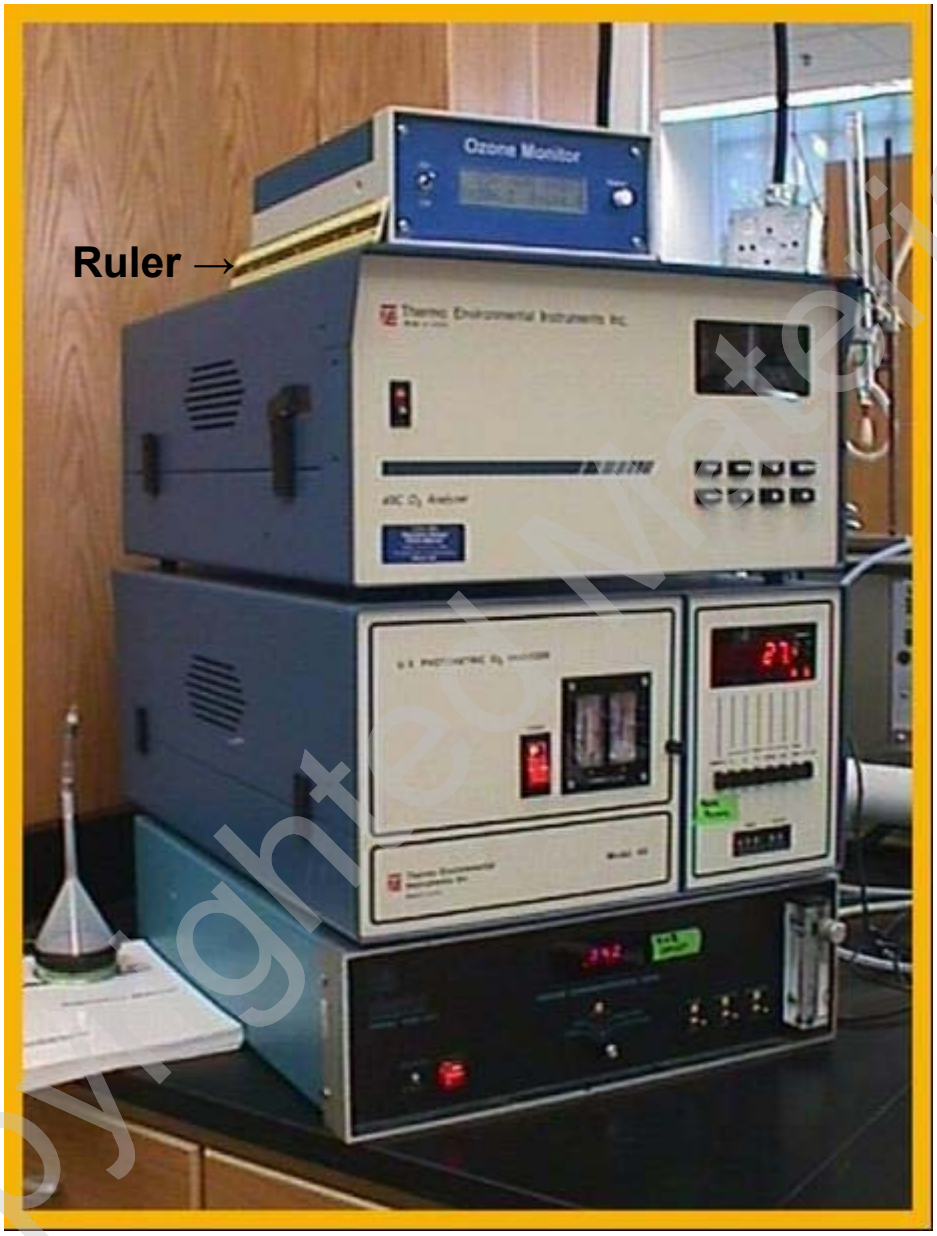

Fig. 2.2 Relative sizes of 2B Tech Model 202, TEI Model 49C, TEI Model 49, and Dasibi Model 1003-AH ozone monitors (top to bottom) as compared to a 12-inch ruler.

temperature, pressure and humidity. For UV-based ozone instruments, temperature and pressure have a significant effect only on the determination of molecular density, which is used to calculate the mixing ratio; fortunately, temperature and pressure are easily measured with high accuracy and precision.

2.2 Discovery of Water Vapor Interference

No water vapor interference is expected for UV absorbance measurements since water vapor does not absorb at the wavelength of 254 nm used for ozone absorption measurements. In an early application of the miniaturized ozone instrument to vertical profiling during a field experiment in Park Falls, WI, very large swings in ozone mixing ratio of several hundred ppbv in both the positive and negative direction were observed as the instrument passed from dry to wet and wet to dry layers of the atmosphere, respectively. In order to test for a humidity effect on the measurement, a Drierite® desiccant scrubber was attached to the inlet of the instrument while operating at ground level. Large excursions in apparent ozone were measured in the negative direction when the drying trap was first attached and in the positive direction when the trap was removed, as seen in *Figure 2.3*. In this experiment, the average ambient ozone measured over the first 300 s was 46 ppbv. Attaching the Drierite scrubber caused a decrease within 20 s (two data points) to an apparent value of -648 ppbv. Over the next 230 s, the apparent ozone mixing ratio recovered to a value of -288 ppbv, at which point the rate of recovery was very slow. At this time, removal of the Drierite trap resulted in an increase within 10 s of apparent ozone to a level of 356 ppbv. Recovery to normal was somewhat faster for

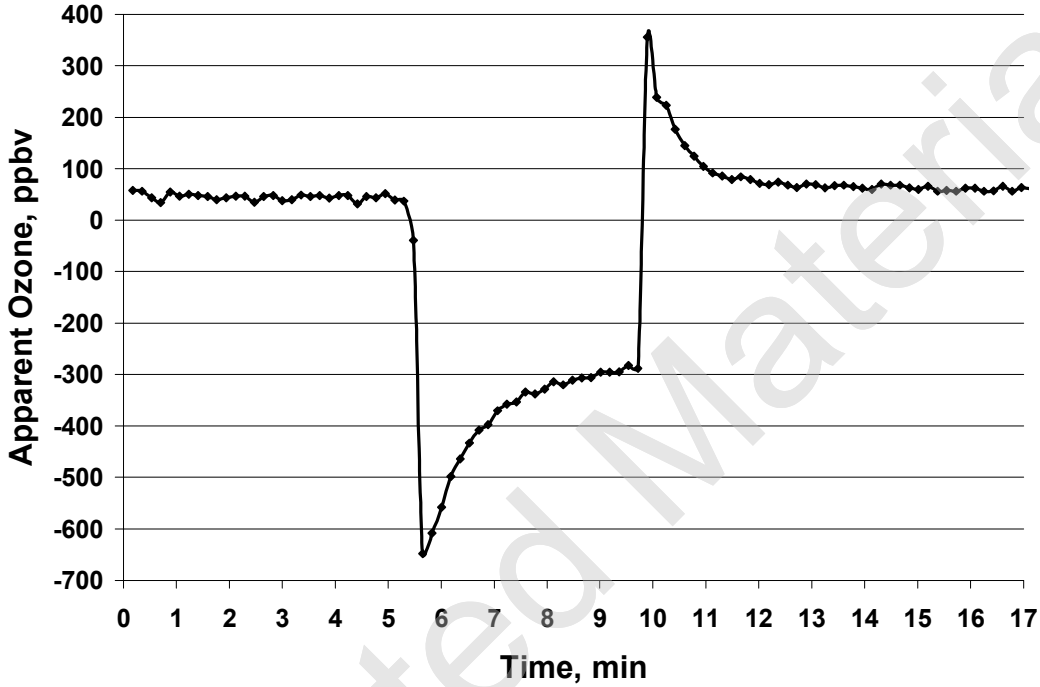

Fig. 2.3. Water vapor effect on apparent ozone reading resulting from attaching at ≈ 5.5 min and removing at ≈ 9.8 min a Drierite® desiccant scrubber on the 2B Tech Ozone Monitor inlet.

the dry-to-wet change, and after 410 s the apparent ozone reading was 97 ppbv, but still well above ambient, especially considering that the sampled ozone was most likely completely destroyed through surface reactions in the Drierite® trap.

This discovery of a water vapor interference was surprising, and initially it was thought to be a unique characteristic of the newly designed instrument. As discussed below, however, it was soon found that various UV absorbance monitors used in atmospheric measurements for several decades exhibit similar water vapor interference. When operated at ground level, the changes in humidity are usually sufficiently slow that large errors in ozone measurements seldom occur and smaller errors of a few ppbv probably go unnoticed.

2.3 Previous Studies Regarding Water Vapor Interference

A review of the literature resulted in only two peer-reviewed articles concerning the possibility of a water vapor interference in UV-absorbance-based ozone instruments: a study by Meyer et al. in 1990 and a 1993 EPA review (Kleindienst et al., 1993). Over the past few years, a few papers discussing anomalies that occur in ozone measurements have been presented at various scientific meetings (Leston and Ollison, 1992; 1994; Hudgens et al., 1994, Ollison et al., 1997; and Maddy, 1998; 1999). In these conference proceedings, it is pointed out that UV ozone instruments often exhibit erratic behavior when sampling on hot, humid days; i.e., when the municipalities are most likely to be out of compliance. Interestingly, as discussed by Parish and Fehsenfeld (2000), it was plausibly argued by Leston and Ollison (1992) that approximately half of the areas designated in 1993 as non-

attainment, may actually have been in compliance with the O_3 standard due to errors in ozone measurements. Unfortunately, no insight into the underlying physical mechanism responsible for the water vapor interference, other than the possibility that water actually condenses within the instrument components, is provided in the non-peer-reviewed literature.

The Meyer et al. experiment utilized three commercial, dual-cell, UV photometers: two from TECO (Model 49) and one from Dasibi (Model 1003-AH). These instruments were plumbed without their ozone scrubbers so that the solenoid, which normally switches between ozone-rich and ozone-free air would now switch between ozone-free dry and humid air. Ambient air was used to produce dry, ozone-free air by passing it through a charcoal filter and molecular sieve. This initial air stream was split with one portion replacing what would be scrubbed air in the instrument. The other stream was split again to ultimately provide humidified air to what is normally the instrument's scrubber by-pass tubing. This moist air stream was humidified to variable levels by bubbling one portion through a temperature-controlled water bath and recombining with dry air by use of mass flow controllers to reach the desired humidity level. With these modifications, any interference from water vapor was measured as an apparent ozone mixing ratio.

In this configuration, Meyer et al. found a measurable water vapor effect ranging between 200 to 800 ppbv equivalent ozone, which they related to the optical differences in light scattering as water vapor interacted with the cell window's surface contaminants and/or irregularities. The paper went on to say that this scattering only affected the instrument's noise and would only be problematic at times when rapid

humidity changes occur at ground level or during vertical profiling in the atmosphere when the instrument passes through alternately wet and dry layers. Meyer et al. did not mention any perturbation of water vapor on the instrument's calibration or zeroing offset nor the specific length of time that the effect persisted other than to state that the effect was not seen in the hourly averaged data.

The Kleindienst et al. studies were run to unequivocally answer the possibility of humidity interferences in UV based ozone instruments raised by Meyer et al. Unlike Meyer et al., the Kleindienst et al. study left the UV based ozone monitors' internal scrubbers intact and varied both humidity and ozone concentrations. Multiple instruments (two TEI 49, two Dasibi 1003-AH, and one Dasibi 1008-AH) were monitored simultaneously with the desired humidity and ozone concentrations mixed in a manifold system through the use of a temperature adjusted, water-bubbling system and a low-voltage mercury lamp, respectively. All instruments were calibrated immediately prior to their use against an EPA standard reference photometer on the above-mentioned manifold system with ozone in dry air.

A first set of experiments was run at three ozone concentrations of 85, 125, and 320 ppbv and three dew point temperatures of 11, 17, and 23°C corresponding to a relative humidity (RH) of approximately 40, 60 and 80%, respectively. This resulted in ozone readings with relative differences ranging from 0.64% to 7.5% with an average 2.9% relative difference from nominal ozone concentrations. Although the instruments were zeroed and spanned with dry air before each experiment there was no attempt to independently verify the ozone concentrations during the humid air runs, which may explain the relatively high deviation from correct values. It must be

further stressed that the "ozone/humid air mixtures were allowed to equilibrate for at least an hour before measurements were made" and that "following equilibration, readings were taken for a single ozone concentration at a single RH for 0.5 hour" (Kleindienst et al., 1993). This is significant because readings were not recorded for variable humidity changes nor for the at least hour-long periods when the instruments were allowed to equilibrate before data collection commenced.

A second set of experiments where ambient laboratory temperatures were kept approximately 5 °C lower than the air stream in the manifold system also were carried out. This was done in an attempt to replicate ambient monitoring during summer months where condensed water sometimes forms in the inlet tubing. The procedure was the same as the first set of experiments, but this time the ozone concentrations were monitored throughout the procedure and calculated via dilution to give known concentrations. The same dew points were utilized as in the previous experiment, but this time only the two higher ozone concentrations of 200 and 325 ppbv were used. It should be noted that the average relative errors from the first set of experiments were highest for the 85 ppbv ozone measurements discarded from this second set of experiments.

This set of experiments resulted in ozone readings with relative differences from nominal ozone concentrations ranging from 0.28% to 1.4% and an average relative difference of 0.53%. Kleindienst et al. determined this discrepancy not to be problematic. Although Kleindienst et al. also saw both an initial 100 to 150 ppbv positive spike, followed by periodic 50 ppbv positive and negative spikes in some instruments (Figure 2.4) and noisier operation in others during periods of humidity

changes, they concluded that this would have no effect upon the hourly averaged ozone readings: "While it was possible for a single hourly average to have a systematically higher value because of a positive deviation (depending on the length of the period), it would be followed by an hourly average that was lower (and vice versa)." They went on to say that any problem with water could be prevented by always operating the instruments at temperatures above the dew point, although they also noted that this often times does not occur during the summer months when ambient terrestrial ozone measurements are at their most critical importance in determining compliance of a municipality with EPA air quality standards. Even though they noted there was difficulty in equilibrating the instruments following rapid relative humidity changes, Kleindienst et al. did not comment on how these spikes and instabilities might affect when and how an instrument should be calibrated so as not to result in spurious ozone measurements.

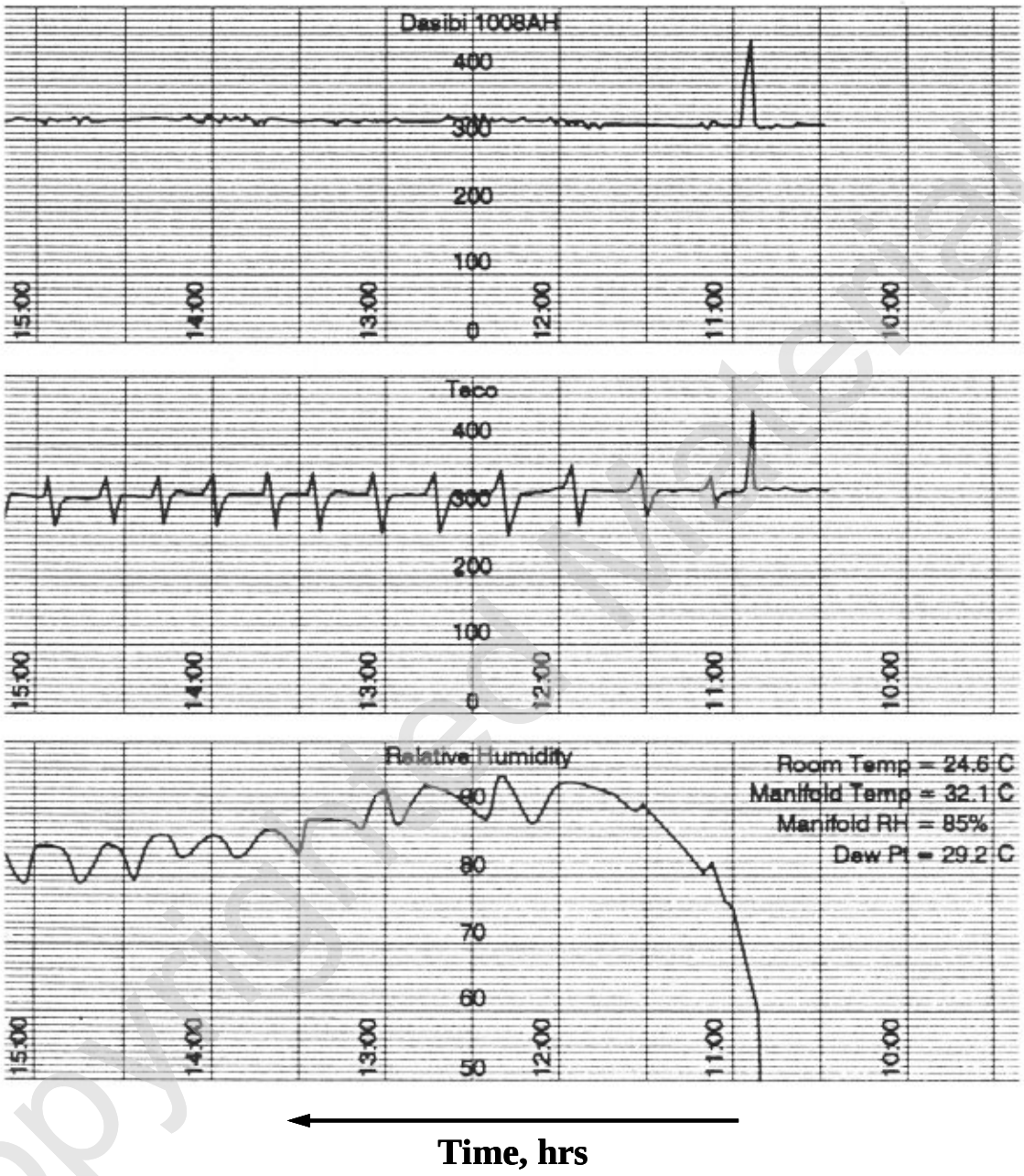

Fig. 2.4. Responses of Dasibi 1008AH and TEI 49 (TECO) ozone instruments to a step change from 0 to 85% RH. Adapted from Kleindienst et al. (1993).

2.4 Experimental Setup of Water Vapor Interference Testing

As a result of the Meyer et al. and Kleindienst et al. papers and our field data using the 2B Tech ozone monitor, it was decided to perform our own studies with UV-absorption-based ozone monitors in order to determine their practical limitations in collection of ambient ozone measurements during periods of humidity fluctuations. Multiple instruments (TEI 49, TEI 49C, Dasibi 1003-AH, and 2B Tech Model 202) were monitored as the humidity of zero air was manipulated through the use of a temperature regulated humidity generator constructed by former graduate student Christine Karbiwnyk (Karbiwnyk et al., 2002). The humidity generator, shown in *Figure 2.5*, consists of a micro-porous polytetrafluoroethylene (PTFE) tube surrounded by a thermally regulated water jacket. By adjustment of the water temperature and the ratio of air flowing through the PTFE versus bypass tubing, any desired relative humidity can quickly be attained. All ozone monitors were calibrated immediately prior to their use against a standard reference photometer following the guidelines described in the EPA transfer standards manual (McElroy, 1979). To ensure that only zero air was tested, the ozone monitors sampled from an air stream, which always exceeded the flow needed by the instruments, with the overflow venting into the laboratory. Ozone was never generated in this set of experiments in order to isolate the humidity effect on the ozone monitors.

The instruments were equilibrated to the laboratory's ambient humidity (between 12 to 14% RH at 23°C) by running for at least 4 hours before the commencement of each experiment. Each run consisted of checking the instrument by verifying its zero with zero air generated from ambient room air (again 12 to 14%

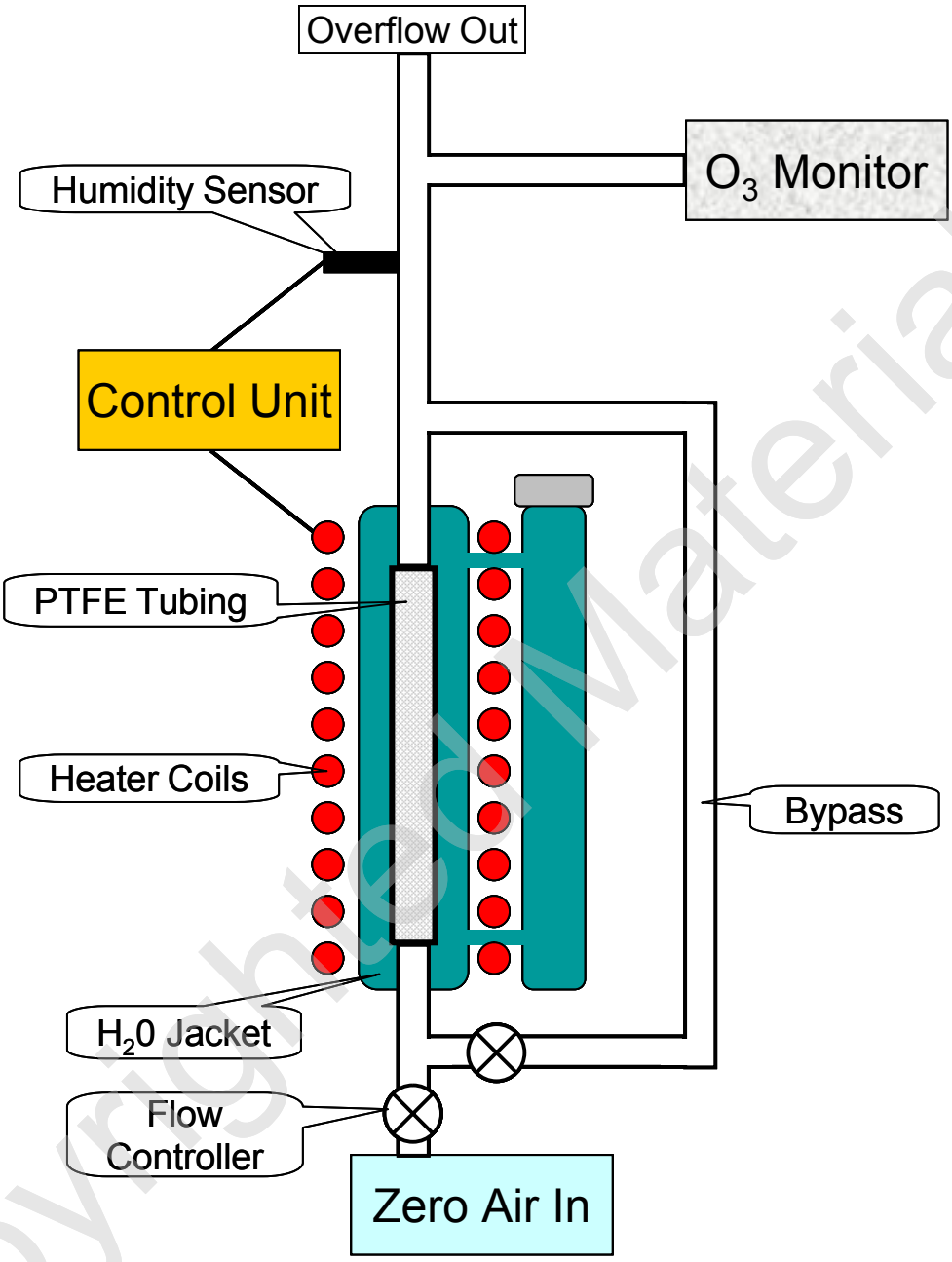

Fig. 2.5. Schematic diagram of apparatus for measuring apparent changes in ozone during changes in humidity of zero air. Humidity generator portion adapted from Karbiwnyk et al. (2002).

RH) using a 3M Mersorb Indicator Chemical Cartridge air as an external ozone scrubber. This was followed by rapid valve switching to ultra high purity tank air at 0% RH, next switching to zero air adjusted to 90% RH, and finally switching again to 0% RH air. Although extreme, this rapid change in relative humidity was sought in order to maximize any effect that might be observed as well as to mimic the various air layers an instrument would sample during flight.

2.5 Experimental Findings of Water Vapor Interference Testing

Much like the Meyer et al. and Kleindienst et al. studies, we too found measurable water vapor interference in all the ozone monitors tested. Even though all instruments were exposed to the same water vapor transients, the responses were of different magnitudes and direction depending upon the instrument evaluated.

Figure 2.6 shows the apparent deviations from 0 ppbv ozone measured by a TEI Model 49 ozone monitor. Positive spikes on the order of 8 ppbv occurred when changing from humid to dry air and persisted for 5 – 10 minutes. A negative spike of -25 ppbv ozone arose over the course of 35 minutes when changing from dry to humid air and flattened out showing no signs of recovery even a full hour after the initial humidity change. The noise of the instrument also increased by a factor of two over that of its normal operation as a result of the humidity changes.

The effect on a newer model TEI, the 49C, is shown in *Figure 2.7*. As with the older model 49, the direction of the spikes remain the same, although in this case the peaks are sharper and of greater magnitude. A positive 300 ppbv spike occurred when switching from humid to dry air with recovery to zero occurring after 5

minutes. A negative spike of 210 ppbv resulted from a switch to humid air but never fully recovered even after 70 minutes had passed. It should be noted that if the instrument were calibrated any time during the depressed, yet stable, region found between the 30 to 85 minute time period that an error of +13 ppbv ozone would have been added to the instrument zero. This would result in erroneously elevated ozone readings at least until the next time the instrument is calibrated. This potential danger of incorrectly calibrating ozone monitors was never addressed by either the Meyer et al. or Kleindienst et al. studies.

The Dasibi instrument showed an opposite effect from the two TEI instruments to the same humidity changes (Figure 2.8). There was a positive 50 ppbv spike when changing from dry to humid air and a negative spike when changing from humid to dry. Although the Dasibi did recover from the humidity changes in approximately 5 minutes, its readings were much noisier than usual as a result of the experiment.

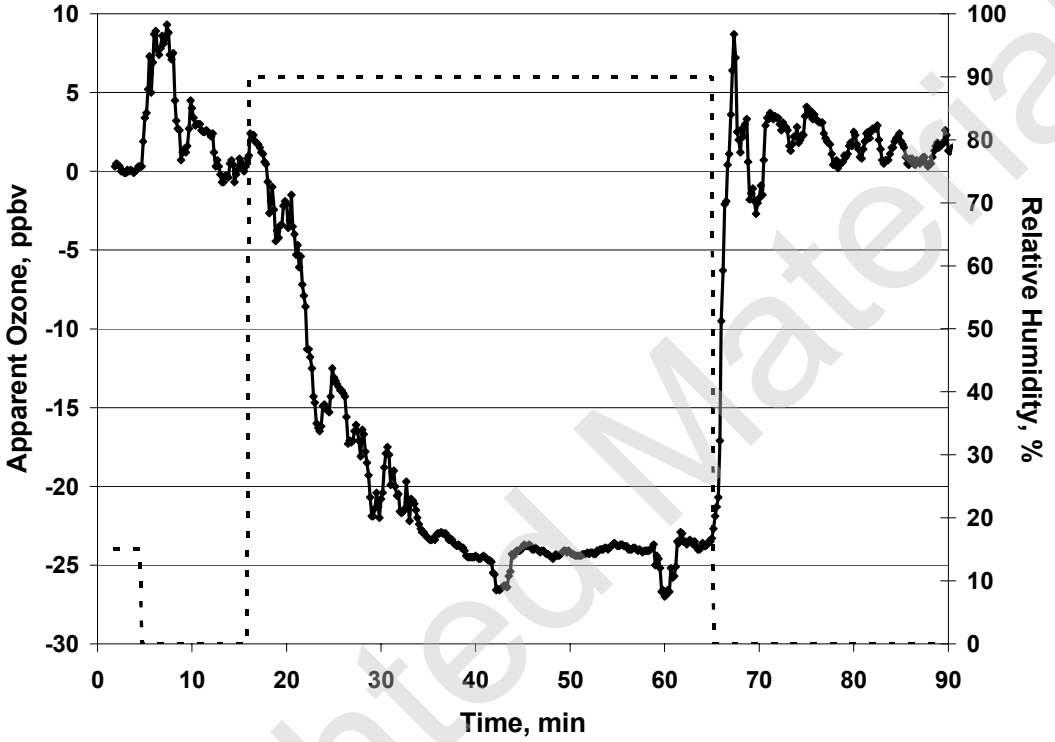

Fig. 2.6. Water vapor effect on apparent ozone reading for TEI Model 49 resulting from changes in the relative humidity of zero air.

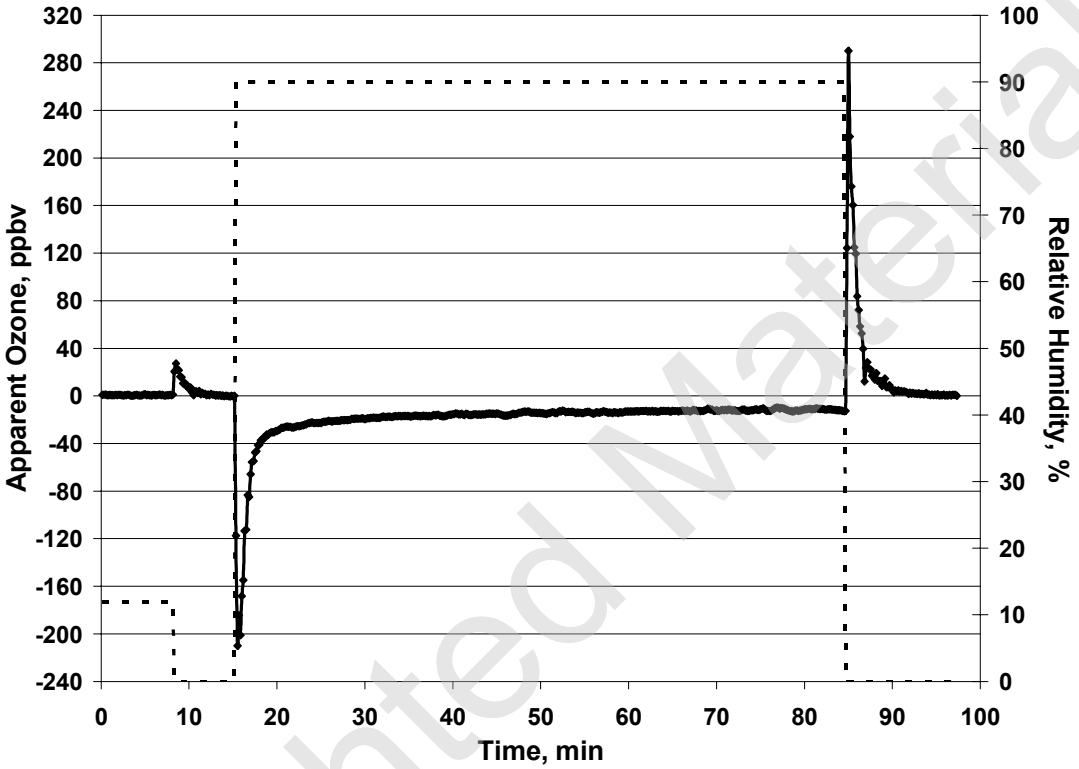

Fig. 2.7. Water vapor effect on apparent ozone reading for TEI Model 49C resulting from changes in the relative humidity of zero air.

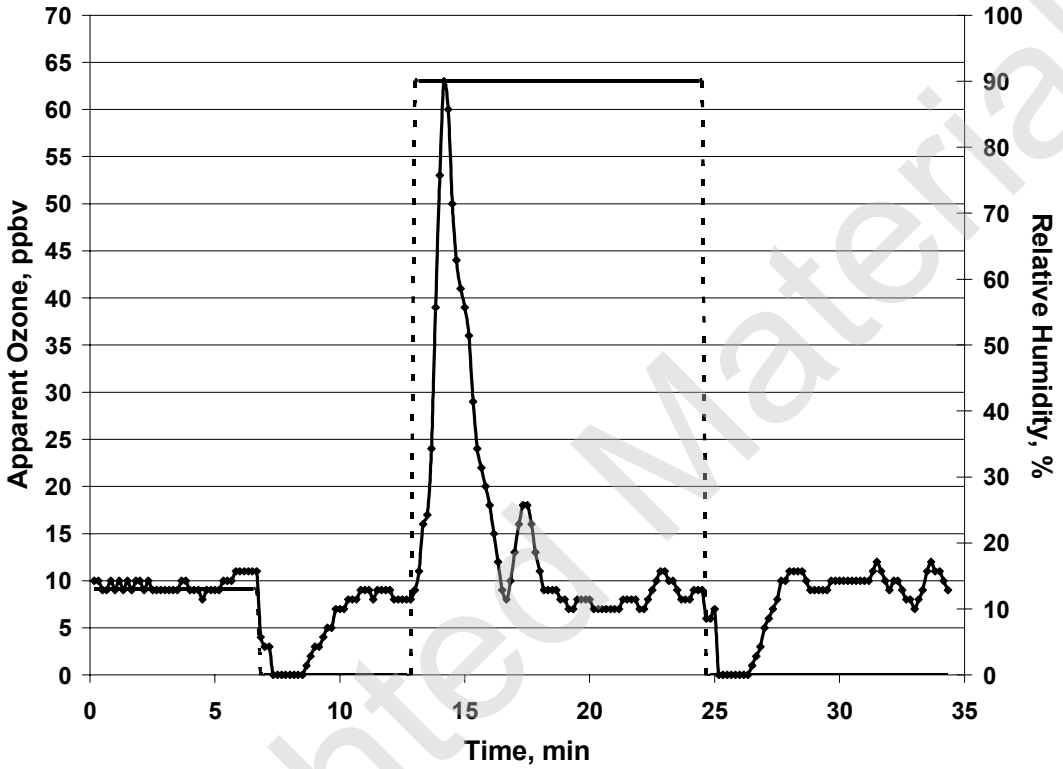

Fig. 2.8. Water vapor effect on apparent ozone reading for Dasibi Model 1003-AH resulting from changes in the relative humidity of zero air. Note that a 10 ppbv offset from zero was applied to better see any negative zero drift since the instrument does not display negative values.

The 2B Tech instrument had, by far, the largest offsets in apparent ozone readings of any of the instruments tested. Like the Dasibi, it too became noisier than usual and had a positive spike (550 ppbv) when changing from dry to humid air and a negative offset (-300 ppbv) when switching from humid to dry conditions (Figure 2.9). Much like the TEI instruments, the 2B Tech ozone monitor showed no signs of fully recovering from the humidity changes even after an hour at 90% RH.

These experiments clearly demonstrate significant humidity interference in all UV-absorption-based ozone monitors tested despite the fact that water does not absorb at 254 nm and therefore should not provide a response to humidity change. This incongruity implies a complex interaction of water with components of the ozone instruments. A mechanism behind these interactions must be established that is capable of not only explaining the direction and magnitude of the instruments' offsets but more importantly clarify how these offsets might hamper current ozone monitoring practices. An understanding of the humidity interference and the development of a method capable of negating the effect in all UV-absorption-based ozone monitors is the primary goal of this thesis.

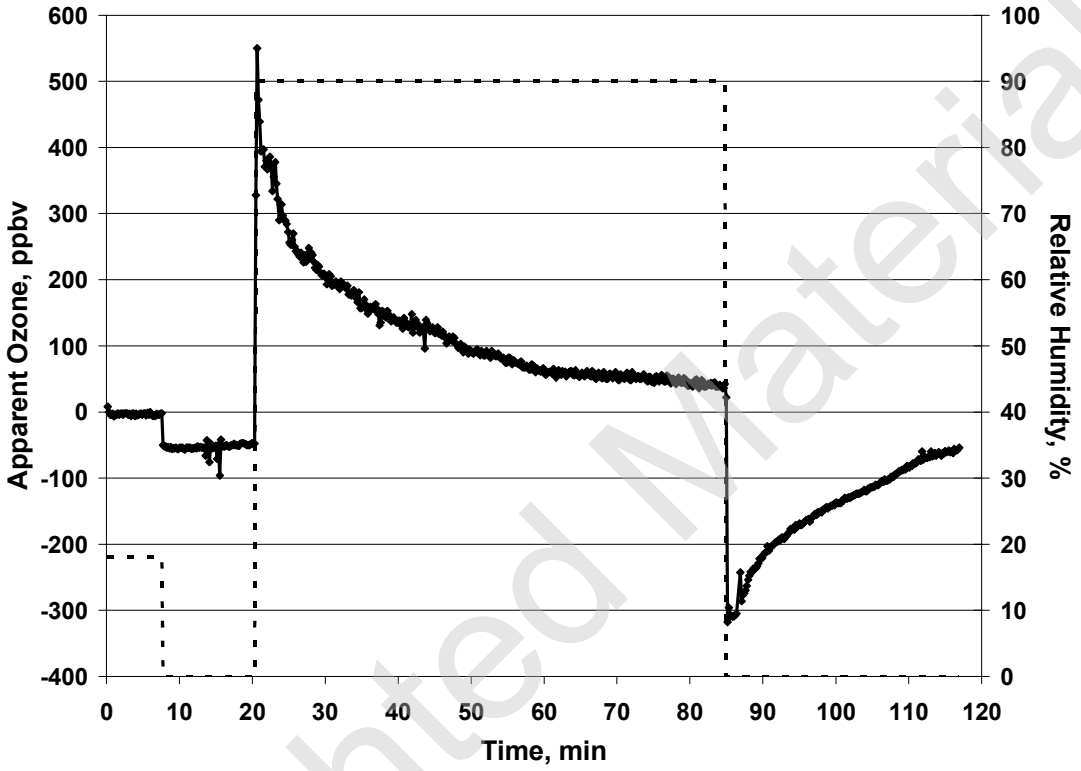

Fig. 2.9. Water vapor effect on apparent ozone reading for 2B Tech Ozone Monitor resulting from changes in the relative humidity of zero air.

Chapter 2 – References

Bognar, J.A. and J. W. Birks. "Miniaturized Ultraviolet Ozonesonde for Atmospheric Measurements." *Anal. Chem.* 68 (**1996**): 3059-3062.

Balsley, B.B., J.W. Birks, M.L. Jensen, K.G. Knapp, J.B. Williams and G.W. Tyrrell. "Ozone Profiling Using Kites." *Nature* 369 (**1994a**): 23.

Balsley, B.B., J. W. Birks, M. L. Jensen, K. G. Knapp, J. B. Williams and G. W. Tyrrell. "Vertical Profiling of the Atmosphere for Ozone Using Kites." *Environ. Sci. Technol.* 28 (**1994b**): 422A-427A.

Deshler, T. and D.J. Hofmann. "Ozone Profiles at McMurdo Station, Antarctica, the Austral Spring of 1990." *Geophys. Res. Lett*. 18 (**1991**): 657-660.

Helmig, D., J. Boulter, D. David, J.W. Birks, N.J. Cullen, K. Steffen, B.J. Johnson and S.J. Oltmans. "Ozone and Meteorological Boundary-Layer Conditions at Summit, Greenland during 3-21 June 2000." *Atm. Environ.* 36 (**2002**): 2595-2608.

Hudgens, E.E., T.E. Kleindienst, F.F. McElroy, and W.M. Ollison. "A Study of Interferences in Ozone UV and Chemiluminescent Monitors." *Proceedings of Air and Waste Management Association International Symposium on Measurements of Toxics and Related Air Pollutants, Research Triangle Park, N.C.* Pittsburgh: Air & Waste Management Assoc., **1994**. 405-415.

Karbiwnyk, C.M., C. S. Mills, D. Helmig and J. W. Birks. "Minimization of Water Vapor Interference in the Analysis of Non-Methane Volatile Organic Compounds by Solid Adsorbent Sampling." *J. Chrom. A* 958 (**2002**): 219-229.

Kleindienst, T.E., E.E. Hudgens, D.F. Smith, F.F. McElroy and J.J. Bufalini. "Comparison of Chemiluminescence and Ultraviolet Ozone Monitor Responses in the Presence of Humidity and Photochemical Pollutants." *J. Air Waste Mange. Assoc*. 43 (**1993**): 213-222.

Knapp, K.G., B.B. Balsley, M.L. Jensen, H.H. Hanson and J.W. Birks. "Observation of the Transport of Polluted Air Masses from the Northeastern United States to Cape Sable Island, Nova Scotia, Canada During the 1993 North Atlantic Regional Experiment Summer Intensive." *J. Geophys. Res.* 103 (**1998a**): 13399-13411.

Knapp, K.G., M.L. Jensen, B.B. Balsley, J.A. Bognar, S.J. Oltmans, T.W. Smith and J.W. Birks. "Vertical Profiling Using Complementary Kite and Tethered Balloon Platforms at Ferryland Downs, Newfoundland, Canada: Observation of a Dry, Ozone-Rich Plume in the Free Troposphere." *J. Geophys. Res.* 103 (**1998b**): 13389-13397.

Komhyr, W.D and T. B. Harris. "Development of an ECC-Ozonesonde." *NOAA Tech. Rep. ERL 200-APCL 18ARL-149*. Washington: GPO, **1971**.

Leston, A. and W. Ollison. "Estimated Accuracy of Ozone Design Values: Are They Compromised by Method Interference?" *Proceedings of Air and Waste Management Association Conference on Tropospheric Ozone: Nonattainment and Design Value Issues, Boston, MA*. October 27-30, 2003. Pittsburgh: Air & Waste Management Assoc., **1992**. 451-456.

Leston, A. and W. Ollison. "Estimated Accuracy of Ozone Design Values: Are They Compromised by Method Interference?" *Proceedings of Air and Waste Management Association International Symposium on Measurements of Toxics and Related Air Pollutants, Research Triangle Park, N.C.* Pittsburgh: Air & Waste Management Assoc., **1994**. 2-18.

Maddy, J.A. "A Test That Identifies Ozone Monitors Prone to Anomalous Behavior While Sampling Hot and Humid Air." Paper 98-MPB.O2P in *Proceedings of the Air and Waste Management Association Meeting, San Diego, C.A.* June 14th-18th, 1998. Pittsburgh: Air & Waste Management Assoc., **1998**.

Maddy, J.A. "Evaluating a Heated Metal Scrubbers Effectiveness in Preventing Ozone Monitor's Anomalous Behavior During Hot and Humid Ambient Sampling." Paper 99-451 in *Proceedings of the Annual Air and Waste Management Association Meeting, St. Louis, M.O.* Pittsburgh: Air & Waste Management Assoc., **1999**.

McPeters, R.D., D.J. Hofmann, M. Clark, L. Flynn, L. Froidevaux, M. Gross, B. Johnson, G. Koenig, X. Liu, S. McDermid, T. McGee, F. Murcray, M.J. Newchurch, S. Oltmans, A. Parrish, R. Schnell, U. Singh, J.J. Tsou, T. Walsh, and J.M. Zawodny. "Results from the 1995 Stratospheric Ozone Profile Intercomparison at Mauna Loa." *J. Geophys. Res. – Atmos.* 104 (**1999**): 30,505-30,514.

Meyer, C.P., C.M. Elsworth and I.E. Galbally. "Water Vapor Interference in the Measurement of Ozone in Ambient Air by Ultraviolet Absorption." *Rev. Sci. Instrum.* 62 (**1991**): 223-228.

McElroy, F.F. *Transfer Standards for Calibration of Air Monitoring Analyzers for Ozone - EPA-600/4-79-056*. Research Triangle Park, N.C.: U.S. EPA Environmental Monitoring and Support, **1979**.

Nardi, B., W Bellon, LD Oolman, and T Deshler. "Spring 1996 and 1997 Ozonesonde Measurements Over McMurdo Station, Antarctica." *Geophys. Res. Lett*. 26 (**1999**): 723-726.

Ollison, W.M., T.E. Kleindienst and C.D. McIver. "A Study of Interferences in Ambient Ozone Monitors." *Proceedings of Air and Waste Management Association International Symposium on Measurements of Toxics and Related Air Pollutants, Research Triangle Park, N.C.* Pittsburgh: Air & Waste Management Assoc., **1997.** 215-217.

Parish, D.D. and F.C. Fehsenfeld. "Methods for Gas-phase Measurements of Ozone, Ozone Precursors and Aerosol Precursors." *Atmos. Enviro.* 34, (**2000**): 1921-1957.

Schulz, A., M. Rex, N.R.P. Harris, G.O. Braathern, E. Reimer, R. Alfier, I. Kilbane-Dawe, S. Eckermann, M. Allaart, M. Alpers, B. Bojkov, J. Cisneros, H. Claude, E. Cuevas, J. Davies, H. DeBacker, H. Dier, V. Dorokhov, H.. Fast, S. Godin, B. Johnson, B. Kois, Y. Kondo, E. Kosmidis, E. Kyro, Z. Litynska, I.S. Mikkelsen, M.J. Molyneux, G. Murphy, T. Nagai, H. Nakane, F. O'Connor, C. Parrondo, F.J. Schmidlin, P. Skrivankova, C. Varotsos, C. Vialle, P. Viatte, V. Yushkov, C. Zerefos, P. von der Gathen. "Arctic Ozone Loss in Threshold Conditions: Match Observations in 1997/1998 and 1998/1999." *J. Geophys. Res. – Atmos.* 107 (**2001**): 7495-7503.

Schulz, K.J. "Measurements of Landscape-Scale Fluxes of Carbon Dioxide at Two AmeriFlux Sites Using a New Vertical Profiling Technique." Ph.D. Thesis, University of Colorado, Boulder, Colorado (**2003**).

Schulz, K.J., M.L. Jensen, B.B. Balsley, K. Davis, and J.W. Birks. "Tedlar Bag Sampling Technique for Vertical Profiling of Carbon Dioxide Through the Atmospheric Boundary Layer with High Precision and Accuracy." *Environ. Sci. & Tech.* 38, (**2004**): 3683-3688.

Chapter 3

The Delineation of and a Proposed Mechanism for Water Vapor Interference in UV-Based Ozone Monitors

3.1 Humidity Interference Theory

Based upon the preliminary experiments presented in Chapter 2 of this thesis, it was postulated that the cause of the water vapor interference exhibited by the various ozone monitors centered upon the interactions of water with the surface of the absorption cell's walls. The reasoning behind this hypothesis was as follows: 1) Based on the design of these instruments, only the cell and/or the scrubber could lead to the observed offsets. 2) The humidity offset was apparent even when ozone was not present in the system – signifying that water was not affecting the ozone scrubber's efficiency since no ozone existed in the first place. 3) There were opposite offsets observed depending upon manufacturer for identical experiments – it was assumed from the literature that each instrument utilized the same ozone destroying catalyst leaving the cell as the only other unknown capable of causing the reversed signals in the different ozone monitors. 4) It was known that at least two of the manufacturers have different coatings on their cell walls – these different coatings might account for the observed opposite-sign signals.

Our hypothesis also was based on the observation that it was the *change* in water in the cell that led to the observed offsets in ozone readings. We supposed the ozone scrubber helped modulate the water on the cell walls by acting as a reservoir to either dry or humidify the air stream. As shown in *Figure 3.1* the ozone scrubber contains a catalytic material having a large surface area capable of being moistened

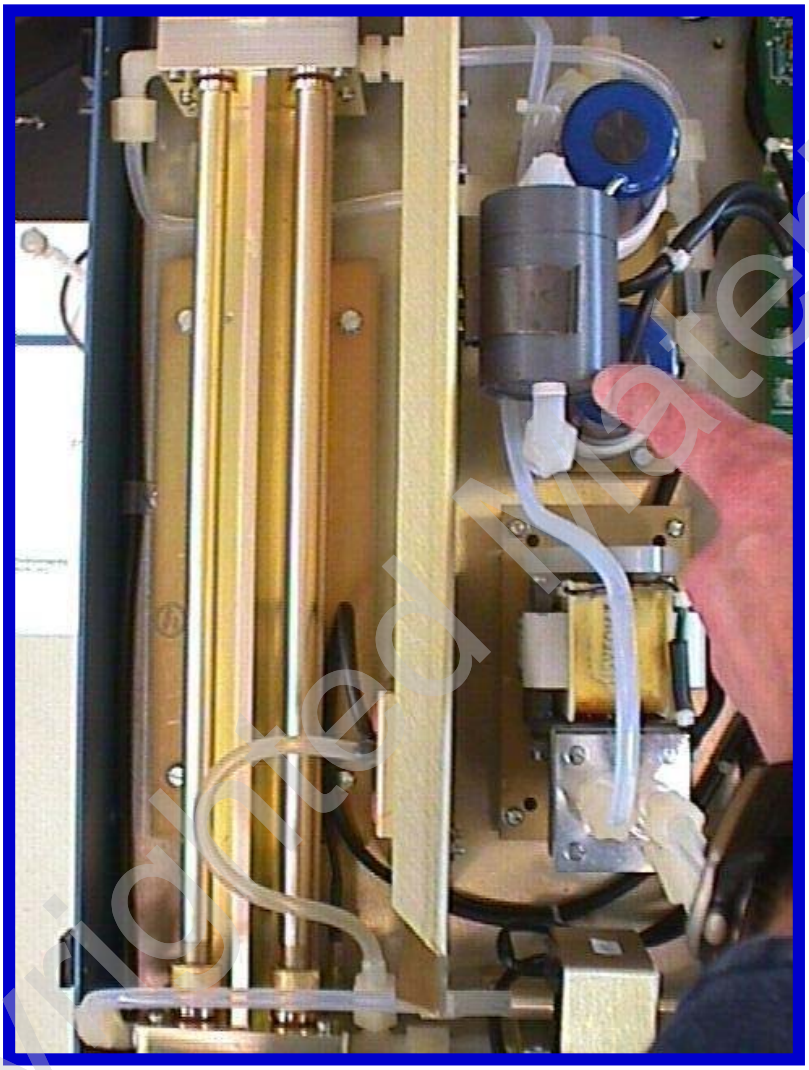

Fig. 3.1 Upper case removed from TEI Model 49 ozone monitor. Grey colored, cylinder-shaped scrubber indicated. Approximate scrubber canister dimensions as follows: 8 cm high, 4.5 cm diameter, 125 cm^3 internal volume, with 550 cm^2 of geometric surface area.

or dried depending on whether a wet or dry air stream passed, respectively, through it. For example, if an instrument were exposed to dry air for an extended time period, the ozone scrubber material would slowly dry out. If the air stream were later humidified then the scrubber material would act as a dry reservoir capable of removing humidity from the moist air stream as it passed through the scrubber. This would result in relatively dry air passing through the cell when the solenoid switches to the scrubber and more humid air when the solenoid switches to the by-pass side. In essence, the solenoid provides a means to quickly modulate the relative humidity in the cell as it switches back and forth between scrubbed and unscrubbed air. The converse of the example described above where the scrubber acts as a moist reservoir also can be imagined. In either case, rapid changes in humidity would lead to modulation of water vapor in the cell as it switches between I and I_0 readings.

In order to check our hypothesis and as a starting point to begin unraveling the convoluted nature of the water vapor interaction, it was decided to replicate the humidity experiments described in Chapter 2, but this time employing a systematic approach to reduce water's variability within the cell. These experiments centered upon the 2B Tech ozone monitor as it was currently under development and provided the most favorable platform to modify.

3.2 Factors Affecting the Water Vapor Interference: Scrubber Surface Area

If the scrubber's surface area did indeed aid in modulating water vapor then a decrease in the amount of catalyst material should result in a reduction of the observed water interference. *Figure 3.2* shows the original prototype scrubber found

Fig. 3.2 2B Technologies original, large ozone scrubber, its smaller replacement, and U.S. quarter for comparison. 1) Larger-sized scrubber dimensions as follows: 7 cm high, 1.7 cm diameter, 16 cm^3 internal volume, with 185 cm^2 of geometric surface area. 2) Smaller-sized scrubber dimensions as follows: 1 cm high, 0.3 cm diameter, 0.07 cm^3 internal volume, with 1.5 cm^2 of geometric surface area.

in the 2B Technologies' ozone monitor and its replacement. The original (larger) scrubber contains an excess of catalyst material providing a much larger surface area to either dry or moisten the air passing through it as water is either adsorbed or desorbed from its surface.

A replication of the humidity experiments discussed in Chapter 2 was carried out and the results are shown in *Figure 3.3*. A humidity generator was again used to create a 90% R.H. zero air stream and the 2B Technologies ozone monitor was quickly cycled between dry and moist zero air containing no ozone molecules. As discussed in Chapter 2, the 2B Technologies ozone monitor showed the maximum change when going from dry to moist air, and for this reason it was decided to focus the following figures on only that portion of the curve. *Figure 3.3* shows an approximate 33% reduction (from ≈ 600 to 400 ppbv) in apparent ozone deviation as a result of decreasing the ozone scrubber surface area. As seen in the earlier experiment, the modified instrument, with the smaller scrubber, does not ever fully recover to zero within the 40 minutes monitored following the humidity change, but unlike the unmodified instrument both its decay and plateau of ≈ 80 ppbv ozone equivalent is reached more quickly at ≈ 15 minutes.

Consistent with our hypothesis, this can be explained as being due to the reduced catalyst surface area of the smaller scrubber more quickly becoming equilibrated with the 90% R.H. air, thus allowing the cell's humidity level to more quickly equilibrate between I and I_0 readings. Even though the scrubber surface area was decreased by ≈ 99% , the magnitude of the humidity affect only decreased by a third. It should be noted that nothing further could be gained by decreasing the

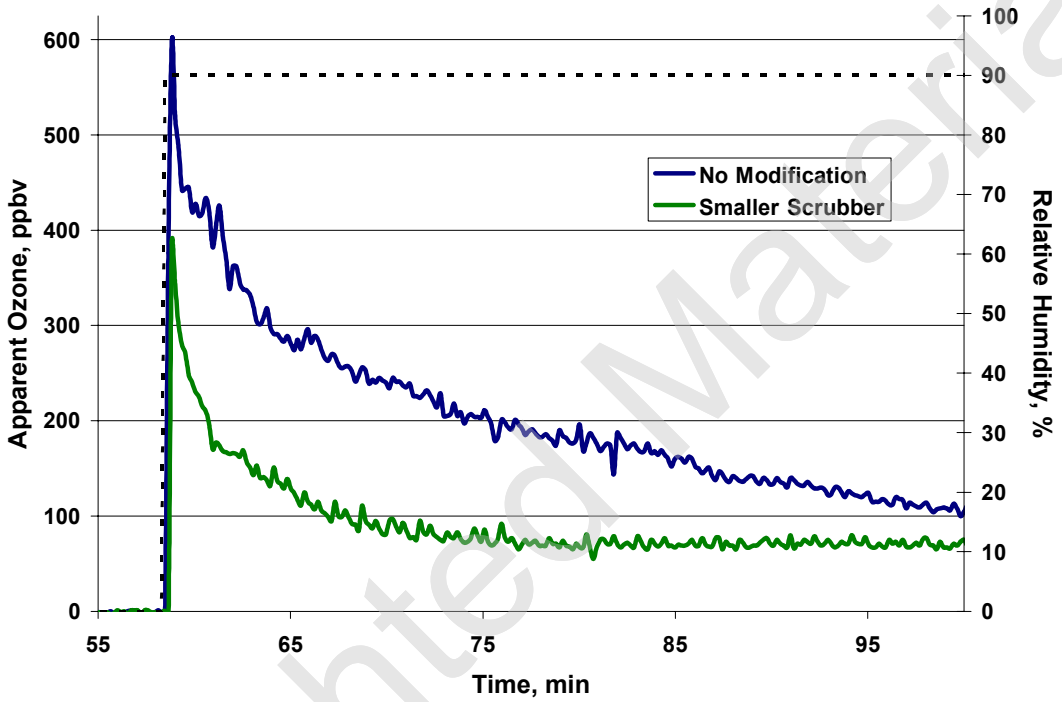

Fig. 3.3 Diminished water vapor effect on apparent ozone reading for the 2B Tech Ozone Monitor resulting from changes in the relative humidity of zero air as a result of a decrease in ozone scrubber size.

number of active sites on the scrubber surface since this reduction would be below the critical amount needed for 100% destruction of ozone at ambient levels. Although this finding agrees with our hypothesis by showing that the scrubber does indeed play a role, the minimal physical limitation of the scrubber size has been reached without any indication of how water vapor itself interacts in the cell. For these reasons, subsequent steps to reduce the water effect focused on the cell itself.

3.3 Factors Affecting the Water Vapor Interference: Optics Cell Composition

The first of these experiments involved the chemical composition of the cell. Given that water vapor itself cannot directly absorb 254 nm light, it was postulated that water must be depositing on the cell's surface and somehow affecting the ozone monitor. If this were true, the cell surface could be changed to make it less hydrophilic, thus decreasing the apparent ozone offset. Although the 2B Tech instrument's cell windows are composed of fused quartz, in order to pass 254 nm light, the original cell walls were composed of less expensive borosilicate glass. Borosilicate glass substitutes boron oxide particles in place of some of the alkali oxides (most commonly sodium and potassium) found in soft glass. Although borosilicate glass, commonly sold under the trade name Pyrex®, has fewer impurities as contrasted to soft glass, its residual alkali salts still provide many hydrophilic surface sites for water absorption. Fused quartz, however, is a highly pure form of silicon dioxide with a low occurrence of impurities. For instance, General Electric™ states its fused quartz as having "a nominal purity of 99.995 weight % SiO_2" and "less than 50 ppmw total elemental impurities" (General Electric Inc., 2002). If the

relative amount of cell impurities does affect the ozone offset then the use of a 'cleaner' fused quartz cell should result in a decrease of the offset.

To test this hypothesis, the instrument with the smaller ozone scrubber was further modified by replacing the borosilicate cell with a fused quartz cell and the experiment replicated. *Figure 3.4* illustrates an additional 60% reduction (from ≈ 400 to 160 ppbv) in apparent ozone deviation as a result of the change in cell material. For comparison, the result for the unmodified design also is shown. As seen in the earlier experiment, the modified instrument with the fused quartz cell does not ever fully recover to zero in the period shown following the humidity change. The fused quartz cell also results in a 5 minute quicker decay, which plateaus at half the value (≈ 40 ppbv ozone after only ≈ 10 minutes time). These findings help confirm our hypothesis concerning an interaction of water on the cell surface, since a decrease in the number of water absorption sites directly decreases the ozone offset.

3.4 Factors Affecting the Water Vapor Interference: Optics Cell Temperature

Although these results were promising, the apparent ozone artifact remains and further steps were needed to further reduce it. Since the previous experiment appeared to show a direct relationship between water absorption and the spurious ozone reading, it was decided to elevate the cell temperature above ambient in order to reduce water absorption onto the cell surface. The cell was wrapped in a copper sheeting to increase the heat transfer rate and to create a thermal mass to stabilize the cell's temperature. To this was attached the 2B Tech ozone monitor's 5 volt lamp voltage regulator as well as an additional 100 Ω resistor. Note that the cell could not

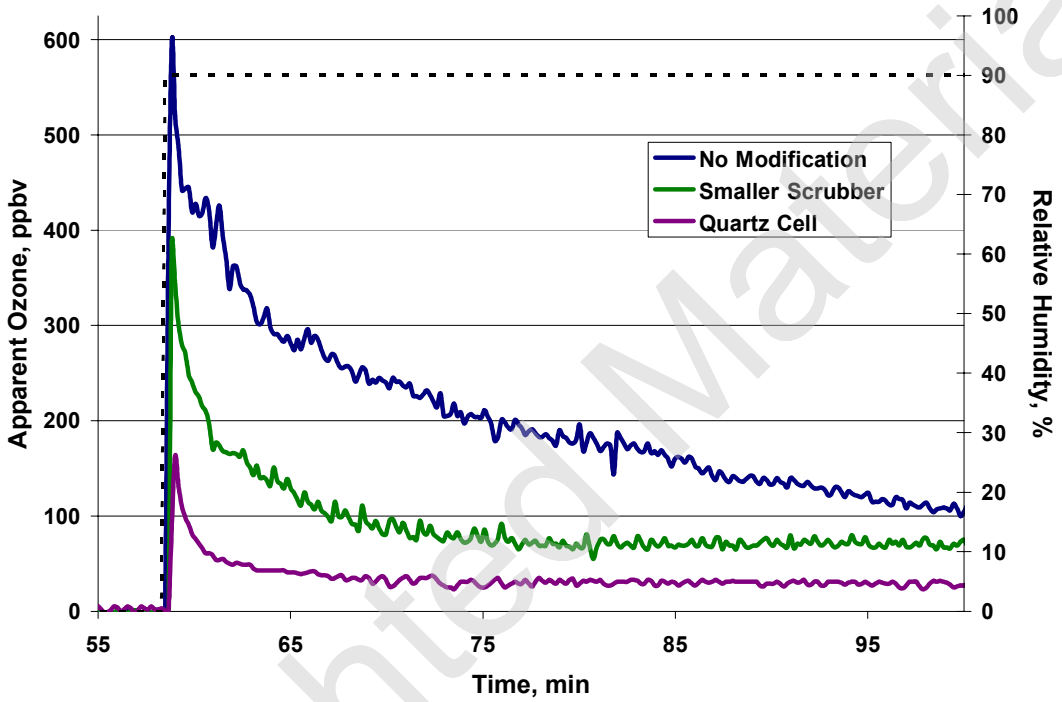

Fig. 3.4 Diminished water vapor effect on apparent ozone reading for the 2B Tech Ozone Monitor resulting from step changes in the relative humidity of zero air as a result of the following additive changes: 1) decrease in ozone scrubber size, and 2) switching from a borosilicate to a fused quartz cell.

be made any warmer without drastically increasing the power consumption of the O_3 monitors. The waste heat from the regulator and resistor heated the copper sheeting, raising the cell temperature to approximately 33°C or ≅10°C above the ambient lab temperature.

Figure 3.5 reveals an additional 50% reduction (from ≈ 160 to 80 ppbv) in apparent ozone deviation as a result of heating the cell. As before, the earlier results are also shown for sake of comparison. As seen in the earlier experiment, the modified instrument with the heated cell does not ever fully recover to zero in the period shown following the humidity change. The instrument with the heated cell has a similar decay rate (≈ 10 minutes) to the previous results, but unlike before the apparent ozone reading plateaus at ≈ 15 ppbv ozone. These findings further support our hypothesis concerning an interaction of water on the cell surface, given that an increase in temperature, which is expected to decrease the coverage of water on the cell surface, directly decreases the ozone offset.

3.5 Factors Affecting the Water Vapor Interference: Optics Cell Cleanliness

In order to further test our hypothesis concerning water's interaction with the cell surface it was decided to remove any adsorbed chemicals or particulate matter from the cell surface through cleaning. Any chemicals and/or particles present would provide additional hydrophilic sites to which water could adsorb. The cell was flushed with HPLC grade methanol and dried with air, and a replicate of the above experiment run again. The results are shown in *Figure 3.6*. At this scale, the water vapor effect appears to completely vanish as a result of the cleaning; however, as seen

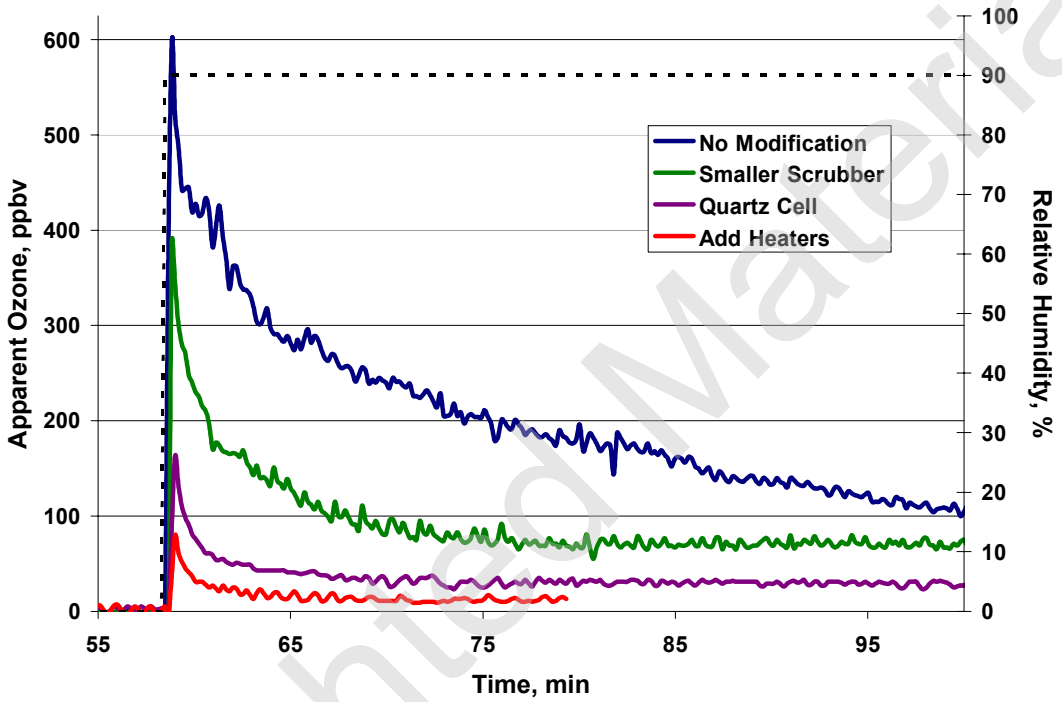

Fig. 3.5 Diminished water vapor effect on apparent ozone reading for the 2B Tech Ozone Monitor resulting from step changes in the relative humidity of zero air as a result of the following additive changes: 1) decrease in ozone scrubber size, 2) switching from a borosilicate to a fused quartz cell, and 3) increasing the cell temperature with heaters.

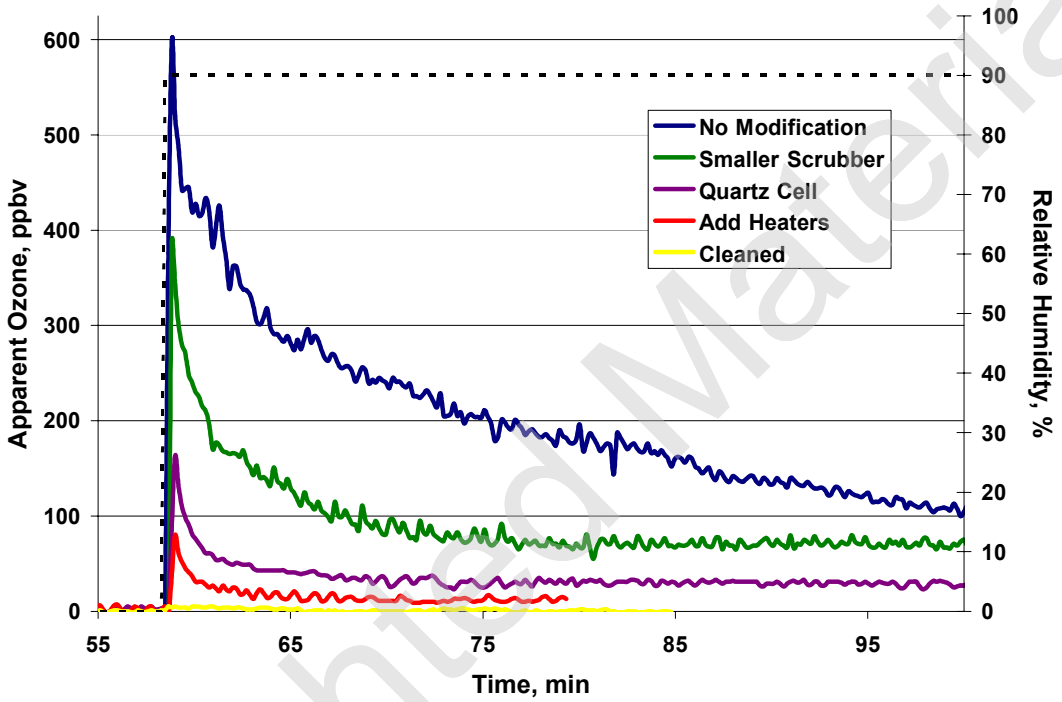

Fig. 3.6 Diminished water vapor effect on apparent ozone reading for the 2B Tech Ozone Monitor resulting from step changes in the relative humidity of zero air as a result of the following additive changes: 1) decrease in ozone scrubber size, 2) switching from a borosilicate to a fused quartz cell, 3) increasing the cell temperature with heaters, and 4) cleaning the cell.

in *Figure 3.7* a small effect is still present. Although the offset is quite small (only 5 ppbv ozone), the decay rate still takes ≈ 10 minutes to recover while the ozone monitor's readings remain much noisier than usual as a result of the sudden change in humidity. At this point it appeared that the humidity effect was reduced to a level, which might be sufficient for sampling hourly averages of ozone, but this impression was short-lived. Within two hours of sampling ambient air, the 2B Tech Ozone Monitor returned to the previous state shown in *Figure 3.5* as its cell became 'polluted' from particulates and aerosols in ambient air. It should be noted that cleaning with methanol also helped both TEI instruments but their cells fouled in a shorter 20-minute period of sampling. These findings again supported our hypothesis concerning an interaction of water on the cell surface given that a decrease in the adsorption sites for water to the cell surface directly reduces the apparent ozone offset.

3.6 Factors Affecting the Water Vapor Interference: O_3 Scrubber Material

Since neither continuous cleaning of an instrument nor changing of the optics bench were a viable option for the 2B Tech monitor it was decided to refocus efforts on the catalyst material found in the scrubber as a means to remove the humidity interference. This material is hopcalite. Hopcalite is a mixture of catalytic manganese dioxide, copper oxide, and a small amount of silver oxide ($Cu_xMn_yO_z$, where the ratio of x:y is most commonly 3:7). Hopcalite was developed during WWI by the War Department's newly founded Defense Chemical Research Section for use in gas masks in gun turrets and below deck locations of ships where

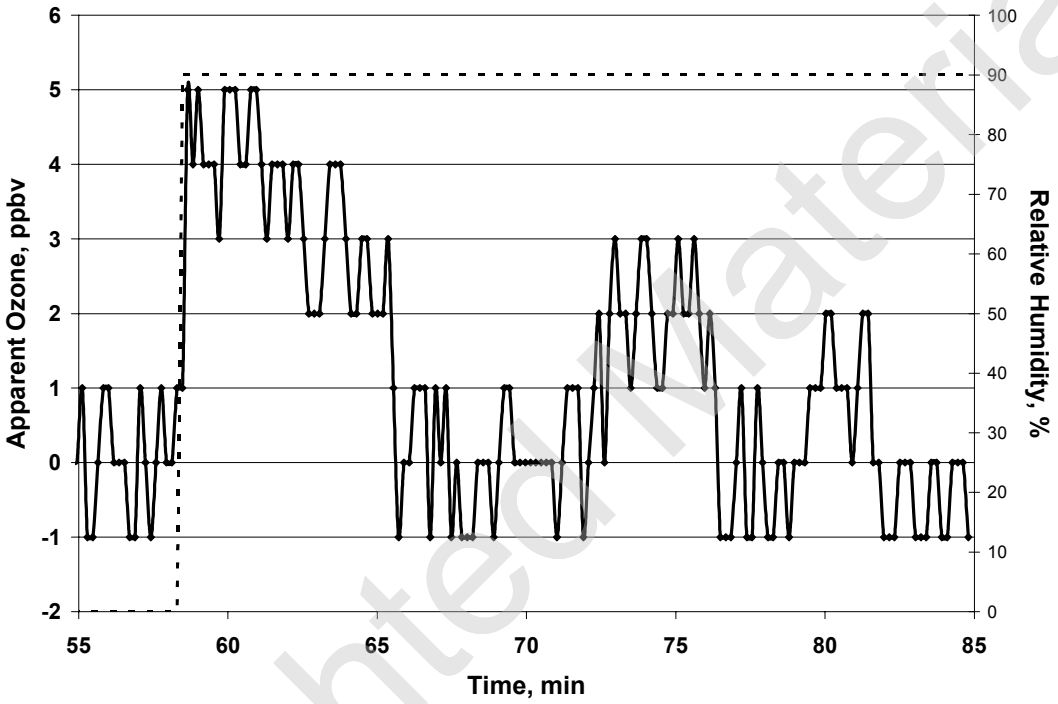

Fig. 3.7 Expanded view of the "Cleaned" yellow line from Figure 3.6.

carbon monoxide concentrations were a concern, as hopcalite effectively catalyzes the oxidation of CO (Bliss, 1955). In addition to its use as an ozone scrubber in ozone monitors, hopcalite currently is used in chemical traps of exhaust pumps, mercury vapor sampling systems, carbon monoxide detectors, and even high-end scuba gear for CO scrubbing.

The hopcalite used in the earlier experiments was provided by Supelco and taken from their line of gas desorption tubes. Since neither the exact ratio of the metal oxides is disclosed by the manufacture nor is the true oxidation state of the Cu and Ag oxides known, we adopted the Edisonian approach of trying a variety of catalysts to discover whether any were more effective at ozone destruction than the Supelco hopcalite. If any were, it was assumed we could decrease the amount of scrubber material in order to minimize the humidity effect. *Figure 3.8* shows a sampling of this effort. While there was a pronounced humidity effect due to the ≈ 26 cm^2 of geometric surface area of each material used, one catalyst, the Süd-Chemie Black, was found to have the desired trait of being less friable than the others. For this reason it was used in the 2B Tech ozone monitors for a period of time. (Currently, the 2B Tech instruments make use of a proprietary extruded alumina impregnated with a hopcalite-type material. However, this material also has a high affinity for water.) The results for tests of a variety of commercially available ozone-destruction catalysts convinced us that it was not probable that additional work with the scrubber material would result in a reduction of the water vapor interference. For this reason, focus returned to the ozone monitor's cell in hope of better understanding the phenomenon.

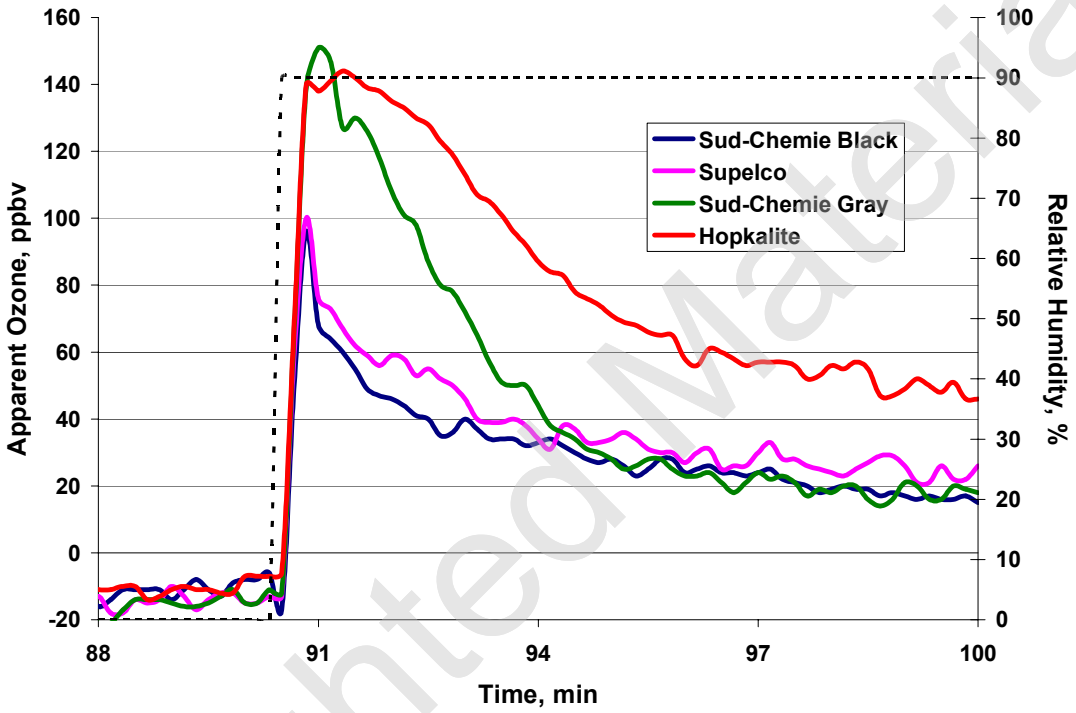

Fig. 3.8 Water vapor effect on apparent ozone reading for various catalysts in 2B Tech Ozone Monitor resulting from changes in the relative humidity of zero air. *Note there is ≈ 26 cm^2 of geometric surface area of each catalyst.*

3.7 Relative Humidity and Water Layer Formation on Quartz Surfaces

Although our experiments clearly showed that the scrubber modulates water vapor in the cell and that the cell surface composition and temperature play a role in the humidity effect, the physical phenomena occurring on the cell surface had not been delineated. First, is it possible to have a dry and then wet layer on the cell surface or is there always a thin layer of water on the surface that only thickens as the humidity level increases? This question was answered by Dana Sedin's work in the Rowlen lab at the University of Colorado. This work centered on adhesion forces experienced by an AFM tip as a result of a capillary bridge of liquid water formed between the surface and the AFM tip. The work, as seen in *Figure 3.9*, clearly shows a dependency on humidity and the pull-off force needed to free a SiO_2 AFM tip from the surfaces of mica and quartz. Below the transition point of ≈ 24% relative humidity there is "insufficient water on the surface to allow for capillary condensation" (Sedin et al., 2000). Above this transition point there is a "tip-surface interaction force" equal to "the sum of the … force in liquid water and the capillary force" (Sedin et al., 2000). This work went on to model the interfacial free energy force the SiO_2 tip would experience on quartz in the presence of water vapor (low RH) and in a liquid water layer (high RH) and found it to be in close agreement with the measured results shown in *Figure 3.9*. These findings verify that there exist two water regimes on the cell's quartz surface, which vary as a function of relative humidity. The fluctuation in this water layer can be modeled and the results compared to the data as a way of explaining the opposite effects observed in the TEI and 2B Tech instruments.

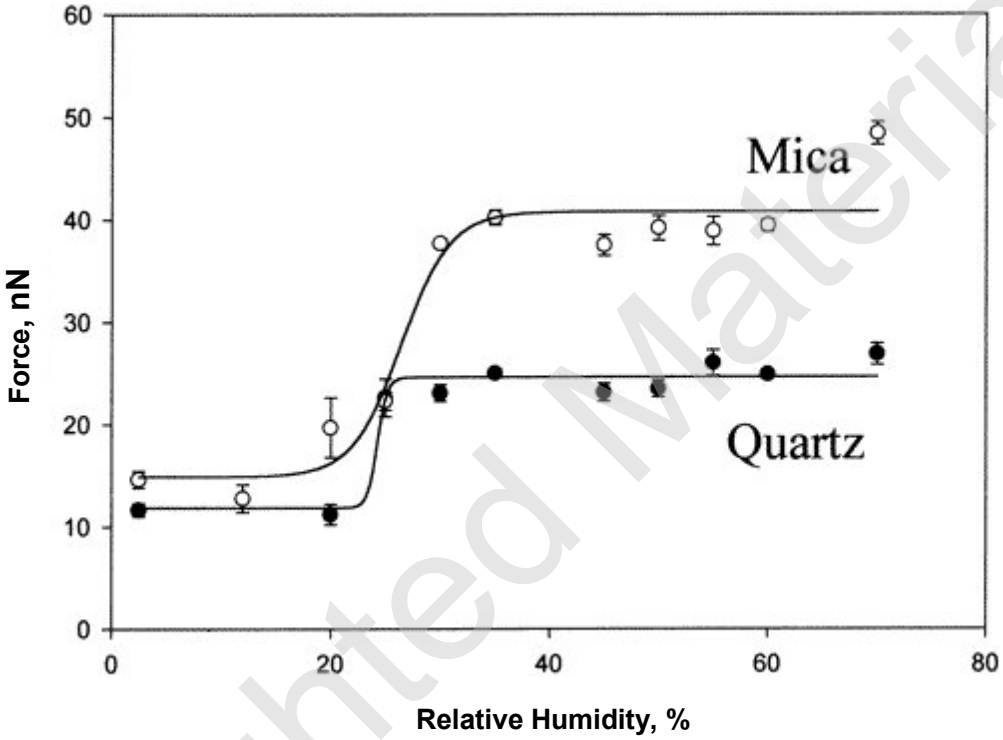

Fig. 3.9 Increase in measured pull-off force as a function of relative humidity. Note capillary bridge forms between SiO_2 AFM tip above the transition point, ≥ 24% R.H. Adapted from Sedin and Rowlen (2000).

3.8 Proposed Model of Light Interaction with Cell's Surface

As a starting point in discussing the complicated interaction of uncollimated light during its passage through the absorption cell, it is useful to consider the various physical phenomena which occur inside the cell: These include the degree of *refraction* and varying *reflection* and *transmission* rates at an interface between two different media, *total internal reflection*, where certain angles of light are trapped in a medium, and finally *absorption* and *scattering* at a surface. *Figure 3.10* reveals patterns, which differ substantially to the naked eye, created by light reflecting through the optical cells of the two instruments - with the TEI cell appearing to have a finer structure than the 2B Tech monitor.

As earlier shown in *Figure 2.6*, the TEI Model 49 instrument experiences a negative offset when switching from dry to humid zero air. Another way of envisioning this is that the scrubber acts to relatively dry the scrubbed gas stream, I_o, as compared to the wetter, I, bypass gas stream. From the Beer-Lambert law, a negative absorbance or concentration offset should result when I_o is smaller than I. This means that a physical phenomenon must exist which results in *less* light at the TEI detector whenever it sends relatively drier air from the scrubber into the cell.

Conversely, the 2B Tech monitor experiences a positive offset (*Figure 3.4*) when switching from dry to humid air. Again, the scrubber acts to dry the scrubbed gas stream for I_o measurements as compared to the wetter bypass gas stream for which intensity I is measured. From the Beer-Lambert law, a positive absorbance or concentration offset should result when I is smaller than I_o. This means that a physical phenomenon which results in *more* light at the 2B Tech detector must exist

Fig. 3.10 Visible light pattern differences between optics cell of TEI Model 49 (shown in top frame) and 2B Tech (bottom frame).

whenever it sends relatively drier air from the scrubber into the cell. *Figure 3.11* clearly illustrates both instruments' effects.

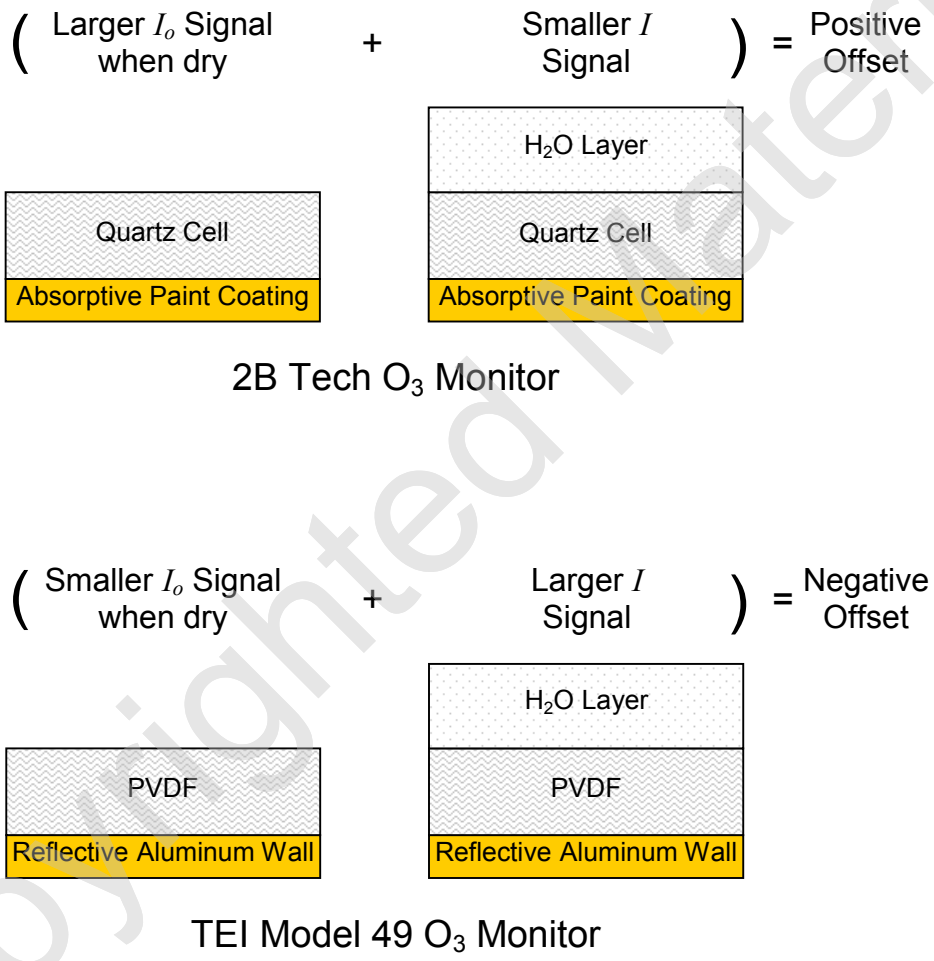

Fig. 3.11 Overview of events leading to apparent ozone offsets in both 2B Tech and TEI Model 49 ozone monitors when switching from dry to humid air. PVDF = polyvinylindine fluoride.

First let us explore reflection losses in each instrument. Normal reflection coefficients, R, are easily calculated from indices of refraction* of the two media in which the light is traveling. For example, the air/quartz interface found in the 2B Tech monitor is calculated as follows:

$$R = \left(\frac{n_{quartz} - n_{air}}{n_{quartz} + n_{air}} \right)^2 , \text{where } n_{quartz} = 1.459, n_{air} = 1.000 \qquad (1)$$

$$R = 0.0348 \text{ or } \approx 3.5\% \qquad (2)$$

This points out that the majority of light, in this case 96.5%, is transmitted into medium of higher index of refraction. Table 3.1, compares the reflectivity and transmission rates for both the wet and dry interfaces found in the two instruments.

Interface	% Reflection	% Transmission
2B Tech air/quartz	3.5	96.5
2B Tech air/water	2.0	98.0
2B Tech water/quartz	0.2	99.8
TEI air/PVDF	3.0	97.0
TEI air/water	2.0	98.0
TEI water/PVDF	0.1	99.9

Table 3.1 Reflection at various interfaces in 2B Tech and TEI ozone monitors illustrating that the vast majority of light is ultimately transmitted into the quartz or PVDF media, respectively. (Multiple internal reflections are not taken into account since their contributions are proportional to the square and higher powers of the reflection coefficient.)

***** *Please note that the more common indices of refraction based on the weighted mean (589.26 nm) of the yellow sodium doublet lines are utilized in all subsequent calculations since the indices of refraction at 253.7 nm are not known for all media. (Although the sodium-D indices are slightly smaller than those of the UV-wavelengths this will not affect the validity of the relative, qualitative trends and theory presented in the following sections.)*

What is immediately evident from the preceding data table is that direct reflection off either the cell wall or water layer occurs only to a small extent and that a dry cell reflects more light to the detector than a wet one. These findings are in agreement with the 2B Tech data where we find that a dry cell during an I_o measurement results in a positive offset. However, the table is not in agreement with the recorded negative offset present in the TEI monitor where there is greater light intensity whenever the optics cell is humidified during *I* measurements. These findings give the first insight into the observed difference between the two instruments by demonstrating that directly reflected light must makes up proportionally more of the detected signal in the 2B Tech instrument than in the TEI instrument. It is further inferred that proportionally more of the transmitted light which has entered the water/polyvinylindine fluoride (PVDF) layers in the TEI monitor escapes to propagate onward to its detector than does the light transmitted into the water/quartz layers of the 2B Tech monitor.

3.9 Physical Variations in Optics Affect Light Interactions

There are physical differences between the two instruments, which can account for the transmitted light providing a larger portion of the measured signal intensity in the TEI Model 49 than in the 2B Tech monitor. The primary distinction is the material, which makes up the cell walls in each instrument. As represented in *Figure 3.11*, the TEI monitor's optics cell is a shiny metal tube which reflects much more of the transmitted light than the highly absorptive matte black paint layer coating the optics cell of the 2B Tech Ozone Monitor. Due to this considerable loss

of transmitted light in the 2B Tech monitor, the initially reflected portion imparts the majority of the detected signal and explains why this instrument experiences less observed signal when wet as this water layer decreases reflectivity from 3.5% to 2.0% (Figure 3.12). It is further hypothesized that the different phenomenon of Total Internal Reflection (TIR) must take place in the TEI monitor since it experiences the opposite result of a larger signal when wet.

TIR is the reflection of all incident light at the boundary between two surfaces and only occurs when the following two conditions are met: 1) the light is in the more dense medium and approaching the less dense medium and 2) the angle of incidence is greater than the critical angle, Θ_c. As shown in *Figure 3.13*, the cell of the TEI Model 49 is coated with polyvinylindine fluoride (PVDF) or Kynar®. PVDR is a translucent material with an index of refraction of 1.42. As modeled in the examples "A" and "B" the majority of the light, 98% and 97% respectively, is transmitted into the cell coating where it can reflect and scatter at each interface. If the incident angle of this scattered and reflected light is $\geq \Theta_c$ then the light becomes trapped in the PVDF layer as TIR occurs. Θ_c are calculated as follows. For example Θ_{c1}:

$$n_1 \sin\theta_{c1} = n_2 \sin 90^\circ, \text{ where } n_1 = n_{PVDF} = 1.42,\ n_2 = n_{H20} = 1.33 \quad (3)$$

$$1.42 \bullet \sin\theta_c = 1.33 \bullet \sin 90^\circ \quad (4)$$

$$\theta_c \approx 69.5^\circ \quad (5)$$

In the TEI Model 49, when there is an absence of water on top of the PVDF coating the critical angle for the PVDF/air interface is 44.8° whereas with a water layer the

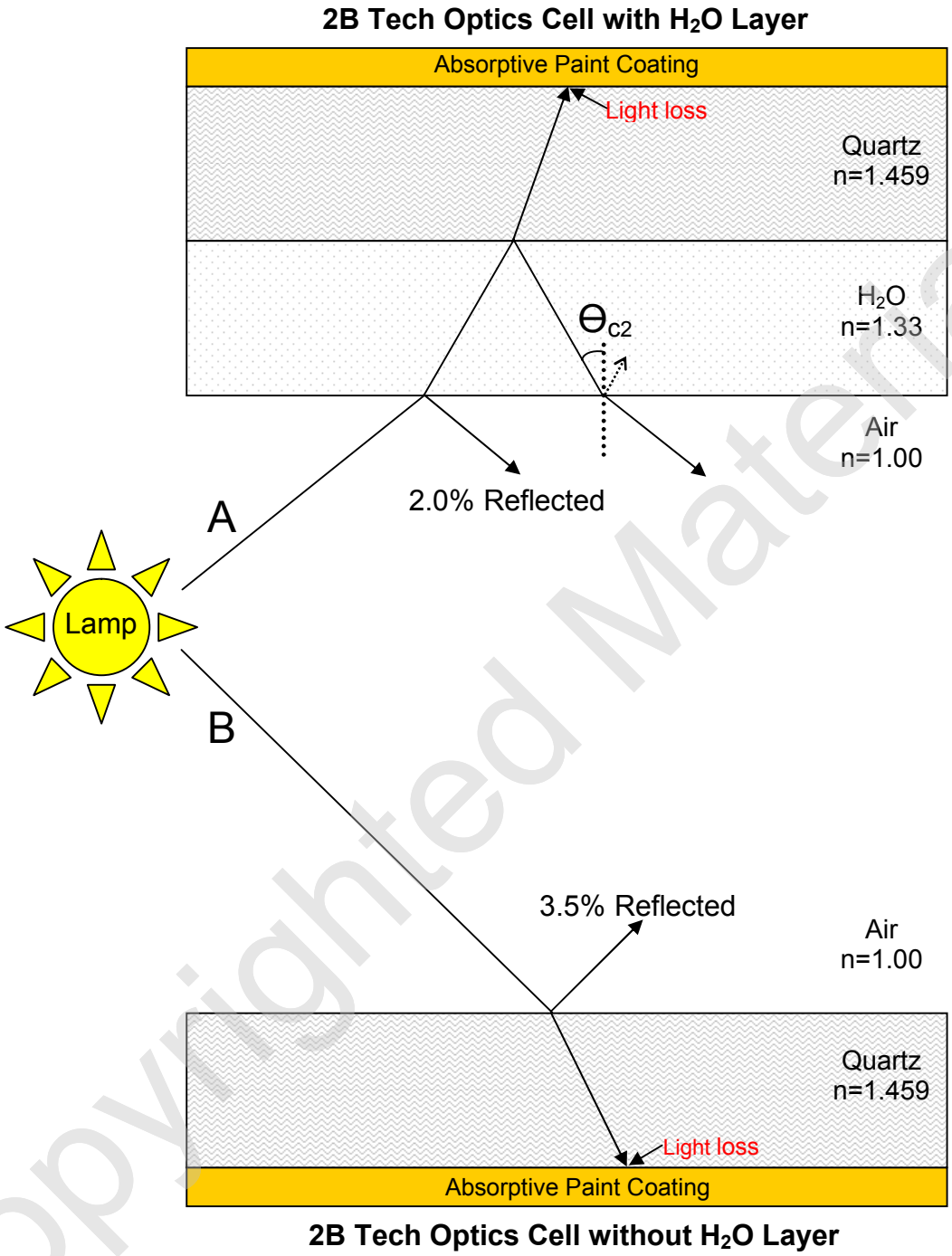

Fig. 3.12 Representation of light paths in 2B Tech optics cell. Example "A" propagates less light to the detector than "B" as a direct result of water being less reflective than dry quartz (2.0% versus 3.5%). TIR does not play a role in the 2B Tech optics cell as light transmitted into the water and quartz layers is not reflected by the painted quartz surface.

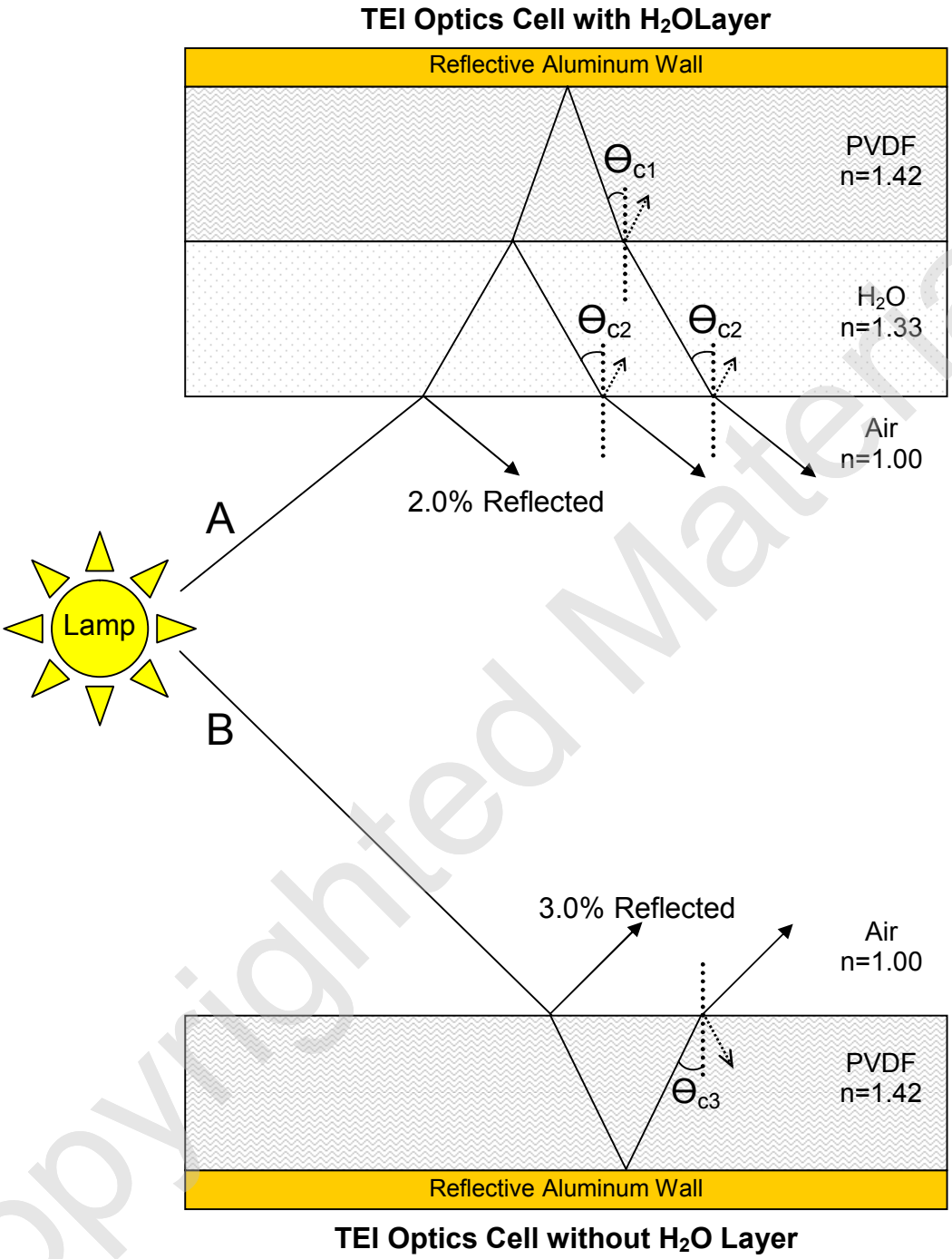

Fig. 3.13 Representation of light paths in TEI Model 49 optics cell. Example "A" propagates more light to the detector than "B" even though "B" initially reflects more light. The water layer allows more light to escape the coating by better matching the index of refraction of the PVDF layer thus relatively decreasing the amount of total internal reflection versus the PVDF/air interface. Dotted arrows denote trapped light from incidence angles $\geq \Theta_c$ for each interface. $\Theta_{c1} = 69.5°$, $\Theta_{c2} = 48.8°$, $\Theta_{c3} = 44.8°$

critical angle is 69.5° for the PVDF-water interface. The net result is that more of the light (24.7° more) transmitted into the PVDF layer and subsequently reflected off the shiny cell wall can escape from this PVDF layer when there is water coating it. Since the majority (> 97 %) of the light in the cell was transmitted into the water and PVDF layers anything that helps it escape would boost the detected intensity of the measured I signal, overwhelming the initial I_o measurement and result in a negative humidity offset. The water layer does this by decreasing the amount of light lost to the detector through TIR by better matching the index of refraction of the PVDF layer versus the PVDF/air interface. As a result, more of the transmitted light "escapes" the PVDF layer when the optics cell is humid thereby dominating the proportionally smaller initially reflected light signal. Furthermore, this explanation fits the observed negative offset present in the TEI Model 49 data when switching from dry to humid air.

3.10 Conclusions

The humidity effect is a function of adsorbed water on the cell walls and varies due to the ozone scrubber which acts as reservoir to either dry or moisten scrubbed air (I_o) depending on instrument history. Consistent with this proposed mechanism, a number of factors, such as a reduction in the scrubber size and cell's affinity for H_2O, were found to reduce but not eliminate the water vapor interference. A model of refraction, reflection, and TIR qualitatively explains the observed opposite humidity effects present in the 2B Tech and TEI instruments under the same experimental conditions. Due to its painted surface, reflected light

dominates the signal in the 2B Tech monitor whether humid or dry. Whereas reflected light only dominates the signal in the TEI monitor when the optics cell is dry. Conversely, an increase in transmitted light intensity is observed in the TEI monitor when the optics cell is humid as a result of a decrease in TIR when a water layer is present. Collimation of the light so that it never reaches the cell surface would solve the water vapor interference problem, but this requires prohibitively expensive optics and a more powerful light source. Furthermore, lasers in the UV currently do not exist without the expense and complexity of frequency doubling. A more practical approach, for use in inexpensive, lightweight, low power instruments to equilibrate the humidity of ozone-scrubbed and unscrubbed air, is discussed in Chapter 5.

Chapter 3 – References

Bliss, A.B. "Arthur Beckett Lamb." *JAC*, 77 (**1955**): 5773-5780.

General Electric Inc. "Chemical Composition." Accessed 10th April **2005**. <http://www.gequartz.com/en/chemical.htm> (**2002**).

Sedin, D.L. and K.L. Rowlen. "Adhesion Forces Measured by Atomic Force Microscopy in Humid Air." *Anal. Chem.* 72 (**2000**): 2183-2189.

Chapter 4

Use of TiO_2 Photocatalysts in Reducing Water Vapor Interference to Negligible Levels

4.1 Focus Upon Titanium Dioxide Reactors

As shown in the previous chapter, a means to minimize the difference in humidity of ozone-scrubbed and unscrubbed air is needed to resolve the water vapor interference problem. Various catalyst beds made up of small particles were shown to contribute to the water interference due to their large surface areas which are capable of desorbing and adsorbing water to and from the air stream. As a result, it was decided to focus upon an ozone destroying method with very little surface area as compared to that found in the aforementioned particle-bed reactors. A basic model of this plan is a length of hollow tube capable of destroying ozone. A search of the literature quickly focused upon the utilization of photocatalytic reactors, composed of titanium dioxide (TiO_2) surfaces immobilized on glass or metal tubes with ultraviolet light excitation, as the most likely method capable of both efficiently destroying ozone while introducing relatively little surface area to the ozone scrubber.

TiO_2 was chosen because it is nearly the perfect semiconductor photocatalyst. It is chemically and biologically inert, stable and regenerative, inexpensive, nontoxic, easy to produce, and capable of quickly catalyzing reactions; not being activated by visible light is its only major shortcoming. Although the field of TiO_2-photocatalytic chemistry originated in 1972, with the water splitting experiments of Fujishima and Honda, it did not experience true growth (*Figure 4.1*) until the early 1990's. At that time, research began to focus upon the remediation of both gas and water streams

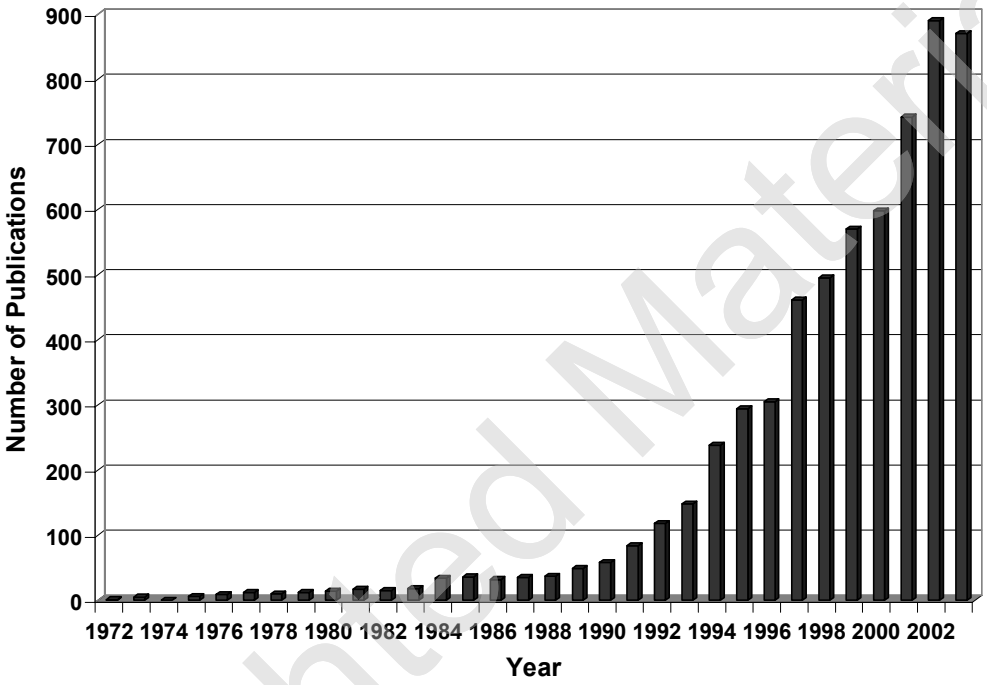

Fig. 4.1 Number of publications concerning TiO_2 photocatalyst per year. Adapted from Blake (2001) and Carp et al. (2004).

through the photocatalytic-degradation of various organics including viruses, bacteria, fungi, algae, and VOCs (Blake, 2001 and Carp et al., 2004). Other photoactivated TiO_2 research areas include self-cleaning, superhydrophilic surfaces (Wang et al., 1998), organic synthesis (Worsley et al., 1995), photoconversion of metals (Skubal and Meshkov, 2002), and most importantly for this thesis, sensitized decomposition of ozone (Gonzàlez-Elipe et al., 1981).

4.2 Band Theory of Solids

As opposed to the discrete energy states and isolated orbitals present in an individual atom, the outermost electrons of atoms present in a crystalline solid are not confined to or associated with any particular atom in the solid and can experience intermittent potential shifts. The possible energies of these electrons are, therefore, free to form a valence band (V.B.) composed of a sea of overlapping orbitals in the solid. Higher energy, unoccupied outer orbitals also overlap to form a conduction band (C.B.) which is separated from the valence band by a band gap (E_g). This band structure (band theory) is indispensable in explaining the properties of solids as it provides a useful way to visualize (*Figure 4.2*) the difference between conductors, insulators, and semiconductors such as TiO_2. Unlike conductors, where the V.B. overlaps the C.B., and insulators, where the electrons in the V.B. are separated by an insurmountable gap from the C.B., a semiconductor has a band gap small enough that thermal or other excitations (such as a photon) can promote an electron from the V.B. across the gap and into the C.B..

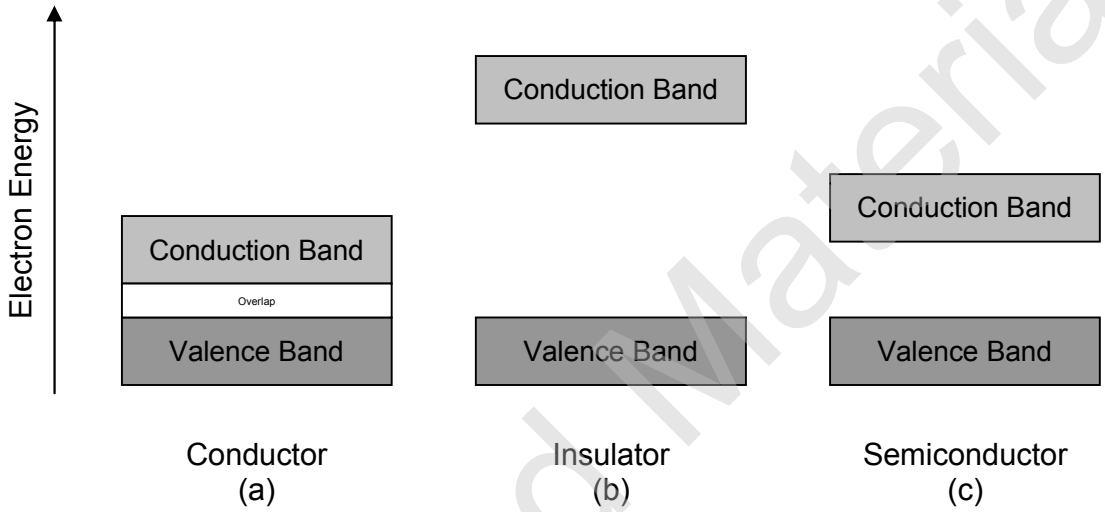

Fig. 4.2 Energy Bands in Solids: a) overlap of valence band (V.B.) and conduction band (C.B.) electron energies provides conduction charge carriers, b) large, forbidden gap between V.B. electron energies and C.B., and c) intermediate band gap of semiconductor which confers possibility of promoting some electrons from the V.B. to the C.B.

4.3 Semiconductor Photoexcitation

Unlike traditional catalytic processes which occur at elevated temperatures, photocatalysis readily takes place at ambient conditions since photonic excitation is employed in lieu of thermal energy. As shown in *Figure 4.3A*, titanium dioxide is a semiconductor photocatalyst with a band gap energy of 3.2 eV. When irradiated with super-band gap photons of less than 385 nm, the band gap transitional energy is exceeded and an electron is promoted from the V.B. to the C.B.. This charge separation creates an electron/hole pair with an adequately long lifetime available such that it can diffuse to the catalyst's surface where it initiates redox reactions with surface-bound reactants. This is possible because, unlike a conductor, a semiconductor lacks an overlap of interband energy states capable of immediately aiding the recombination of the electron/hole pairs.

4.4 General Mechanism of Semiconductor Photocatalyst Redox Reactions

Figure 4.3A, illustrates the hole in the top energy level of the valence band. This valence electron deficiency at this energy level determines the oxidizing ability of a photo-induced hole. In contrast, the energy level of the electron at the bottom of the conduction band establishes the reduction potential of the photocatalyst, with each energy designating the ability of the system to drive oxidations and reductions. From a thermodynamic perspective, an adsorbed species can be reduced if it has a more positive redox potential than the conduction band electrons, and conversely oxidized if it has a more negative redox potential than the valence band holes. A schematic of this is shown in *Figure 4.3B* and is represented by the following general equation:

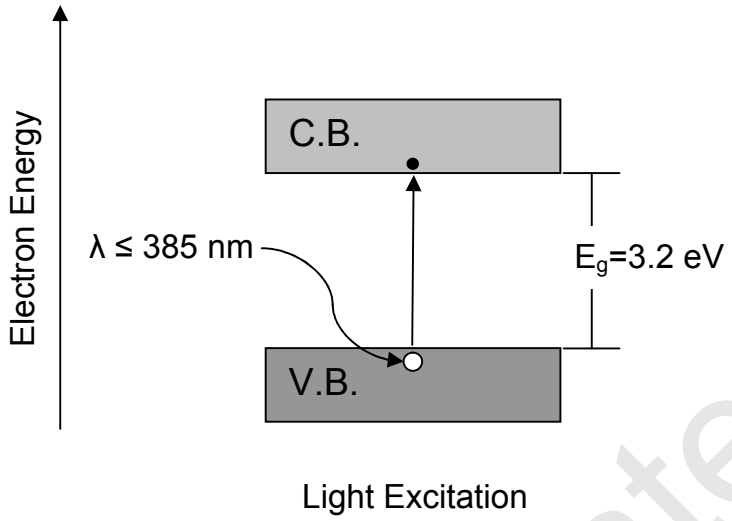

Fig. 4.3A Creation of a reactive electron/hole pair in a TiO_2 semiconductor through the super-band gap, light induced promotion of a V.B. electron across the band gap (E_g) and into the C.B..

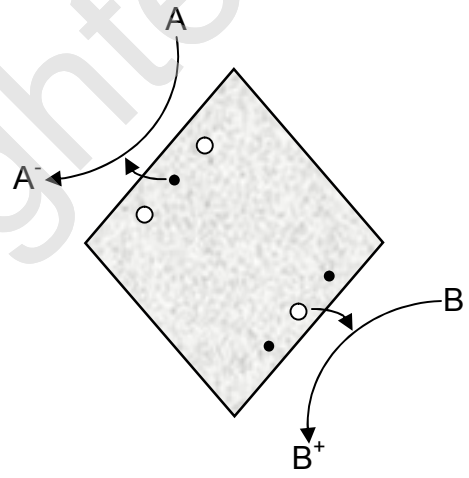

Fig. 4.3B Redox reactions occurring after migration of electrons and holes to TiO_2 surface: adsorbed acceptor species "A" is reduced by conduction band electron while adsorbed donor species B is oxidized by valence band hole.

$$A_{ads} + B_{ads} \xrightarrow[TiO_2]{h\upsilon \geq 3.2\,eV} A^-_{ads} + B^+_{ads} \qquad (1)$$

In most cases, the oxidation half of this reaction leads to the formation of hydroxyl radicals ($HO^\bullet$) on the catalyst surface. These radicals, with an oxidative capacity (E^o=2.80V) exceeded by only that of fluorine, act to non-selectively oxidize other species present in the system and help explain the seemingly universal application of TiO_2 photocatalysis in the degradation of a wide variety of microorganisms and both organic and inorganic compounds.

4.5 Sensitized Decomposition of Ozone Over Photoactive TiO_2

The established reaction scheme of photo-induced catalysis of the inorganic molecule, O_3, over TiO_2 also hinges upon the formation of the $HO^\bullet$ radical. As is seen in the subsequent reaction scheme (Gonzàlez-Elipe et al., 1981; Ohtani et al., 1992, and Mills et al., 2003a), following the formation of the electron (e^-)/hole (h^+) pair (Equation 2) and the reduction of ozone to the O_3^- ion (Equation 3), the photogenerated hole reacts with a surface hydroxyl group to oxidize it to a hydroxyl radical (Equation 4). Both the O_3^- ion and the $HO^\bullet$ radical react with ozone molecules (Equation 5 & 6, respectively) to form the O_4^- ion; direct support for the formation of the O_3^- and O_4^- intermediates is provided by the electron paramagnetic resonance (epr) studies of Gonzàlez-Elipe et al.. As a result of its reactivity, the O_4^- ion quickly reacts, with the most probable reactants being either O_3 (Equation 7) or the O_3^- ion (Equation 8). The summation of the reaction scheme gives an overall,

reduced chemical equation where the final product is simply molecular oxygen (Equation 9).

$$TiO_2 \xrightarrow{h\upsilon \geq 3.2\,eV} h^+ + e^- \quad (2)$$

$$e^- + O_3 \longrightarrow O_3^- \quad (3)$$

$$h^+ + OH^- \longrightarrow HO^\bullet \quad (4)$$

$$O_3^- + O_3 \longrightarrow O_4^- + O_2 \quad (5)$$

$$HO^\bullet + O_3 \longrightarrow O_4^- + H^+ \quad (6)$$

$$O_4^- + O_3 \longrightarrow 2O_2 + O_3^- \quad (7)$$

$$H^+ + O_3^- + O_4^- \longrightarrow 3O_2 + OH^- \quad (8)$$

$$2O_3 \xrightarrow[TiO_2]{h\upsilon \geq 3.2\,eV} 3O_2 \quad (9)$$

4.6 Experimental Setup of TiO_2 Photoreactors

As a means to quickly ascertain the general effectiveness and overall feasibility of utilizing TiO_2 as a scrubber material in UV-based ozone monitors, a slurry of the common tetragonal form of TiO_2 (anatase) was used in coating the inside of a quartz tube. This tube (6.5 mm O.D., 5.0 mm I.D., and 12 cm in length) was allowed to dry in an oven for an hour at 120 °C following each of its three slurry coats in order to provide a stable, uniform TiO_2 coating. This coated quartz tube, with a large 12-inch black light placed next to it, was positioned in-line with the inlet

air line which supplied ozone rich air to each of the various ozone monitors. As the light was turned on, a noticeable decrease in ozone concentration was clearly evident on both the TEI Model 49 and 2B Tech Ozone Monitors. With the success of this initial "proof of concept" experiment, efforts turned toward creation of a viable alternative capable of replacing the standard hopcalite scrubber in the 2B Tech Ozone Monitor without sacrificing this miniaturized instrument's critical power and size requirements.

As it is not possible to utilize a large, power intensive external light source in the small and sometimes battery-operated 2B Tech Ozone Monitor, the first hurdle to overcome was finding suitable miniaturized lamps capable of providing super-band gap energy without themselves creating ozone. These lamps, supplied by JKL Components Inc., are 12 cm in length, 3.2 mm O.D., with no output below 315 nm, and λ_{max} = 365 nm. In an effort to increase light intensity over the TiO_2 surface, it was decided to arrange the lamp and tube in an annular configuration. As shown in *Figures 4.4A & B*, the UV lamp is concentrically placed inside the photoreactor tube. This setup provides equal and maximum radiation intensity over the entire photoactive interior surface while also increasing the rate of mass transfer to the surface by effectively decreasing the air space inside the reactor. The 90° elbows provided a means to secure the lamp in the center of the reactor while also allowing air to flow through the system. This experimental arrangement was also utilized in later experiments where the photoactive surface support was switched from quartz to various types of metallic Ti tubing.

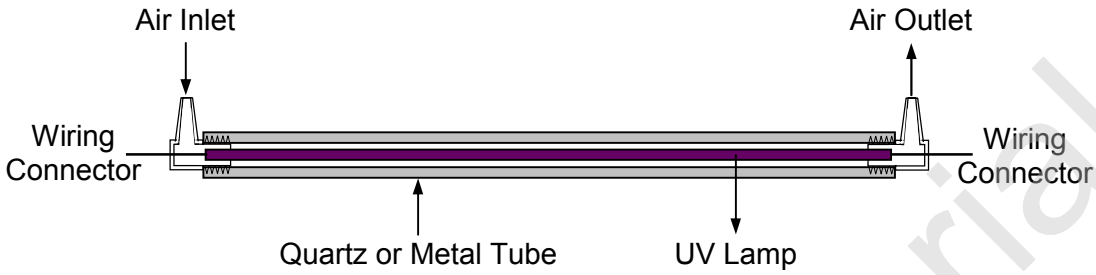

Fig. 4.4A Bisected, longitudinal view of UV lamp concentrically-centered in either a quartz or metal tube. The lamp's electrical wiring passes through nylon elbow air connectors which are attached to the ends of the photoreactor tube.

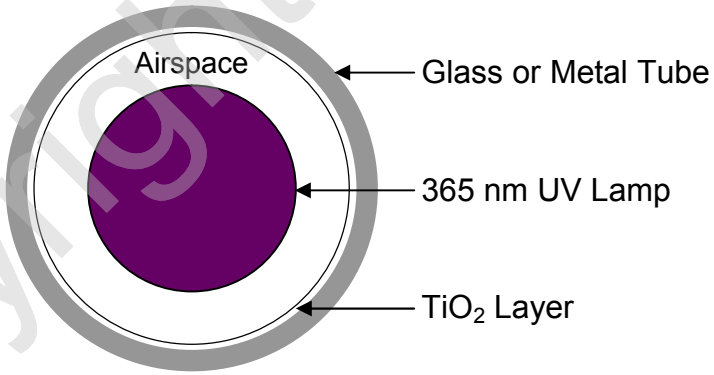

Fig. 4.4B Orthogonal, cross-sectional slice from middle section of Figure 4.4A. Note thin TiO_2 layer on inner surface of tube.

4.7 Experimental Findings from TiO_2 Coated Glass Tube Photoreactors

As demonstrated previously in Chapter 3, excessive scrubber surface area inherently leads to humidity interference in UV-based ozone monitors. With this awareness, it was decided that the first test of the hollow tube photoreactor as an internal ozone scrubber must be to ascertain its intrinsic capacity to adsorb and desorb water vapor, thus leading to inaccurate ozone readings. Duplicating the humidity experiments described in Chapter 3, the findings shown in *Figure 4.5* confirm a small but clearly evident humidity effect. This effect, however, is ±5 ppbv instead of the ±80 ppbv present when the standard hopcalite scrubber is in use. This finding was promising as it furthers our assumption that a scrubber such as a hollow tube, with little or no surface area, is critical in eliminating the humidity effect.

The next trial was to assess the new photocatalyst scrubber's activity level. In these experiments, relative humidity and ozone concentrations are held constant. The UV-lamp current, however, is modulated. This allows for the actual ozone concentration to be determined and compared to the catalyst's degree of ozone destruction, while also giving some insight into the rate at which ozone decomposition occurs. Furthermore, the experiments are run twice: once with the water vapor concentration at 0% R.H. and again at 100% R.H.. Duplicating the experiment at these two humidity extremes allows the possibility of pinpointing water's potential positive or negative interference in the photocatalysis of O_3 in the TiO_2 reactor tube.

In the case of a 0% R.H. air sample, *Figure 4.6A* shows an ≈ 93% decrease in O_3 concentration (from ≈ 450 ppbv to ≈ 35 ppbv) when the UV-lamp activates the

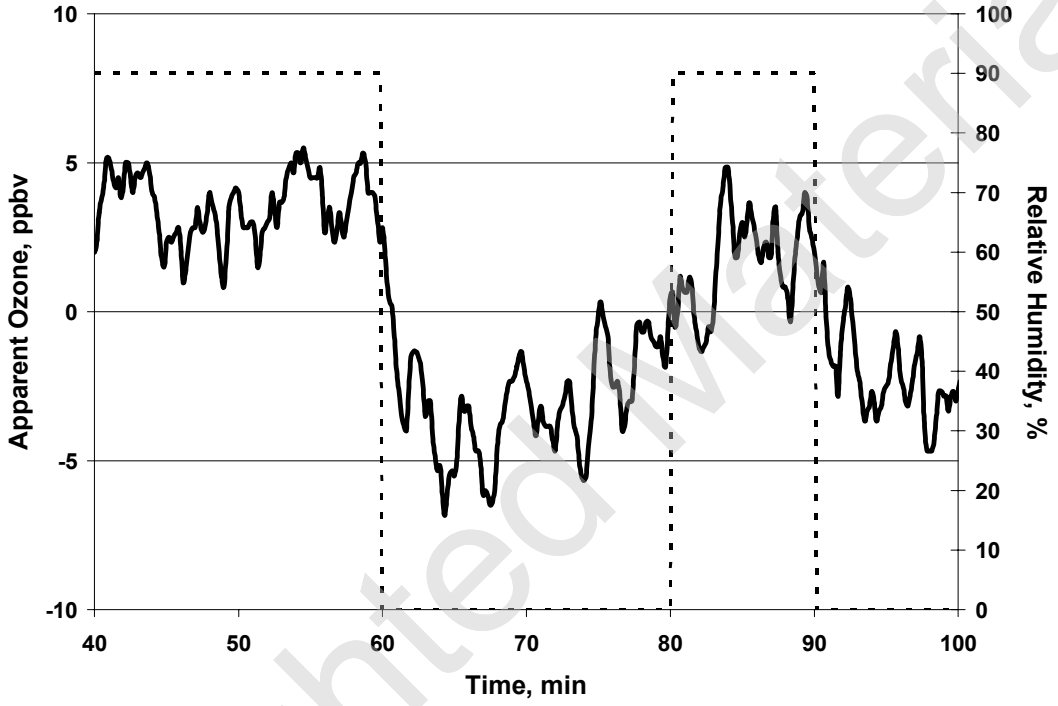

Fig. 4.5 1 minute running average of water vapor effect on apparent ozone reading for 2B Tech Ozone Monitor resulting from changes in the relative humidity of zero air with TiO_2-coated quartz tube in place of standard hopcalite ozone scrubber.

TiO_2 surface. This result was encouraging for our first application of the photocatalyst as it suggested that perhaps modifying either the lamp intensity, surface area, or air space could result in 100% O_3 destruction. To verify this effectiveness, the experiment was run again at 90% R.H. The results are shown in *Figure 4.6B*. Water vapor negatively influenced the degree of O_3 destruction, causing its concentration to be reduced by roughly half from ≈ 600 ppbv to ≈ 300 ppbv. Although it may also appear that the rate of decomposition was slower in the humid air experiment, this is only a visual artifact of the different time axes of the two figures. Nevertheless, Figure 4.6B shows that water continues to be an interference in our determination of O_3 via UV-based instruments. This time, however, it is not due to cell wall interactions but rather interference with photocatalytic processes in the scrubber itself.

4.8 Explanation of Water Vapor Interference in the Decomposition of O_3 on TiO_2 Coated Glass Tube Photoreactors

A great deal of research has been conducted concerning the effect of various parameters such as concentration on the photocatalytic efficiency of TiO_2, with particular significance given to the importance of relative humidity (Peral & Ollis, 1992, Zorn et al., 2000). Unfortunately for this project involving the inorganic molecule O_3, the majority of other studies have centered upon water's interaction in the degradation efficiency of *organic* molecules (Sauer and Ollis, 1994; Jacoby et al., 1995; Cao et al., 2000; Kim and Hong, 2002), with no research investigating the interference of water on O_3 photodecomposition being reported during the course of

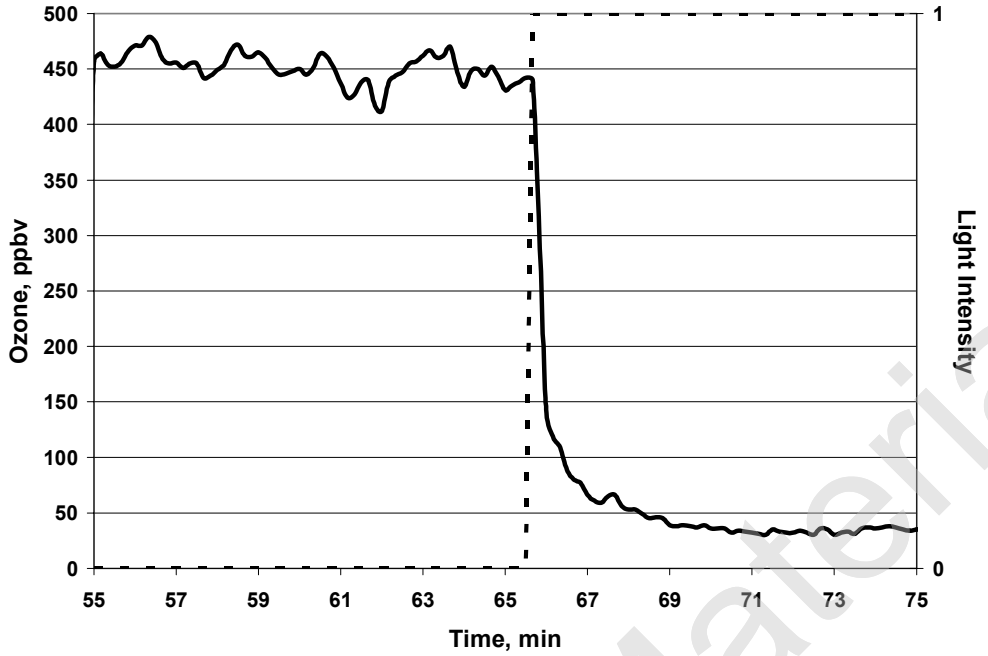

Fig. 4.6A Reduction in ozone concentration as a result of decomposition over photoactivated TiO_2 coated quartz tube in 0% R.H. air. Note that the second y-axis is light intensity and not R.H..

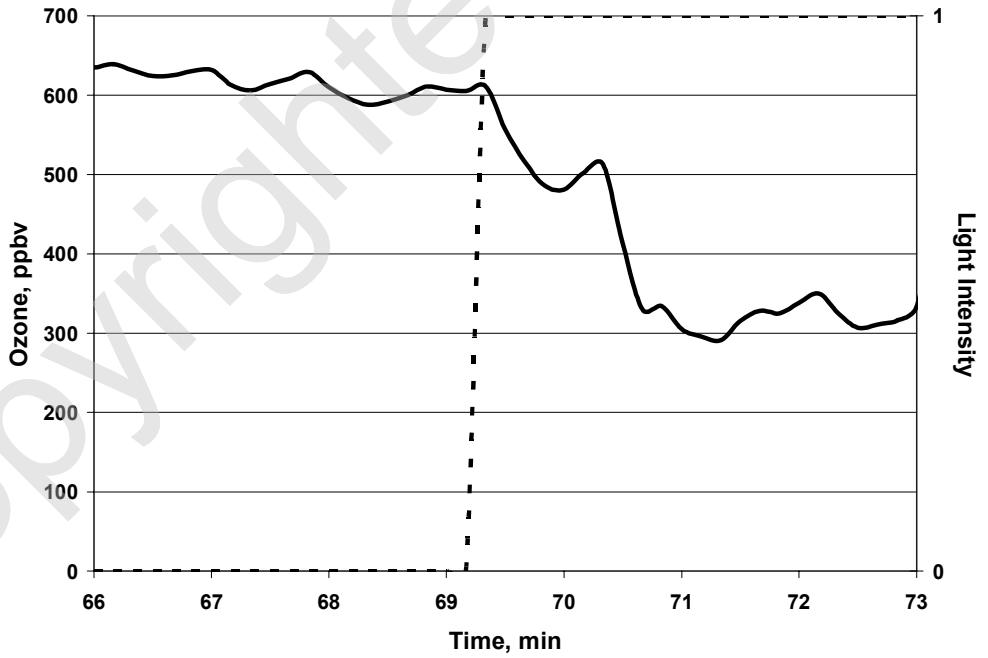

Fig. 4.6B Reduction in ozone concentration as a result of decomposition over photoactivated TiO_2 coated quartz tube in 100% R.H. air.

this research study. Water's interference is the result of catalyst surface inhibition since water vapor does not absorb at 365 nm and therefore could not attenuate the UV light source. Photocatalyst inhibition can occur through a combination of water interactions including: competing for active sites, shortening of the electron/hole pair lifetime, or even interfering with the mass transfer of ozone to the catalyst surface.

As was shown in the preceding reaction scheme (*Equations 2 - 9*), the photodegradation of O_3 requires the uninterrupted supply of hydroxyl radicals and subsequently, a mechanism capable of continually replenishing the hydroxylated surface. It is of no surprise then that research exists which confirms that a certain degree of humidity is required to maintain these surface hydroxyls and hence catalyst activity (Maira et al., 2001, Coronado et al., 2003). Furthermore, it has been shown that this humidity also stops deactivation by cleaning away partially oxidized products from the TiO_2 surface (Phillips and Raupp, 1992; Ameen and Raupp, 1999; Maria et al., 2001). However, when humidity rises above an equilibrium concentration, water vapor interference produces deleterious consequences. Water adsorbs onto the surface, creating a competition for active sites between the compounds to be oxidized and the extra water molecules (Sauer and Ollis, 1994; Obee & Brown, 1995; Lichtin & Avudaithai, 1996), thus lowering the effective catalytic activity of the TiO_2 (Park et al, 1999). Water adsorption has been shown to further reduce the photocatalytic oxidation rate by altering surface band bending in a manner favoring electron-hole recombination which consequently shortens the lifetime of the electron-hole pair (Park et al, 1999).

Water's ability to hinder the photocatalyst activity is further complicated at even higher relative humidity. In these cases, depending upon the texture, surface characteristics, and size of the TiO_2 particles there is not only the adsorbed water occupying and covering active sites (Henderson, 1996), but also variable amounts of weakly adsorbed water clusters (Vichi et al., 2000). This means that in regions of thicker water layers, humidity not only affects the adsorption of the compound directly to the TiO_2 surface, but it also further affects the photocatalytic activity through solvation and thus mass transfer of the compound to the catalyst surface (Cao et al., 2000). Under these conditions, a model which only assumes that water and ozone compete for the same sites will not fully explain the rate of the photocatalytic processes. Although the influence of adsorption on the overall kinetics of the photocatalytic oxidation of organics has been previously considered (Sauer and Ollis, 1994; Lichtin & Avudaithai, 1996; and Kim and Hong, 2002), a more thorough study of the role of water clusters has not occurred. This is unfortunate as there is much confusion and conflicting data concerning water's interactions. One can find instances in the literature where there is not only the earlier reported decrease in photoactivity due to water (Jacoby et al., 1995; Lichtin & Avudaithai, 1996, Cao et al., 2000; and Kim and Hong, 2002), but also enhancement (Jacoby et al., 1995; Kim and Hong, 2002; Einaga et al., 2002) as well as no effect shown (Peral and Ollis, 1992; Fu, 1995), sometimes for the same molecule. Although understanding the disparities due to differing experimental conditions such as the texture and size of the photocatalyst particles and the specific photocatalyzed molecule and its concentration is important, a full explanation of the complicated nature of water's interactions is

beyond the scope of this thesis. What can be learned and utilized from the literature is that an increase in surface area and subsequently the number of active sites is the most straightforward approach to increasing TiO_2 photoactivity.

4.9 Experimental Findings with Oxidized Titanium Tube Photoreactors

In an attempt to address concerns of the potentially friable nature and shock stability of the slurry coated glass tubes, it was decided to instead employ solid metal Ti tubes in the experimental setup shown earlier in *Figure 4.4A*. As was done with slurry-coated tubes, the intrinsic humidity effect of the solid Ti metal tubes was first ascertained. The solid metal tubes performed in much the same manner as the slurry coated tubes with an inherent ±5 ppbv humidity effect (*Figure 4.7*). This finding holds true for all subsequent metallic tubes described later in this chapter and again shows the feasibility of employing a hollow tube scrubber in lieu of the standard high surface area scrubbers currently utilized in ozone monitors.

The pure titanium tube reacts with oxygen to form the clear oxide, TiO_2 and appears as a grey tube with a very thin clear, shiny coating on its surface. Pure TiO_2 has an extremely high index of refraction (n_i = 2.70) with an optical dispersion exceeding that of diamond. Electrochemical or heat treatments will increase the oxide layer thickness. As the oxide layer grows thicker interference colors arise as light interacts with the oxide layer. These colors vary with the wavelength and angle of incident light but generally correspond to an oxide layer thickness from 500 Å (violet) to 1,000 Å (orange-red).

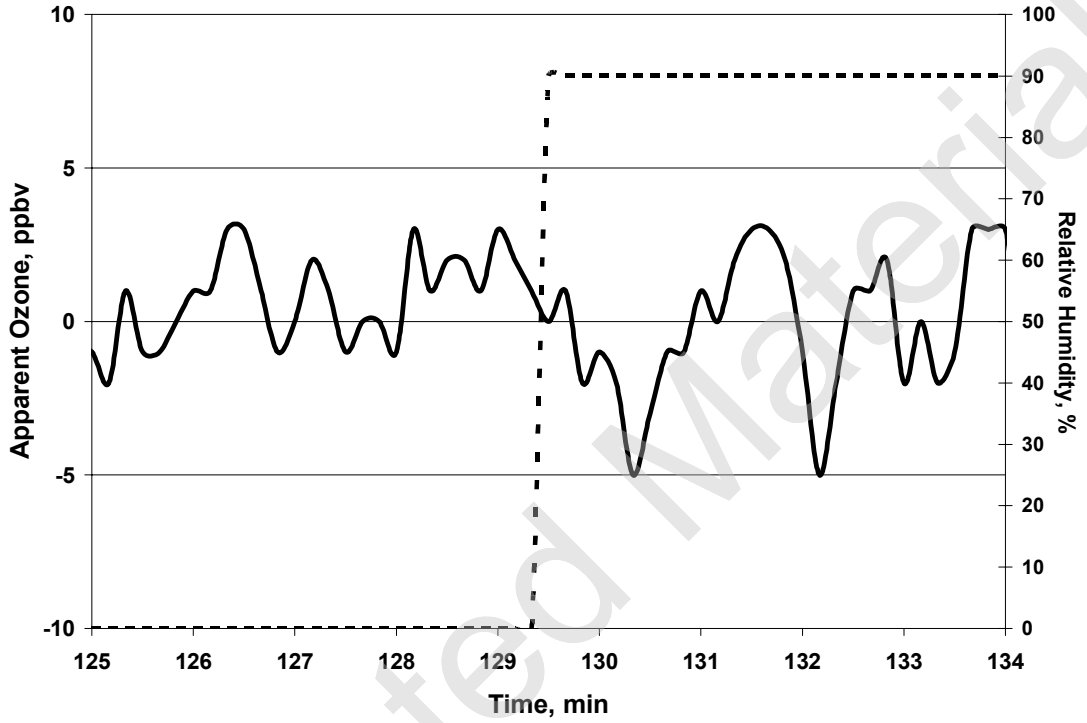

Fig. 4.7 Water vapor effect on apparent ozone reading for 2B Tech Ozone Monitor resulting from changes in the relative humidity of zero air with TiO_2 metal tube in place of standard hopcalite ozone scrubber.

Heating the tubes at 350°C for varying lengths of time produces a range of colors and hence oxide layer thicknesses. These tubes were then utilized in the experimental setup shown earlier in *Figure 4.4A* with the titanium tube photoreactor substituted for the standard hopcalite scrubber in the 2B Tech Ozone Monitor to test the tube's abilities to destroy ozone. Results are shown in *Figure 4.8* with a clear oxide layer photoreactor destroying ≈ 38% O_3; a blue colored oxide layer photoreactor destroying ≈ 45% O_3; and the gold colored oxide layer photoreactor destroying ≈ 75% of the ozone at 0% R.H. Results under higher R.H. are not shown, as the activity of the TiO_2 photoreactor only decreases as water occupies the photocatalyst active sites. The best of these results show the solid metallic Ti tubes to be ineffective as an ozone scrubber as well as less effective than the slurry coated glass tubes. As expected it is seen that there is a direct correlation with an increase in oxide layer thickness with the activity of the TiO_2 photocatalyst. It should be noted that there is an optimal thickness for the catalyst film layer, as it is porous with the interfacial layer being proportional to the thickness of the catalyst. There are limitations to this thickness, in that there is both an increased resistance to internal mass transfer of the species undergoing oxidation as well as an increase in the likelihood of electron/hole recombination with increasing TiO_2 layer thickness. However, this optimal thickness has recently been found to be thicker than previously believed, >1 μm, (Mills et al., 2003b) and much greater than we were able to easily generate in the oven driven oxidation experiments described above. As a result, other methods to generate sufficiently thick TiO_2 photoactive surfaces were pursued, as it was clear that photoactivity was still limited by oxide layer thickness and thus

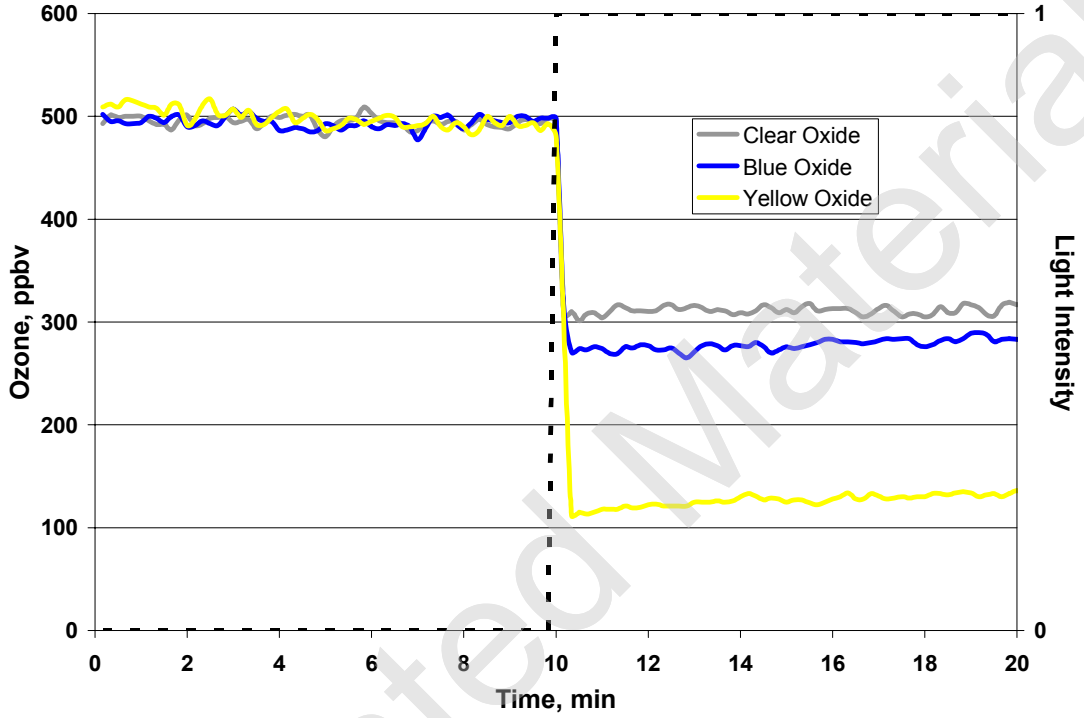

Fig. 4.8 Reduction in ozone concentration in 0% R.H. air as a result of sensitized decomposition over various oxide thicknesses of photoactivated TiO_2 tubes.

number of active sites.

4.10 Experimental Findings from HCl Pretreated Titanium Tube Photoreactors

In an effort to increase the oxide layer thickness, oxide surface area, and number of oxide photoactive sites it was decided to etch the tubes with concentrated HCl acid before baking at 350°C. This was accomplished by soaking the Ti tubes in 14 M HCl for 24 hours at room temperature, rinsing with H_2O, and then baking for 3 hours in a 350°C oven. The resulting pitted, roughened tube surface was dark grey to black in color and closely resembled wet/dry 320 grit sandpaper. These HCl etched tubes were again employed in the experimental setup shown earlier in *Figure 4.4A* where the 365 nm UV lamp was switched on to determine the photocatalyst's ability to effectively destroy ozone.

Results in dry air are shown *Figure 4.9A*, while *Figure 4.9B* illustrates the results in humidified air. These figures clearly display the high photoactivity of the HCl pretreated, metallic Ti tubes. The ozone, at levels many times higher than that commonly found in polluted air, undergoes 100% destruction in the presence of the 365 nm light activated catalyst surface, regardless of the humidity. As mentioned earlier, the HCl acid pretreated Ti tube ozone scrubber inherently exhibits a minute humidity offset of ±5 ppbv, which suggests this photoactive tube to be the long sought after replacement to the standard hopcalite scrubbers present in current ozone monitors. In an effort to further verify the photoactive tube's viability, it was next decided to check the lifetime of the catalyst by continuously running the experiment at elevated ozone levels to see if any appreciable deactivation occurred over time.

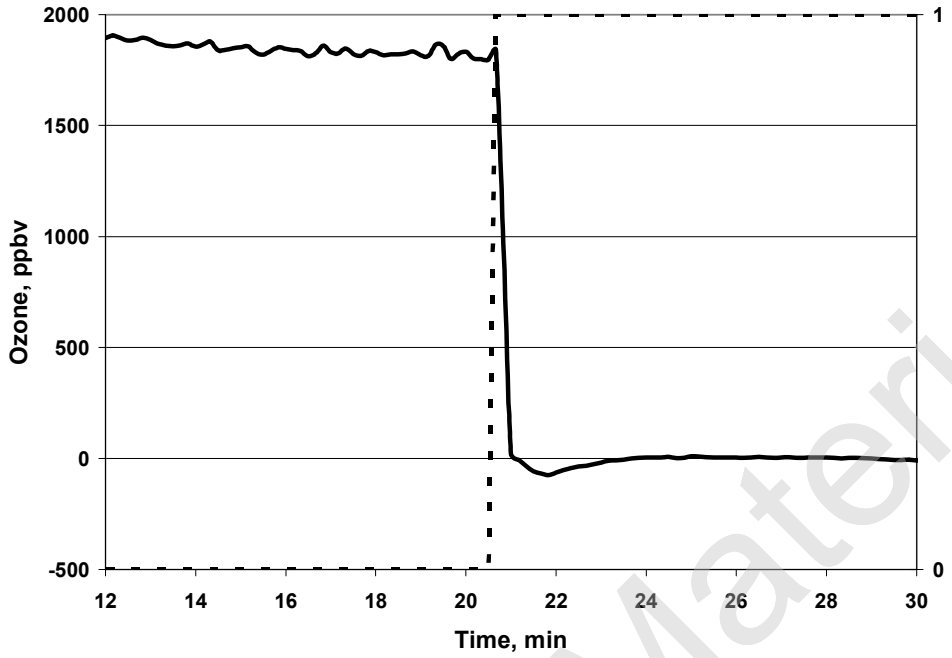

Fig. 4.9A Reduction in ozone concentration in 0% R.H. air as a result of sensitized decomposition over an HCl-etched, photoactivated TiO_2 tube.

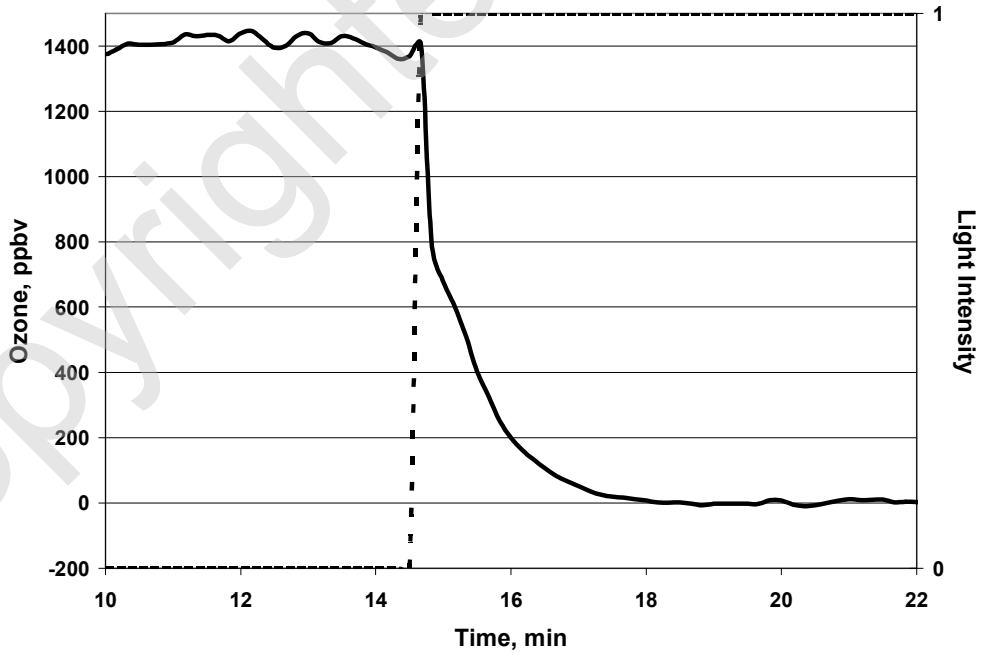

Fig. 4.9B Reduction in ozone concentration in 100% R.H. air as a result of sensitized decomposition over an HCl-etched, photoactivated TiO_2 tube.

Unfortunately the catalyst did lose activity over a period of days as illustrated in *Figure 4.10*. The reason for the decrease in the activity level of the photocatalyst was later determined to be related to the surface characteristics introduced during the halogenation pretreatment.

Although it was first believed that the boost in the photoactivity of the concentrated HCl acid pretreated Ti tube was purely a function of the physical increase in surface area as a result of etching, this was later found to be incorrect. A literature search showed that halogenation pretreatment *chemically* affects the Ti tube surface by leaving behind halogen anions which increase the activity rate of the photocatalyst. The chloride ions can trap photogenerated holes as they occur and thus inhibit the recombination of electron/hole pairs. Additionally, the chloride ions can be converted to chlorine radicals by the photogenerated holes and then react with adsorbed hydrocarbon species, speeding up the mineralization rate of adsorbed contaminants that can occupy active sites, and thus poisoning the photocatalyst surface over time (d'Hennzel et al., 1990; Amama et al., 2002; Lewandowski and Ollis, 2003). It has been determined that this increase in activity is directly linked to the concentration of the HCl utilized in acid pretreatment (Amama et al., 2002) and that periodic regeneration of the chloride ions is needed to restore the heightened photoactivity. It is believed that the trends shown in *Figure 4.10* represent the depletion of the chloride ions over time. It is further postulated that these ions and not the increase in surface area was the primary source of the improved photocatalyst activity noted in *Figures 4.9A & B*. These findings further indicate that over time both anthropogenic and naturally occurring hydrocarbon pollutants may significantly

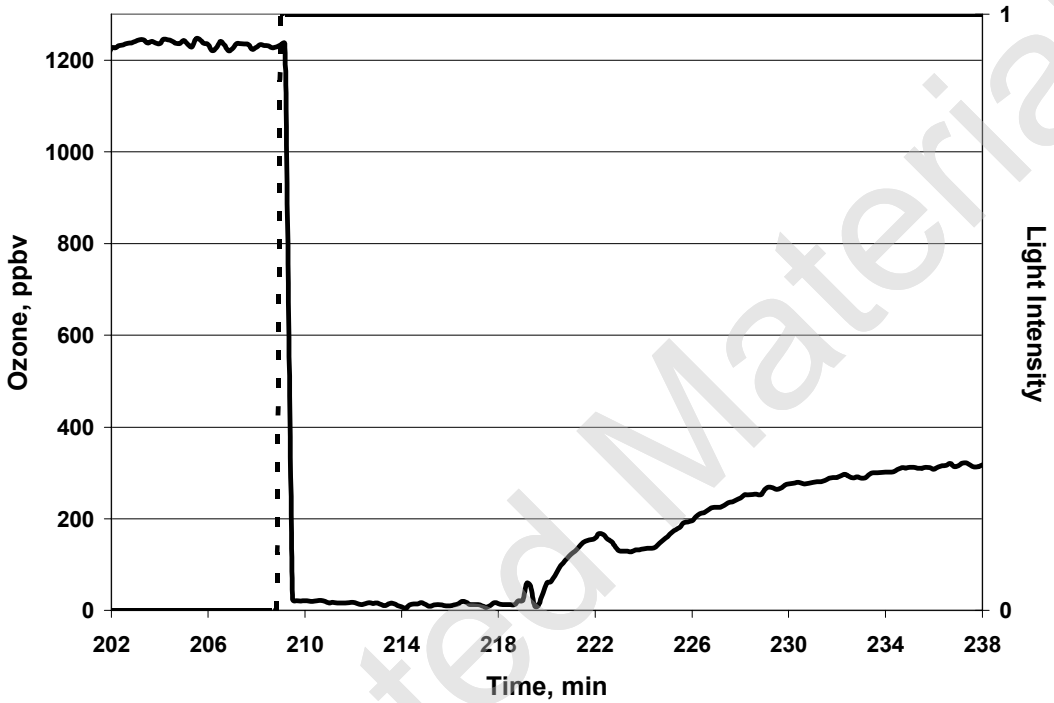

Fig. 4.10 Decrease in catalytic activity of a HCl-etched, photoactivated TiO_2 tube after ≈ 3.5 days of continuous use shown as ozone concentration increase despite constant photoactivation of the catalyst surface.

decrease the efficiency of any TiO_2 photocatalyst, making it unsuitable for use as a scrubber in ozone monitors. As it is not practical to continually regenerate the chloride ions in a real world instrument, further experiments were undertaken to find alternate means of increasing the efficiency and activity of TiO_2 photocatalysts.

4.11 Experimental Findings from Ti/Al/V Alloy Tube Photoreactors

In an attempt to further enhance the activity of the photocatalyst for oxidizing O_3, efforts focused upon the use of doped TiO_2 semiconductors, as this produces an enhanced efficiency in other photocatalytic systems (Martin et al., 1994; Serpone et al., 1994; Wilke and Breuer, 1999). TiO_2 particles can be interstitially doped with different cations, forming either mixed oxides and/or surface oxide clusters, depending upon both the dopant concentration and annealing treatment (Soria et al., 1991). Although the exact photochemical and physical mechanisms of doped semiconductors are complex and not always understood (Zhao et al., 1999), our efforts further focused upon p-type semiconductors since they show greater photoactivity than n-type for ozone decomposition (Imamura et al., 1991; Dhandapani and Oyama, 1997).

When the p-type atoms are added to the semiconductor structure they accept weakly bound electrons from the valence band of semiconductor atoms, resulting in fixed negative charges in the doped atoms and the creation of freely moving positive holes in the semiconductor. p-Type doping is obtained by dissolving cations of valencies lower than that of Ti^{4+} (e.g., Al^{3+}) into the TiO_2 lattice, whereas n-type doping is obtained with cations of valencies higher than +4 (e.g., V^{5+}). The common

Grade 9 titanium alloy composed of 3% aluminum and 2.5% vanadium (Sandvik Materials, 2000) provided a source of commercially available tubes of p-typed doped catalyst material. It should be noted that although vanadium, a n-type dopant, is also present in this alloy, the type dopant with the higher concentration will compensate for the lower concentration dopant, effectively canceling out its effect in the semiconductor. Although doping can lead to shortening of the electron/hole pair lifetime (doping ions can act as trapping sites), doping also increases the quantum efficiency of a compound's photooxidation. Furthermore, vanadium doping affects the particle size, crystal form, and surface structure of the Ti catalyst which in turn influences the concentration of hydroxyl radicals present on the photocatalyst surface (Martin et al., 1994). Due to its potential to affect both quantum efficiency and surface hydroxyl concentration, tubes of the Grade 9 Ti alloy were utilized in the same experimental setup shown earlier in *Figure 4.4A* where the 365 nm UV lamp was activated to determine the photocatalyst's ability to effectively destroy ozone.

Results in dry air are shown *Figure 4.11A*, whereas *Figure 4.11B* illustrates the findings in humidified air. Although these figures display a high photoactivity of the Ti/Al/V alloy tubes, they fail to show 100% destruction of ozone. The ozone undergoes 92% destruction in the presence of the 365 nm light activated catalyst surface when dry and 85% destruction in high humidity air. Unlike the findings from the HCl pretreated catalyst, this level of destruction held constant for several days of continual use, but never reached the 100% destruction required for a viable replacement ozone scrubber.

As an aside, it is known that vanadium doping could lead to a substantial

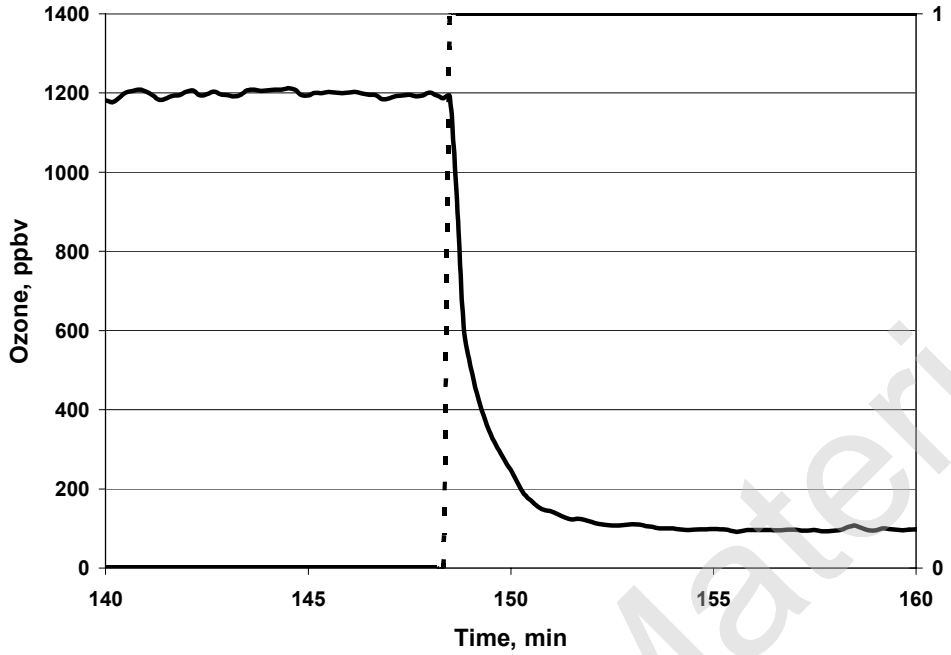

Fig. 4.11A Reduction in ozone concentration in 0% R.H. air as a result of sensitized decomposition over Ti/Al/V alloy tube with a photoactivated p-doped TiO_2 semiconductor layer.

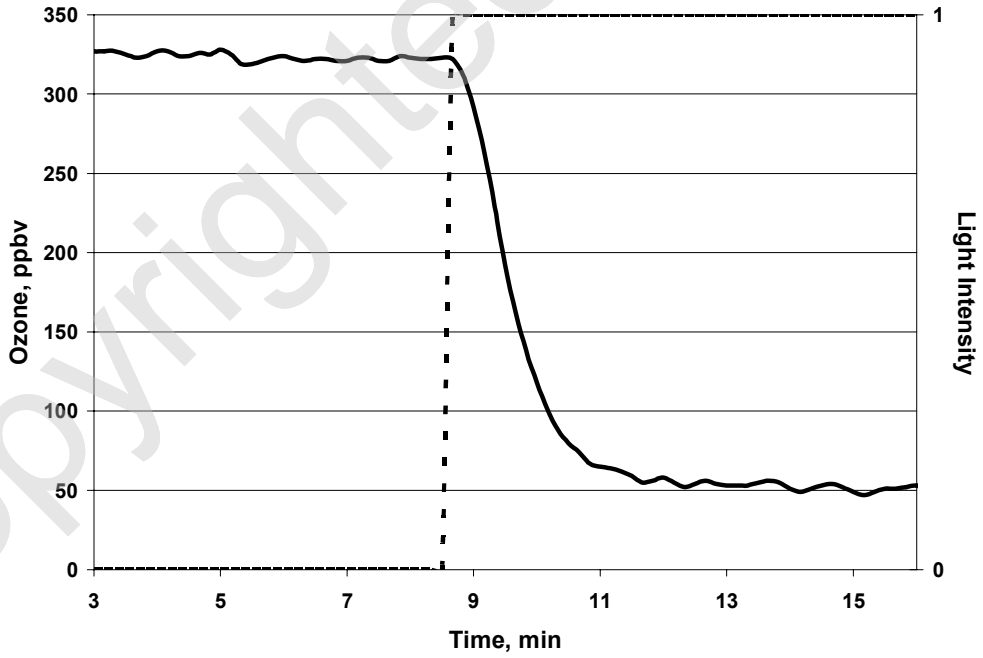

Fig. 4.11B Reduction in ozone concentration in 100% R.H. air as a result of sensitized decomposition over Ti/Al/V alloy tube with a photoactivated p-doped TiO_2 semiconductor layer.

batho-chromic red shift via its introduction of allowed intraband energy states in the photocatalyst (Takeuchi et al., 2000; Anpo et al., 2001). For this reason, experiments were run where these same Ti alloy tubes were also paired with miniature fluorescent bulbs of higher intensity than the 365 nm blacklights to check the viability of a visible light setup. Although higher activity was noted in the visible light region for the alloyed Ti tubes as compared to a standard 100% Ti tube, the overall activity was still less than the photoactivity results at 365 nm. For this reason, the potential use of a visible light activated photocatalyst was abandoned, and the results are not shown in this thesis. Additionally, it should be noted that unlike the pure Ti tubes, heat treatment of the Ti/Al/V alloy tubes showed no effect on the level of photocatalyst activity in both the visible and UV light regimes.

Although a single tube of the Ti/Al/V alloy did not destroy sufficient levels of ozone, it did have the advantage of constant ozone destruction over a period of days. Since a single Ti/Al/V photoreactor tube destroys 92 and 85% of the ozone in dry and humidified air respectively, it was proposed that two consecutive tubes might destroy nearly 100% of the sampled ozone. The effectiveness of this arrangement was examined, as shown in *Figure 4.12*, where 100% ozone destruction occurs in a p-doped TiO_2 photoreactor at 0% R.H.. Identical results were also recorded in 100% R.H. air, suggesting an experimental setup had been discovered which was capable of destroying ozone without imparting either a direct or indirect humidity effect upon UV-based ozone monitors.

The photoreactor cell and ozone monitor were tested over a continuous period of several days, where the experimental setup was subjected to a variety of sampling

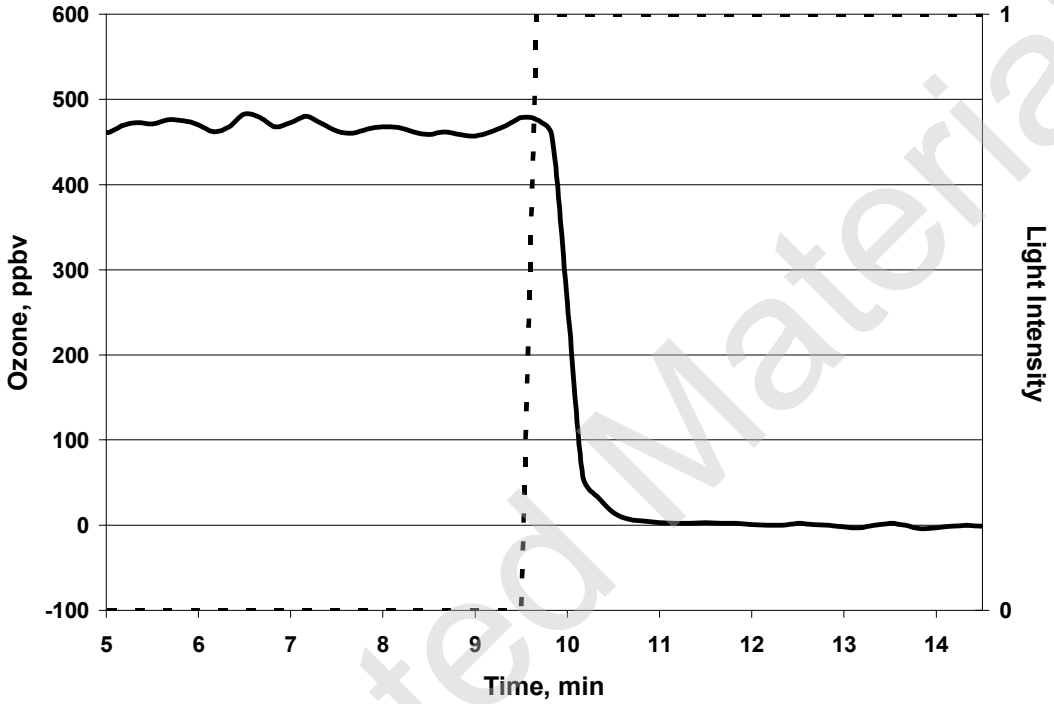

Fig. 4.12 Reduction in ozone concentration in 0% R.H. air as a result of sensitized decomposition over two sequential Ti/Al/V alloy tubes with a photoactivated p-doped TiO_2 semiconductor layer.

regimes and the persistence of 100% ozone destruction was verified. Air was sampled from both ultra-high-purity zero tank air and ambient air at a variety of humidity levels and ozone concentrations created from both lamp and electrical sources. The conditions were varied in an attempt to recreate the possible regimes in which one commonly encounters and operates an UV-based ozone monitor. Even though ozone created from an electrical discharge source is commonly used, it is considered 'dirty' as this method converts organic impurities found in both ambient and tank air into aldehydes and ketones for example, which flow into the ozone monitor and adsorb onto surfaces, fouling the instrument over time. Oxides of nitrogen also are produced by the discharge, and these react with water to form nitrous and nitric acid. An observed decrease in photocatalytic efficiency of the Ti/Al/V allow over a period of 10 to 11 days is probably due to accumulation of products formed in the electric discharge. The result of this fouling of the TiO_2 photocatalyst is shown in *Figure 4.13*, where only 75% of the ozone was destroyed and enhanced signal noise was observed. It should also be noted that with the use of two consecutive alloy tubes the surface area of the scrubber again became an issue as increasing amounts of unreacted species deposited on the catalyst surface. This led to an increase in the inherent humidity offset due to the scrubber, as well as increased noise in the instrument signal during rapid humidity changes. It is theorized that water vapor displaced some of the adsorbed partially mineralized hydrocarbon species, resulting in variable and false ozone readings in the instrument. Again, this inadequacy of the use of TiO_2 photoreactors as an ozone scrubber limits its practicality in the field.

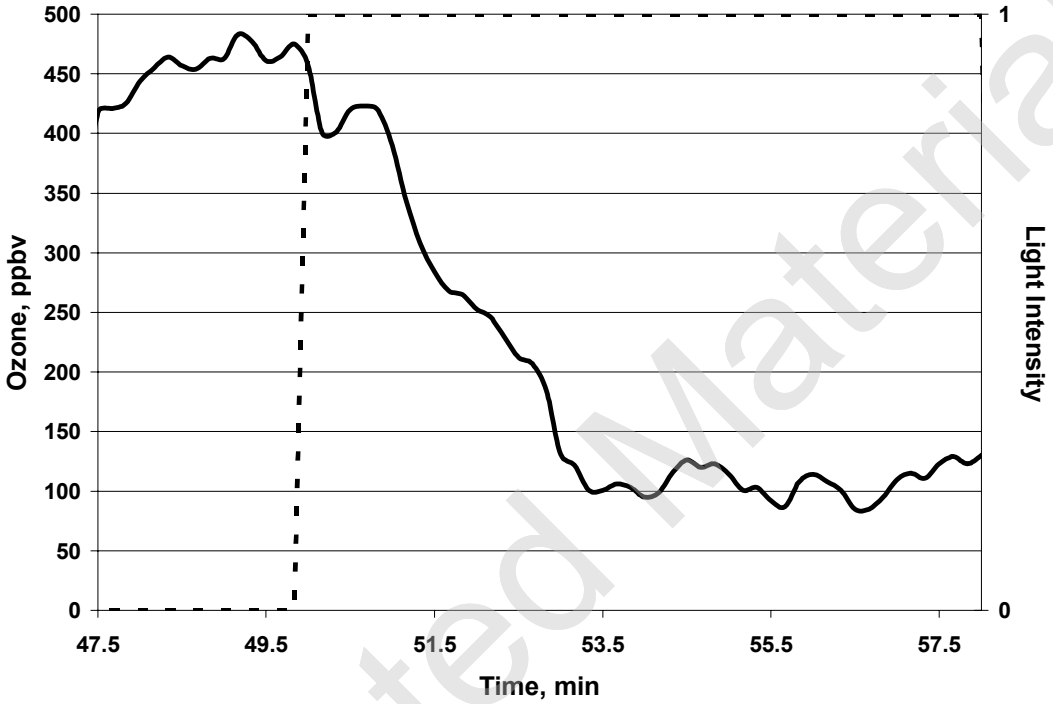

Fig. 4.13 Reduction in ozone concentration in 100% R.H. air as a result of sensitized decomposition over 2 sequential Ti/Al/V alloy tubes with a photoactivated p-doped TiO_2 semiconductor layer.

4.12 Conclusions and Limitations of the Use of TiO_2 Photoreactors as Scrubbers in Ozone Monitors

Although there are reports of the effective use of titanium dioxide photocatalyst films being used repeatedly over many cycles of ozone degradation without any appreciable loss in photocatalytic activity (Gonzàlez-Elipe et al., 1981; Mills et al., 2003a), the experimental setup of these studies differed from our instrument requirements in many ways. One of the more important of these is the physical specification of the photoreactor itself. Our experiments were size and power supply limited to one small 365 nm lamp contained inside a 10-cm long tube with a photoreactor hydraulic diameter of 1.8 mm and a light intensity of 0.25 $mW \cdot cm^{-2}$. The experimental setup of others often employs a 30 cm long tube with a hydraulic diameter of 0.9 mm and a lamp intensity of 5.3 $mW \cdot cm^{-2}$ (Jacoby et al., 1995). This results in ≈ 20 times more light irradiating 3 times the surface area with inherently greater interaction of the air stream with the photocatalyst since the hydraulic diameter is half as large as our photoreactor. Furthermore, other groups have employed recirculating photoreactors (Zorn, 2003) since there is often not enough interaction with the semiconductor surface in the single-pass, flow-type reactor required for use in an ozone monitor. These limits, particular to our specific experimental requirements, are in addition to the general limitations inherent to many TiO_2 photoreactors.

The most common one of these limitations, catalyst deactivation, was encountered over time in many of our experiments. This phenomenon is seldom mentioned in publications, as it is not encountered in those experiments which run for

only a period of hours before being cleaned for the next experiment. Catalyst deactivation is attributed to the buildup of partially reacted intermediates on the TiO_2 surface (Larson and Falconer, 1997) and occurs most easily in single-pass photocatalytic reactors (Sauer and Ollis, 1996). The deactivation (both reversible and irreversible) is further attributed to organic compounds (Peral and Ollis, 1997; Piera et al., 2002) commonly found in ambient air with any contamination of the photoactive surface leading to an accelerated buildup of additional contaminants (Maira et al., 2000), requiring reactivation of the catalyst surface over time.

Regeneration can occur in a variety of ways, the most common being either purging with zero air or a simple water rinse of the photocatalyst surface (Jacoby et al. 1996) to essentially displace and wash away weakly held contaminants. More pervasive intermediate contaminates require thermal regeneration to undergo complete decomposition. Although some specific catalysts display effective thermal regeneration at temperatures below 100 °C (Cao et al., 2000), in many cases these lower temperatures lead to an acceleration of carbonaceous deposits, and in most cases a temperature above 420 °C is required for effective cleaning (Ameen and Raupp, 1999). Another procedure for catalyst regeneration utilizes simultaneous UV illumination and exposure to a humidified air stream. Although this photocatalytic regeneration works for many organics and may be more practical than thermal degradation from a power consumption standpoint, it requires substantially longer cleaning times as well as a device for humidity generation. (Ameen and Raupp, 1999; Cao et al., 2000 and Einaga et al., 2002). It should be noted that none of these

techniques are useful for a viable field instrument, which in some cases is expected to run continuously for months at a time without fouling of the ozone scrubber.

There is one last inherent issue with much of the previous published works in that they often involve the use of tank oxygen for ozone formation and usually do not sample actual ambient air. Although the TiO_2 photocatalyzed reactions are non-selective oxidations resulting in similar oxidation rates for a range of molecules, this may not always be true in real world air sampling where multiple compounds may interact in an unexpected manner. In fact, most experiments have focused on the degradation of a single compound, a situation which would never occur in, for example, a polluted urban environment. Research on this problem has only recently begun, but already has shown that in multi-component systems, compounds with a lower attraction for the photocatalyst surface's active sites did not undergo degradation until after the more reactive compounds had decomposed (Zorn, 2003). Additional research with these real world competitive reactions must occur before implementation of a TiO_2 photocatalytic scrubber in ambient ozone monitoring.

The fundamental disparities listed above between the requirements of a viable field instrument and a bench top photoreactor are currently difficult at best to overcome, but may not be insurmountable with time considering the wide variety of techniques available to optimize the TiO_2 photocatalyst. Sensitization of TiO_2 occurs as the result of differences in crystal structure, smaller particle sizes (Wu and Yu, 2004), structured support material, and the use of various metal dopants and/or dyes (Iliev, 2002; Yu et al. 2003), with these modifications affecting the rate of electron/hole recombination, number and availability of active sites, density of

hydroxyl groups and therefore the overall photocatalytic efficiency of the semiconductor. Although this type of reactor may prove useful in the future, as it does not inherently possess a substantial humidity effect, this method is currently unsuitable for implementation in a field ready ozone monitor as it loses its ozone destroying efficiency over time. A completely different and highly successful approach to solving the issue of the humidity effect is discussed in the final chapter of this thesis.

Chapter 4 – References

Amama, P.B., K. Itoh and M. Murabayashi. "Gas-phase Photocatalytic Degradation of Trichloroethylene on Pretreated TiO_2." *Appl. Catal. B: Env.* 37 (**2002**): 321-330.

Ameen, M.M. and G.B. Raupp, "Reversible Catalyst Deactivation in the Photocatalytic Oxidation of Dilute *o*-xylene in Air." *J. Catal.* 184 (**1999**): 112-122.

Anpo, M., S. Kishiguchi, Y. Ichihashi, M. Takeuchi, H. Yamashita, K. Ikeue, B. Morin, A. Davidson, M. Che. "The Design and Development of Second-Generation Titanium Oxide Photocatalysts Able to Operate Under Visible Light Irradiation by Applying a Metal Ion-implantation Method." *Res. Chem. Intermed.* 27 (**2001**): 459-467.

Blake, D. M. *Bibliography of Work on the Heterogeneous Photocatalytic Removal of Hazardous Compounds from Water and Air: Update Number 4 to October 2001 - NREL/TP-510-31319*. Springfield, VA: Dept. Commerce, **2001.**

Cao, L., Z. Gao, S.L. Suib, T.N. Obee, S.O. Hay and J.D. Freihault. "Photocatalytic Oxidation of Toluene on Nanoscale TiO_2 Catalysts: Studies of Deactivation and Regeneration." *J. Catal.* 196 (**2000**): 253-261.

Carp, O., C. L. Huisman and A. Reller. "Photoinduced Reactivity of Titanium Dioxide." *Prog. Solid State Chem.* 32 (**2004**): 33-177.

Coronado, J.M., M.A. Anderson, I. Tejedor-Tejedor, and M.E. Zorn. "Photocatalytic Oxidation of Ketones in the Gas Phase over TiO_2 Thin Films: A Kinetic Study on the Influence of Water Vapor." *Appl. Catal. B: Env.* 43 (**2003**): 329-344.

d'Hennzel, O., P. Pichat, and D.F. Ollis. "Benzene and Toluene Gas-phase Photocatalytic Degradation Over H_2O and HCl Pretreated TiO_2: By-products and Mechanisms." *J. Photochem. Photobiol. A: Chem.* 118 (**1990**): 197-204.

Dhandapani. B., and S.T. Oyama. "Gas Phase Ozone Decomposition Catalysts." *Appl. Catal. B: Env.* 11 (**1997**): 129-166.

Einaga, H., S. Futamura, and T. Ibusuki. "Heterogeneous Photocatalytic Oxidation of Benzene, Toluene, Cyclohexene and Cyclohexane in Humidified Air: Comparison of Decomposition Behavior on Photoirradiated TiO_2 Catalyst." *Appl. Catal. B: Env.* 38 (**2002**): 215-225.

Fu, X., M. Anderson, and W.A. Zeltner. "The Gas-phase Photocatalytic Mineralization of Benzene on Porous Titania-based Catalysts." *Appl. Catal. B: Env.* 6 (**1995**): 209-224.

Fujishima, A. and Honda, K. "Electrochemical Photolysis of Water at a Semiconductor Electrode." *Nature* 238 (**1972**): 37.

Gonzàlez-Elipe, A.R., J. Soria and G. Munuera. "Photodecomposition of Ozone on Titanium Dioxide." *Z. Phys. Chem. N. F.* 126 (**1981**): 251-257.

Henderson, M.A. "Structural Sensitivity in the Dissociation of Water on TiO_2 Single-Crystal Surfaces." *Langmuir* 12 (**1996**): 5093-5098.

Iliev, V. "Phthalocyanine-Modified Titania-Catalyst for Photooxidation of Phenols by Irradiation with Visible Light." *J Photochem Photobiol A: Chem* 151 (**2002**): 195-199.

Imamura, S., M. Ikebata, T. Ito, and T. Ogita. "Decomposition of Ozone on a Silver Catalyst." *Ind. Eng. Chem. Res.* 30 (**1991**): 217-221.

Jacoby, W.A., D.M. Blake, R.D. Noble and C.A. Koval. "Kinetics of Oxidation of Trichloroethylene in Air via Heterogeneous Photocatalysis." *J Catal.* 157 (**1995**): 87-96.

Jacoby, W.A., D.M. Blake, J.A. Fennell, J.E. Boutler, L.M. Vargo, M.C. George, and S.K. Dolberg. "Heterogeneous Photocatalysis for Control of Volatile Organic Compounds in Indoor Air." *Air Waste Manage. Assoc.* 46, (**1996**): 891-898.

Kim, S.B. and S.C. Hong. "Kinetic Study for Photocatalytic Degradation of Volatile Organic Compounds in Air Using Thin Film TiO_2 Photocatalyst." *Appl Catal B: Environ* 35 (**2002**): 305-315.

Larson, S.A. and J.L. Falconer. "Initial Reaction Steps in Photocatalytic Oxidation of Aromatics." *Catal. Lett.* 44 (**1997**): 57-65.

Lewandowski, M.M. and D.F. Ollis. "Halide Acid Pretreatments of Photocatalysts for Oxidation of Aromatic Air Contaminants: Rate Enhancement, Rate Inhibition, and a Thermodynamic Rationale." *J. Catal.* 217 (**2003**): 38-46.

Lichtin, N.N. and M. Avudaithai. "TiO_2-Photocatalyzed Oxidative Degradation of CH_3CN, CH_3OH, C_2HCl_3, and CH_2Cl_2 Supplied as Vapors and in Aqueous Solution under Similar Conditions." *Env. Sci. Tech.* 30 (**1996**): 2014-2020.

Maira, A.J., K.L. Yeung, C.Y. Lee, P.L. Yue and C.K. Chan. "Size Effects in Gas-phase Photo-oxidation of Trichloroethylene Using Nanometer-Sized TiO_2 Catalysts." *J. Catal.* 192 (**2000**): 185-196.

Maira, A.J., K.L. Yeung, J. Soria, J.M. Coronado, C. Belver, C.Y Lee and V. Augugliaro. "Gas-phase Photo-oxidation of Toluene Using Nanometer-size TiO_2 Catalysts." *Appl. Catal. B: Env.* 29 (**2001**): 327-336.

Martin, S.T., C.L. Morrison, and M.R. Hoffmann. "Photochemical Mechanism of Size-Quantized Vanadium-Doped TiO_2 Particles." *J Phys Chem* 98 (**1994**): 13,695–13,704.

Mills, A., S. K. Lee and A. Lepre. "Photodecomposition of Ozone Sensitized by a Film of Titanium Dioxide on Glass." *J. Photochem. Photobiol. A: Chem.* 155 (**2003a**): 199-205.

Mills, A., G. Hill, S. Bhopal, I.V. Parkin, and S.A. O'Neill. "Thick Titanium Dioxide Films for Semiconductor Photocatalysis." *J. Photochem. Photobiol. A: Chem.* 160 (**2003b**): 185-194.

Obee, T.N. and R.T. Brown. "TiO_2 Photocatalysis for Indoor Air Applications. Effects of Humidity and Trace Contaminant Levels on the Oxidation Rates of Formaldehyde, Toluene, and 1,3-Butadiene." *Env. Sci. Tech.* 29 (**1995**): 1223-1231.

Ohtani, B., S.-W. Zhang, S. Nishimoto and T. Kagiya. "Catalytic and Photocatalytic Decomposition of Ozone at Room Temperature Over Titanium(IV) Oxide." *J. Chem. Soc. Faraday Trans.* 88.7 (**1992**): 1049-1053.

Park, D.R., M. Anpo, J. Zhang, K. Ikeue and H. Yamashita. "Photocatalytic Oxidation of ethylene to CO_2 and H_2O on Ultrafine Powdered TiO_2 Photocatalysts in the Presence of O_2 and H_2O." *J. Catal.* 185 (**1999**): 114-119.

Peral, J. and D. Ollis. "Heterogeneous Photocatalytic Oxidation of Gas-phase Organics for Air Purification: Acetone, 1-Butanol, Butyraldehyde, Formaldehyde, and *m*-Xylene Oxidation." *J. Catal.* 136 (**1992**): 554-565.

Peral, J. and D.F. Ollis. "TiO_2 Photocatalyst Deactivation by Gas-phase Oxidation of Heteroatom Organics." *J. Mol. Catal. A: Chem* 115 (**1997**): 347-354.

Phillips, L.A. and G.B. Raupp. "Infrared Spectroscopic Investigation of Gas-solid Heterogeneous Photocatalytic Oxidation of Trichloroethylene." *J. Mol. Catal.* 77 (**1992**): 297-311.

Piera, E., J. Peral, J.A. Ayllón and X. Doménech. "TiO_2 Deactivation During Gas-phase Photocatalytic Oxidation of Ethanol." *Catal. Today* 76 (**2002**): 259-270.

Sandvik Materials Technology AB. "Product Information: Titanium Grades." Accessed 5 July 2005. <http://www2.sandvik.com/sandvik/0140/internet/se01974.nsf/GenerateFrameset1?readForm&url=http://www2.sandvik.com/sandvik/0140/internet/se01974.nsf/1ab734b4713311544125653d002eb28b/a09783b3907e8b02c1256b0a003bfd18?OpenDocument> (**2000**).

Sauer, M.L. and D.F. Ollis. "Acetone Oxidation in a Photocatalytic Monolith Reactor." *J. Catal.* 149 (**1994**): 81-91.

Sauer, M.L. and D.F. Ollis. "Catalyst Deactivation in Gas–Solid Photocatalysis." *J. Catal.* 163 (**1996**): 215-217.

Serpone, N., D. Lawless, J. Disdier, and J.M. Hermann. "Spectroscopic, Photoconductivity, and Photocatalytic Studies of TiO_2 Colloids: Naked and with the Lattice Doped with Cr^{3+}, Fe^{3+}, and V^{5+} Cations." *Langmuir* 10 (**1994**): 643-652.

Skubal, L.R. and N.K. Meshkov. "Reduction and Removal of Mercury from Water Using Arginine-Modified TiO_2." *J. Photochem. Photobiol. A: Chem.* 148 (**2002**): 211-214.

Soria, J., J.C. Conesa, V. Augugliaro, L. Palmisano, M. Sciavello and A. Scalfani. "Dinitrogen Photoreduction to Ammonia Over Titanium Dioxide Powders Doped with Ferric Ions." *J. Phys. Chem.* 95 (**1991**): 274-282.

Takeuchi, M., H. Yamashita, M. Matsuoka, M. Anpo, T. Hirao, N. Itoh and N. Iwamoto. "Photocatalytic Decomposition of NO Under Visible Light Irradiation on the Cr-ion-implanted TiO_2 Thin Film Photocatalyst." *Catal. Lett.* 67 (**2000**): 135-137.

Vichi, F.M., M.A. Anderson, and M.I. Tejedor-Tejedor. "Effect of Pore-wall Chemistry on Proton Conductivity in Mesoporous Titanium Dioxide." *Chem. Mater.* 12 (**2000**): 1762-1770.

Wang, R., K. Hashimoto, A. Fujishima, M. Chikuni, E. Kojima, A. Kitamura, M. Shimohigoshi, and T, Watanabe. "Photogeneration of Highly Amphiphilic TiO_2 Surfaces." *Adv. Materials* 10 (**1998**): 135-138.

Wilke, K. and H.D. Breuer. "The Influence of Transition Metal Doping on the Physical and Photocatalytic Properties of Titania." *J. Photochem. Photobiol. A: Chem.* 121 (**1999**): 49-53.

Wu, J. and C. Yu. "Aligned TiO_2 Nanorods and Nanowalls." *J. Phys. Chem. B* 108 (**2004**): 3377-3379.

Worsley, D., A. Mills, K. Smith, and M.G. Hutchings. "Acid Enhancement Effect in the Clean Oxidation of Toluenes Photocatalyzed by TiO_2." *J Chem Soc, Chem Comm.* (**1995**): 1119-1120.

Yu, J.C., Y. Xiea, H.Y. Tanga, L. Zhanga, H.C. Chanb and J. Zhao. "Visible Light-Assisted Bactericidal Effect of Metalphthalocyanine-Sensitized Titanium Dioxide Films." *J. Photochem. Photobiol. A: Chem.* 156 (**2003**): 235-241.

Zhao, G., T. Yoko, H. Kozuka, H. Lin and M. Takahashi. "Preparation and Photoelectrochemical Properties of $Ti_{1-x}V_xO_2$ Solid Solution Thin Film Photoelectrodes with Gradient Bandgap." *Thin Solid Films* 340 (**1999**): 125-131.

Zorn, M.E., D.T. Tompkins, W.A. Zeltner and M.A. Anderson,. "Catalytic and Photocatalytic Oxidation of Ethylene on Titania-Based Thin-Films." *Env. Sci. Tech.* 34 (**2000**): 5206-5210.

Zorn, M.E. "Photocatalytic Oxidation of Gas Phase Compounds in Confined Areas: Investigation of Multiple Component Systems." *Proceedings of the 13th Annual Wisconsin Space Conference*. August 14-15, 2003. Green Bay: Wisconsin Space Grant Consortium, **2003**.

Chapter 5

Use of a Nafion® Membrane in Reducing the Water Vapor Interference to Negligible Levels

5.1 Review of Work on the Water Vapor Interference

To review, a practical approach to equilibrate the humidity of ozone-scrubbed and by-pass air for use in inexpensive, lightweight, low power ozone monitors is desired. All previous studies discussed thus far in the thesis revolved around minimizing both the optical cell's and the ozone scrubber's affinity for absorption of water vapor. The physical nature of the cell was modified and heated, and the surface area of the scrubber was reduced to its minimum, while alternative catalysts and methods of ozone destruction were thoroughly explored. At this stage, little or no additional modifications are possible for these portions of the 2B Tech Ozone Monitor. This leaves modifying the air stream itself as the only other means to equilibrate the relative humidity of the ozone-scrubbed (I_o) and by-pass air (I).

Drying the inlet air with a heater or employing a chemical absorbent to remove all moisture from the inlet line of the ozone monitor could easily accomplish this. Unfortunately, these methods will also destroy all or some portion of the analyte, ozone, as it readily decomposes on most surfaces, especially heated ones. One could also attempt the opposite approach of heavily humidifying the inlet air in hopes that both the ozone-scrubbed and by-pass air will remain near 100 % R.H.. Again, this method poses potential problems in that ozone will most likely be destroyed while passing through a moistened membrane, water can potentially condense inside the ozone monitor, and the water source would need to be

replenished over time, making long-term operation of the monitor more difficult. Each of these approaches focuses upon one extreme or the other (either 100 % drying or humidifying the air) when what is really desired is a means to equilibrate both the ozone-scrubbed and by-pass air streams to the *same* humidity - keeping in mind that it is not a specific humidity level that is problematic, but rather the rapid change in humidity which brings about the undesired humidity effect. It is with this in mind that a completely different approach was attempted and discussed in the following sections.

5.2 Focus Upon Nafion® Polymer for Cancellation of Humidity Modulation

A membrane is required which can both quickly remove water from a moist air stream while also quickly adding water to a dry one, bringing each air stream to an equal relative humidity. Furthermore, this membrane material should have little or preferably no reactivity with the ozone molecule. Perma Pure, LLC of Toms River, N.J. is the only licensed manufacturer of a proprietary membrane named Nafion®. As shown in *Figure 5.1*, Nafion® is the modified, sulfonated form of Teflon® and for this reason, it is highly resistant to chemical attack including reactions with ozone. The sulfonic acid groups impart ionic properties to the bulk Teflon® polymer matrix, allowing absorption of up to 13 waters of hydration (22% $^{w}/_{w}$) to occur (Perma Pure LLC, 2004). Furthermore, the absorption and desorption of water is very fast, requiring only 200 ms to occur (Robinson, 1999). This signifies that roughly a one-meter length of small diameter Nafion® tubing is sufficient to equilibrate the different humidity gas streams present in the 2B Tech Ozone Monitor.

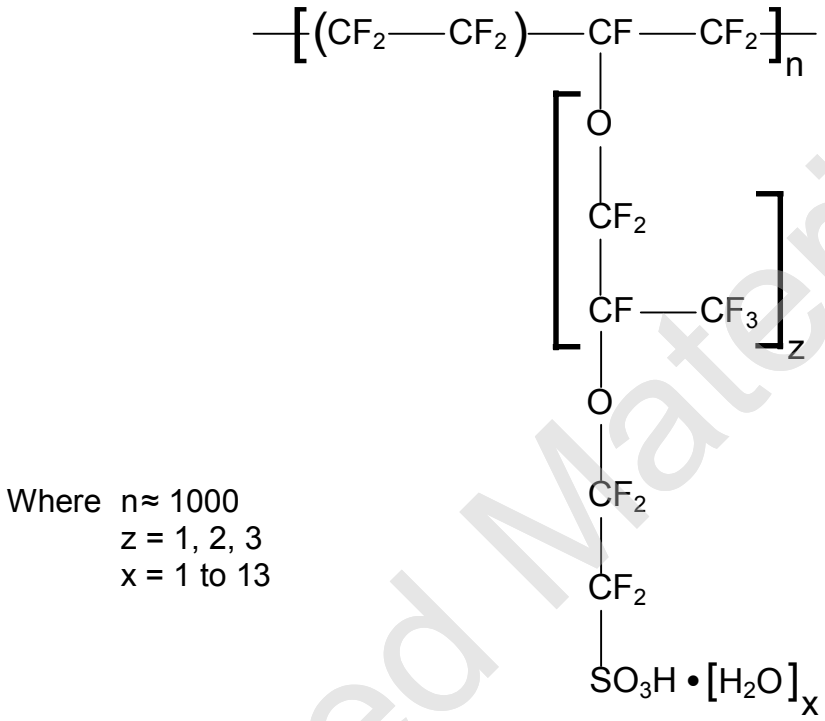

Fig. 5.1 Molecular structure of Nafion® co-polymer consisting of a tetrafluoroethylene (Teflon®) backbone with perfluoro-3,6-dioxa-4-methyl-7-octene-sulfonic acid side-chains (Perma Pure LLC, 2004).

5.3 Testing of Nafion® Polymer for Potential Use in Ozone Monitors

Along with examining the usefulness of Nafion® tubing as a humidity equilibrator in the 2B Tech Ozone Monitor, it is important to also verify both its drying ability and capacity for interacting with ozone. Firstly, to test the humidity equilibration, air of varying R.H. was drawn through a Nafion® tube of the following dimensions: 1-meter length, 1.07 mm I.D., and 1.35 mm O.D. The pump of a 2B Tech Ozone Monitor was used for this to assure identical flow rates to those found in an instrument, ≈ 1 $L \cdot min^{-1}$. The humidities of the various air streams were measured both before and after passing through the Nafion® tube. The results are shown in *Table 5.1*. Neither the beginning relative humidity nor the order in which the various air streams were measured affected the outcome. In each case the air stream was equilibrated to the relative humidity (≈ 39.2%) of the ambient air surrounding the Nafion® tube, proving Nafion's® ability to modulate the often different humidity levels found in both the ozone-scrubbed and by-pass air streams present in every UV-based ozone monitor.

In an effort to check the ability of Nafion® to pass ozone, the aforementioned humidity experiment was duplicated, although in this experiment, the air stream's

	Relative Humidity %	
Air Stream	**Before Nafion® Tube**	**After Nafion® Tube**
Dry Tank Air	0.2	39.3
Humidified Air	93	39.4
Room Air	39.2	39.2

Table 5.1 Modulation of relative humidity of dry and moist air to the R.H. of ambient room air as a result of passing through a length of Nafion® tubing.

ozone level was measured instead of R.H. Ozone was generated, spanning concentrations commonly encountered in ambient air, and measured both before and after passing through the Nafion® tube; the results of this experiment are shown in *Figure 5.2*. The chart clearly shows the high correlation (R^2=1.0000) of ozone before and after passing through the Nafion® tube. From the slope of the line, it can be determined that only 0.33% of ozone is lost while passing through the Nafion® tube. The observed miniscule positive offset of 0.2681 ppbv ozone is within the noise of the instrument. Nafion's® capacity to pass >99% of the ozone analyte molecule demonstrates the polymer's effectiveness for use in UV-based ozone monitors.

5.4 Experimental Setup and Results of Utilizing Nafion® Humidity Modulator

The 1 meter length of Nafion® tubing is spooled inside a small box with an inlet and outlet. Before sealing, the interior of the box is filled with a small amount of slightly moistened cotton fibers to provide both a slight reservoir humidity source and shock support to the Nafion® tubing. The now self-contained humidity modulator component is then placed in-line in the ozone monitor after the solenoid switching valve and before the optics cell *Figure 5.3*. The remainder of the ozone monitor is unchanged and identical to the one shown in an earlier chapter *Figure 1.5*.

A replication of the humidity experiments discussed in Chapter 2 and 3 was carried out, and the results are shown in *Figure 5.4*. A humidity generator was again used to create a 90% R.H. zero air stream, and the 2B Technologies Ozone Monitor was quickly cycled between dry and moist zero air containing no ozone molecules. Unlike previous experiments, there is no significant change in ozone signal when

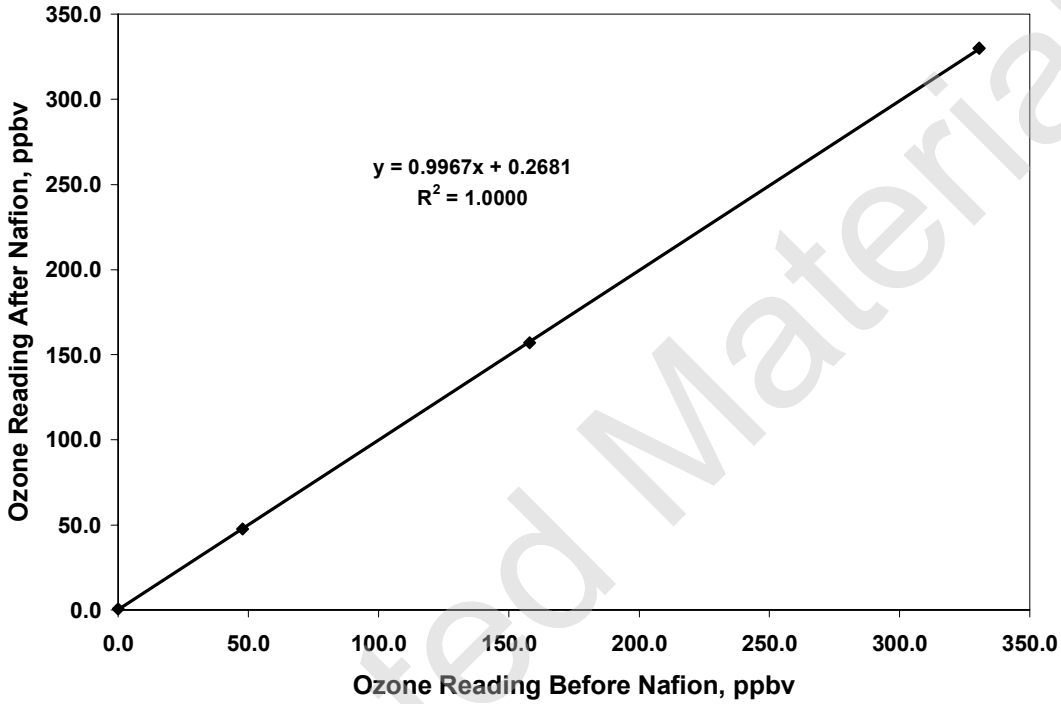

Fig. 5.2 Ozone loss on Nafion® humidity modulator. The Nafion® passes 99.7% of ozone over 0 to 330 ppbv range with excellent precision.

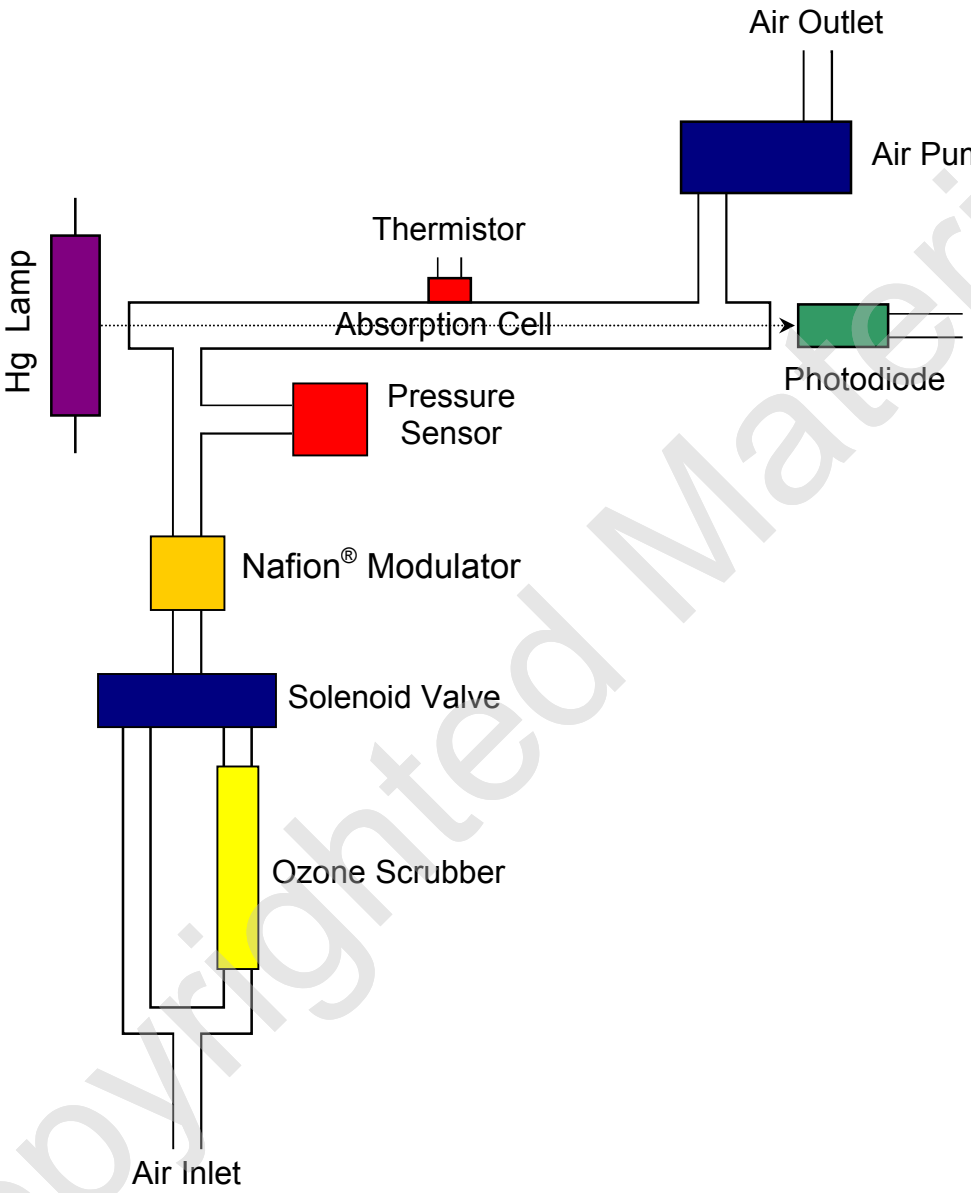

Fig. 5.3 Schematic diagram of UV-based ozone monitor with Nafion® humidity modulator located between the solenoid valve and absorption cell.

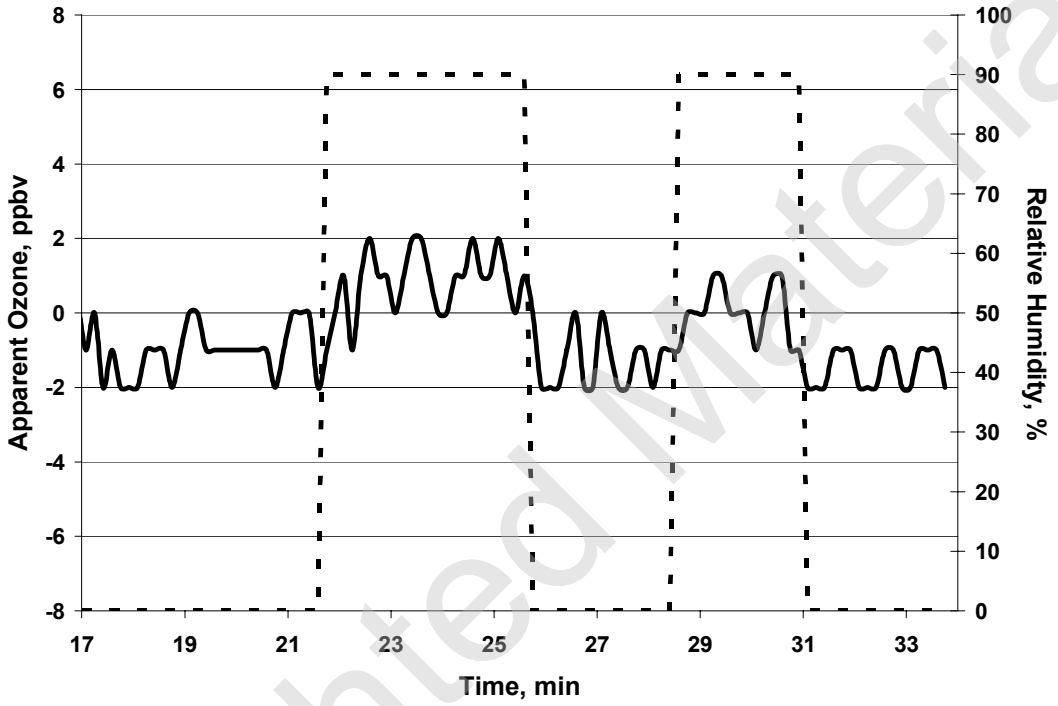

Fig. 5.4 Apparent ozone reading for 2B Tech Ozone Monitor resulting from changes in the relative humidity of zero air with Nafion® humidity modulator located between the solenoid valve and absorption cell.

going from dry to moist air, where only a small apparent ozone offset of ± 2 ppbv is present. Furthermore, the ozone monitor undergoes this change in one instrument reading (10 seconds). The magnitude of the water vapor effect for this improbably large and sudden R.H. change is now negligible. The scale of this effect is clearly shown in *Figure 5.5*. In contrast to other instruments which undergo -200, +80, +60, and -25 ppbv changes in ozone signal when relative humidity increases under the same experimental conditions and require up to an hour to equilibrate after changes in relative humidity, the Nafion® modified 2B Tech Ozone Monitor is an order of magnitude superior on both the magnitude of ozone offset as well as the time period required for recovery (± 2 ppbv and 10 seconds, respectively). At last, a practical method to equilibrate the relative humidity of the ozone-scrubbed (I_o) and by-pass air (I) in UV-based ozone monitors has been established eliminating an interference and solving a significant problem in analytical/atmospheric chemistry.

5.5 Conclusions

In this thesis work, significant and sometimes large water vapor interference inherent in essentially all commercially available ozone monitors was positively identified for the first time. Prior knowledge of this interference was mostly anecdotal, with the only published studies either dismissing it as being solved in newer instruments or incorrectly identifying its source. In this work the mechanism of the interference was elucidated, the interference being caused by changes in the transmission efficiency of light through the UV absorption cell as a result of adsorption of water molecules to the cell surface. The water vapor concentration

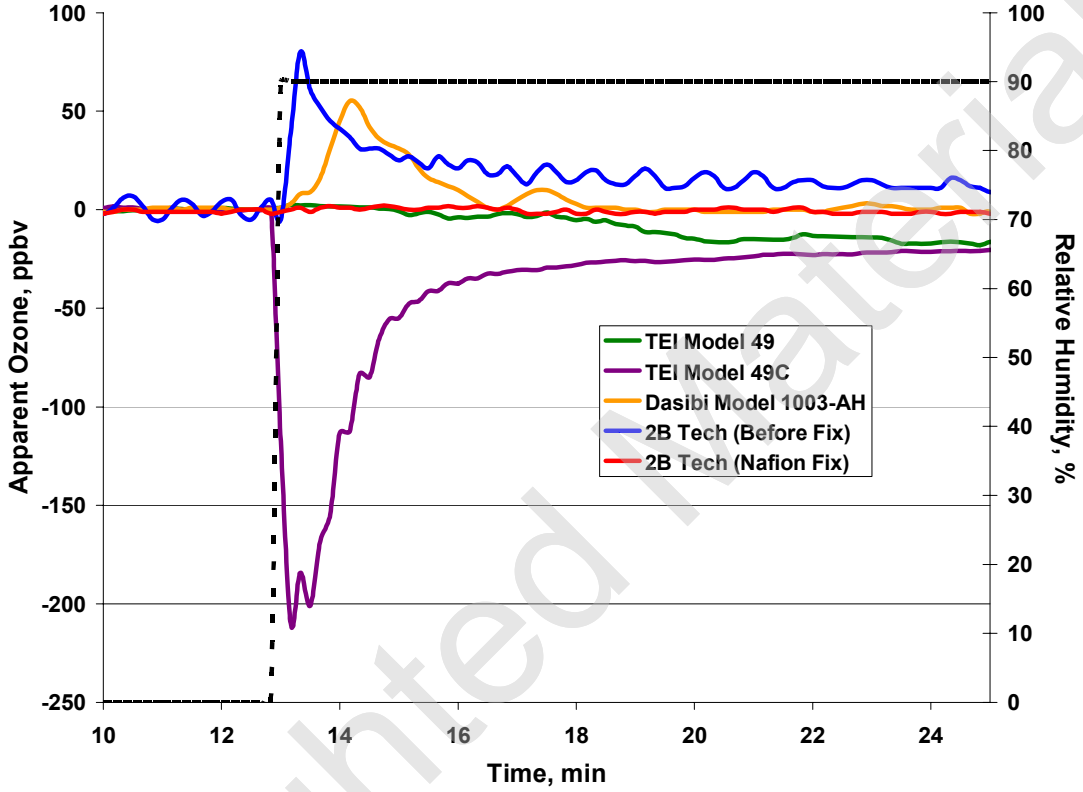

Fig. 5.5 Contrasting water vapor effect on apparent ozone reading for TEI Model 49, TEI Model 49C, Dasibi Model 1003-AH, 2B Tech Ozone Monitor prior to Nafion® humidity modulator, and 2B Tech Ozone Monitor after introduction of Nafion® humidity modulator.

within the cell and therefore transmission of the cell is modulated by the ozone destruction catalyst, which acts as a water vapor reservoir. Consistent with this mechanism, a number of factors were found to reduce or eliminate the water vapor effect. These include heating the absorption cell, changing the composition of the absorption cell, reducing the nature and/or surface area of the ozone destruction catalyst, and, finally, use of a Nafion® tube to equilibrate the humidities of scrubbed and unscrubbed air.

The use of a Nafion® tube for elimination of the water vapor interference, discovered here, was introduced as an option in 2B Technologies Ozone Monitors in early 2004 under the trade name DewLine™. The DewLine™ is either a coil of Nafion® tubing exposed to air in the interior of the instrument case or a coil of Nafion® tubing enclosed in a small plastic box packed with silica gel to serve as a humidity buffer. To date, DewLines™ have been installed in more than fifty 2B Tech Ozone Monitors with no reported adverse effects such as loss of ability to equilibrate water vapor, decreased sensitivity to ozone or large shifts in the instrument zero. The National Oceanic and Atmospheric Administration Climate Monitoring and Diagnostics Laboratory (NOAA/CMDL) incorporate DewLines™, for example, in 2B Technology Ozone Monitors employed on a fleet of light aircraft. Those instruments are used to obtain vertical profiles of ozone on a weekly basis at numerous sites in the U.S. The complete elimination of the water vapor interference presented in this thesis is critical, not only in making valid ozone measurements on aircraft flights such as these where rapid changes in humidity are encountered on time scales of seconds or less, but also in ambient monitoring sites across the globe where

large humidity variations often occur as a result of weather fronts and/or calibration methods which can potentially affect the results of ozone monitoring for compliance with environmental standards such as the U.S. Clean Air Act.

Based on its success in field-deployed instruments, the DewLine™ soon will become a standard component of all 2B Technologies Ozone Monitors, including the recently introduced dual beam instrument. Furthermore, a Nafion® tube has been a component of the 2B Technologies Nitric Oxide Monitor, which is based on an ozone titration of NO, since its introduction early in 2005. In the development of that instrument, it was found that a Nafion® tube quantitatively passes nitric oxide as well as ozone.

Chapter 5 – References

Perma Pure LLC. "Our Technology." Accessed 4 July 2005. <http://www.permapure.com/OurTechnology.htm> (**2004**).

Robinson, J.K. "Luminol-Hydrogen Peroxide Detector for the Analysis of Nitric Oxide in Exhaled Breath." Ph.D. Thesis, University of Colorado, Boulder, Colorado (**1999**).

Bibliography

A.S.L. & Associates. "Nonattainment Areas for the 1-Hour Ozone Standard." Accessed 11 July 2005. < http://www.asl-associates.com/currenta.htm> (**2005a**).

A.S.L. & Associates. "Attainment and Nonattainment Areas in the U.S. 8-Hour Ozone Standard." Accessed 11 July 2005. <http://www.asl-associates.com/current8-hra.htm> (**2005b**).

Aimedieu, P and J. Barat. "Instrument to Measure Stratospheric Ozone with High Resolution." *Rev. Sci. Instrum.* 52 (**1981**): 432-437.

Amama, P.B., K. Itoh and M. Murabayashi. "Gas-phase Photocatalytic Degradation of Trichloroethylene on Pretreated TiO_2." *Appl. Catal. B: Env.* 37 (**2002**): 321-330.

Ameen, M.M. and G.B. Raupp, "Reversible Catalyst Deactivation in the Photocatalytic Oxidation of Dilute *o*-xylene in Air." *J. Catal.* 184 (**1999**): 112-122.

Anpo, M., S. Kishiguchi, Y. Ichihashi, M. Takeuchi, H. Yamashita, K. Ikeue, B. Morin, A. Davidson, M. Che. "The Design and Development of Second-Generation Titanium Oxide Photocatalysts Able to Operate Under Visible Light Irradiation by Applying a Metal Ion-implantation Method." *Res. Chem. Intermed.* 27 (**2001**): 459-467.

Balsley, B.B., J.W. Birks, M.L. Jensen, K.G. Knapp, J.B. Williams, and G.W. Tyrell. "Vertical Profiling of the Atmosphere Using High-Tech Kites." *Environ. Sci. Tech.* 28 (**1994a**): 422A-427A.

Balsley, B.B., J.W. Birks, M.L. Jensen, K.G. Knapp, J.B. Williams, and G.W. Tyrell. "Ozone Profiling Using Kites." *Nature* 369 (**1994b**): 23.

Barnes, R.A., A.R. Bandy and A.L. Torres. "Electrochemical Concentration Cell Ozonesonde Accuracy and Precision." *J. Geophys. Res.* 90 (**1985**). 7881-7887.

Birks, J.W. "Oxidant Formation in the Troposphere." *Perspectives in Environmental Chemistry*, Ed. D.L. Macalady. Oxford University Press: New York, **1998**. 233-256.

Blake, D. M. *Bibliography of Work on the Heterogeneous Photocatalytic Removal of Hazardous Compounds from Water and Air: Update Number 4 to October 2001 - NREL/TP-510-31319*. Springfield, VA: Dept. Commerce, **2001.**

Bliss, A.B. "Arthur Beckett Lamb." *JAC*, 77 (**1955**): 5773-5780.

Bognar, J.A. and J. W. Birks. "Miniaturized Ultraviolet Ozonesonde for Atmospheric Measurements." *Anal. Chem.* 68 (**1996**): 3059-3062.

Bowman, L.D. and R.F. Horak. "A Continuous Ultraviolet Absorption Ozone Photometer." *Air Quality Instrumentation, Vol. 2*, Ed. J.W. Scales. Instrument Society of America: Research Triangle Park, N.C., **1972**.

Brewer, A.W. "Measuring Ozone in the Stratosphere." *New Scientist* 2 (**1957**): 32.

Browell, E.V. "Differential Absorption LIDAR Sensing of Ozone." *Proc. IEEE* 77 (**1989**): 419-432.

Cao, L., Z. Gao, S.L. Suib, T.N. Obee, S.O. Hay and J.D. Freihault. "Photocatalytic Oxidation of Toluene on Nanoscale TiO_2 Catalysts: Studies of Deactivation and Regeneration." *J. Catal.* 196 (**2000**): 253-261.

Carp, O., C. L. Huisman and A. Reller. "Photoinduced Reactivity of Titanium Dioxide." *Prog. Solid State Chem.* 32 (**2004**): 33-177.

Chapman, S. "A Theory of Upper-Atmospheric Ozone." *Memoirs of the Royal Meteorological Society* 3 (**1930**): 103-125.

Coronado, J.M., M.A. Anderson, I. Tejedor-Tejedor, and M.E. Zorn. "Photocatalytic Oxidation of Ketones in the Gas Phase over TiO_2 Thin Films: A Kinetic Study on the Influence of Water Vapor." *Appl. Catal. B: Env.* 43 (**2003**): 329-344.

Deshler, T. and D.J. Hofmann. "Ozone Profiles at McMurdo Station, Antarctica, the Austral Spring of 1990." *Geophys. Res. Lett*. 18 (**1991**): 657-660.

d'Hennzel, O., P. Pichat, and D.F. Ollis. "Benzene and Toluene Gas-phase Photocatalytic Degradation Over H_2O and HCl Pretreated TiO_2: By-products and Mechanisms." *J. Photochem. Photobiol. A: Chem.* 118 (**1990**): 197-204.

Dhandapani. B., and S.T. Oyama. "Gas Phase Ozone Decomposition Catalysts." *Appl. Catal. B: Env.* 11 (**1997**): 129-166.

Einaga, H., S. Futamura, and T. Ibusuki. "Heterogeneous Photocatalytic Oxidation of Benzene, Toluene, Cyclohexene and Cyclohexane in Humidified Air: Comparison of Decomposition Behavior on Photoirradiated TiO_2 Catalyst." *Appl. Catal. B: Env.* 38 (**2002**): 215-225.

Finlayson-Pitts, B.J. and J.N. Pitts Jr. *Atmospheric Chemistry*. Wiley & Sons: New York, **1986**.

Finlayson-Pitts, B.J. and J.N. Pitts Jr. "Analytical Methods and Typical Atmospheric Concentrations for Gases and Particles." *Chemistry of Upper and Lower Atmosphere*. Academic Press: San Diego, C.A., **2000a**. 583.

Finlayson-Pitts, B.J. and J.N. Pitts Jr. "Scientific Basis for Control of Halogenated Organics." *Chemistry of Upper and Lower Atmosphere*. Academic Press: San Diego, C.A., **2000b**. 737.

Fontijn, A, A.J. Sabadell, R.J. Ronco. "Homogeneous Chemiluminescent Measurements of Nitric Oxide with Ozone: Implications for Continuous Selective Monitoring of Gaseous Air Pollutants." *Anal. Chem.* 42 (**1970**): 575-579.

Fu, X., M. Anderson, and W.A. Zeltner. "The Gas-phase Photocatalytic Mineralization of Benzene on Porous Titania-based Catalysts." *Appl. Catal. B: Env.* 6 (**1995**): 209-224.

Fujishima, A. and Honda, K. "Electrochemical Photolysis of Water at a Semiconductor Electrode." *Nature* 238 (**1972**): 37.

General Electric Inc. "Chemical Composition." Accessed 10th April 2005. <http://www.gequartz.com/en/chemical.htm> (**2002**).

Gonzàlez-Elipe, A.R., J. Soria and G. Munuera. "Photodecomposition of Ozone on Titanium Dioxide." *Z. Phys. Chem. N. F.* 126 (**1981**): 251-257.

Gregory, G.L., C.H. Hudgins and R.A. Edhal. "Laboratory Evaluation of an Airborne Ozone Instrument That Compensates for Altitude/Sensitivity Effects." *Environ. Sci. Tech.* 17 (**1983**): 100-103.

Güsten, H., G. Heinrich, R. Schmidt and U. Schurath. "A Novel Ozone Sensor for Direct Eddy Flux Measurements." *J. Atm. Chem.* 14 (**1992**): 73-84.

Güsten, H. and G. Heinrich. "On-line Measurements of Ozone Surface Fluxes: Part I. Methodology and Instrumentation." *Atmos. Environ*. 30 (**1996**): 897-909.

Heath, D.F., A.J. Krueger, H.A. Roeder and B.D. Henderson. "The Solar Backscattered Ultraviolet and Total Ozone Mapping Spectrometer (SBUV/TOMS) for NIMBUS G." *Opt. Eng.* 14 (**1984**): 323-331.

Helmig, D., J. Boulter, D. David, J.W. Birks, N.J. Cullen, K. Steffen, B.J. Johnson and S.J. Oltmans. "Ozone and Meteorological Boundary-Layer Conditions at Summit, Greenland during 3-21 June 2000." *Atm. Environ.* 36 (**2002**): 2595-2608.

Henderson, M.A. "Structural Sensitivity in the Dissociation of Water on TiO_2 Single-Crystal Surfaces." *Langmuir* 12 (**1996**): 5093-5098.

Hilsenrath, E. and P.T. Kirschner. "Recent Assessment of the Performance and Accuracy of a Chemiluminescent Rocket Sonde for Upper Atmospheric Ozone Measurements." *Rev. Sci. Instrum.* 51 (**1981**): 1381-1389.

Hudgens, E.E., T.E. Kleindienst, F.F. McElroy, and W.M. Ollison. "A Study of Interferences in Ozone UV and Chemiluminescent Monitors." *Proceedings of Air and Waste Management Association International Symposium on Measurements of Toxics and Related Air Pollutants, Research Triangle Park, N.C.* Pittsburgh: Air & Waste Management Assoc., **1994**. 405-415.

Iliev, V. "Phthalocyanine-Modified Titania-Catalyst for Photooxidation of Phenols by Irradiation with Visible Light." *J Photochem Photobiol A: Chem* 151 (**2002**): 195-199.

Imamura, S., M. Ikebata, T. Ito, and T. Ogita. "Decomposition of Ozone on a Silver Catalyst." *Ind. Eng. Chem. Res.* 30 (**1991**): 217-221.

Jacoby, W.A., D.M. Blake, R.D. Noble and C.A. Koval. "Kinetics of Oxidation of Trichloroethylene in Air via Heterogeneous Photocatalysis." *J Catal.* 157 (**1995**): 87-96.

Jacoby, W.A., D.M. Blake, J.A. Fennell, J.E. Boutler, L.M. Vargo, M.C. George, and S.K. Dolberg. "Heterogeneous Photocatalysis for Control of Volatile Organic Compounds in Indoor Air." *Air Waste Manage. Assoc.* 46, (**1996**): 891-898.

Karbiwnyk, C.M., C. S. Mills, D. Helmig and J. W. Birks. "Minimization of Water Vapor Interference in the Analysis of Non-Methane Volatile Organic Compounds by Solid Adsorbent Sampling." *J. Chrom. A* 958 (**2002**): 219-229.

Keesee, B. "History of the Ozone Layer." Accessed 10th July 2005. <http://www.albany.edu/faculty/rgk/atm101/o3histor.htm> (19th Aug, **2004a**).

Keesee, B. "Measured Ozone Depletion." Accessed 11th July 2005. <http://www.albany.edu/faculty/rgk/atm101/ozmeas.htm> (19th Aug, **2004b**).

Kim, S.B. and S.C. Hong. "Kinetic Study for Photocatalytic Degradation of Volatile Organic Compounds in Air Using Thin Film TiO_2 Photocatalyst." *Appl Catal B: Environ* 35 (**2002**): 305-315.

Kleindienst, T.E., E.E. Hudgens, D.F. Smith, F.F. McElroy and J.J. Bufalini. "Comparison of Chemiluminescence and Ultraviolet Ozone Monitor Responses in the Presence of Humidity and Photochemical Pollutants." *J. Air Waste Mange. Assoc*. 43 (**1993**): 213-222.

Knapp, K.G., B.B. Balsley, M.L. Jensen, H.H. Hanson and J.W. Birks. "Observation of the Transport of Polluted Air Masses from the Northeastern United States to Cape Sable Island, Nova Scotia, Canada During the 1993 North Atlantic Regional Experiment Summer Intensive." *J. Geophys. Res.* 103 (**1998a**): 13399-13411.

Knapp, K.G., M.L. Jensen, B.B. Balsley, J.A. Bognar, S.J. Oltmans, T.W. Smith and J.W. Birks. "Vertical Profiling Using Complementary Kite and Tethered Balloon Platforms at Ferryland Downs, Newfoundland, Canada: Observation of a Dry, Ozone-Rich Plume in the Free Troposphere." *J. Geophys. Res.* 103 (**1998b**): 13389-13397.

Komhyr, W.D. "Electrochemical Concentration Cells for Gas Analysis." *Ann. Geophys*., 25 (**1969**): 203-210.

Komhyr, W.D and T. B. Harris. "Development of an ECC-Ozonesonde." *NOAA Tech. Rep. ERL 200-APCL 18ARL-149*. Washington: GPO, **1971**.

Larson, S.A. and J.L. Falconer. "Initial Reaction Steps in Photocatalytic Oxidation of Aromatics." *Catal. Lett.* 44 (**1997**): 57-65.

Leston, A. and W. Ollison. "Estimated Accuracy of Ozone Design Values: Are They Compromised by Method Interference?" *Proceedings of Air and Waste Management Association Conference on Tropospheric Ozone: Nonattainment and Design Value Issues, Boston, MA.* October 27-30, 2003. Pittsburgh: Air & Waste Management Assoc., **1992**. 451-456.

Leston, A. and W. Ollison. "Estimated Accuracy of Ozone Design Values: Are They Compromised by Method Interference?" *Proceedings of Air and Waste Management Association International Symposium on Measurements of Toxics and Related Air Pollutants, Research Triangle Park, N.C.* Pittsburgh: Air & Waste Management Assoc., **1994**. 2-18.

Lewandowski, M.M. and D.F. Ollis. "Halide Acid Pretreatments of Photocatalysts for Oxidation of Aromatic Air Contaminants: Rate Enhancement, Rate Inhibition, and a Thermodynamic Rationale." *J. Catal.* 217 (**2003**): 38-46.

Lichtin, N.N. and M. Avudaithai. "TiO_2-Photocatalyzed Oxidative Degradation of CH_3CN, CH_3OH, C_2HCl_3, and CH_2Cl_2 Supplied as Vapors and in Aqueous Solution under Similar Conditions." *Env. Sci. Tech.* 30 (**1996**): 2014-2020.

Maddy, J.A. "A Test That Identifies Ozone Monitors Prone to Anomalous Behavior While Sampling Hot and Humid Air." Paper 98-MPB.O2P in *Proceedings of the Air and Waste Management Association Meeting, San Diego, C.A.* June 14th-18th, 1998. Pittsburgh: Air & Waste Management Assoc., **1998**.

Maddy, J.A. "Evaluating a Heated Metal Scrubbers Effectiveness in Preventing Ozone Monitor's Anomalous Behavior During Hot and Humid Ambient Sampling." Paper 99-451 in *Proceedings of the Annual Air and Waste Management Association Meeting, St. Louis, M.O.* Pittsburgh: Air & Waste Management Assoc., **1999**.

Maira, A.J., K.L. Yeung, C.Y. Lee, P.L. Yue and C.K. Chan. "Size Effects in Gas-phase Photo-oxidation of Trichloroethylene Using Nanometer-Sized TiO_2 Catalysts." *J. Catal.* 192 (**2000**): 185-196.

Maira, A.J., K.L. Yeung, J. Soria, J.M. Coronado, C. Belver, C.Y Lee and V. Augugliaro. "Gas-phase Photo-oxidation of Toluene Using Nanometer-size TiO_2 Catalysts." *Appl. Catal. B: Env.* 29 (**2001**): 327-336.

Martin, S.T., C.L. Morrison, and M.R. Hoffmann. "Photochemical Mechanism of Size-Quantized Vanadium-Doped TiO_2 Particles." *J Phys Chem* 98 (**1994**): 13,695–13,704.

Mast, G.M. and H.E. Saunders. "Research and Development of the Instrumentation of Ozone Sensing." *Inst. Soc. Am. Trans.* 1 (**1962**): 325-328.

McCormick, M.P., T.J. Swissler, E. Hilsenrath, A.J. Krueger and M.T. Osborn. "Satellite and Correlative Measurements of Stratospheric Ozone: Comparison of Measurements Made by SAGE, ECC Balloons, Chemiluminescent, and Optical Rocketsondes." *J. Geophys, Res.* 89 (**1984**): 5315-5320.

McElroy, F.F. *Transfer Standards for Calibration of Air Monitoring Analyzers for Ozone - EPA-600/4-79-056*. Research Triangle Park, N.C.: U.S. EPA Environmental Monitoring and Support, **1979**.

McPeters, R.D., D.J. Hofmann, M. Clark, L. Flynn, L. Froidevaux, M. Gross, B. Johnson, G. Koenig, X. Liu, S. McDermid, T. McGee, F. Murcray, M.J. Newchurch, S. Oltmans, A. Parrish, R. Schnell, U. Singh, J.J. Tsou, T. Walsh, and J.M. Zawodny. "Results from the 1995 Stratospheric Ozone Profile Intercomparison at Mauna Loa." *J. Geophys. Res. – Atmos.* 104 (**1999**): 30,505-30,514.

Mehrabzadeh, A.A., R.J. O'Brien, T.M. Hard. "Optimization of Response of Chemiluminescence Analyzers." *Anal. Chem.* 55 (**1983**): 1660-1665.

Meyer, C.P., C.M. Elsworth and I.E. Galbally. "Water Vapor Interference in the Measurement of Ozone in Ambient Air by Ultraviolet Absorption." *Rev. Sci. Instrum.* 62 (**1991**): 223-228.

Middlebrook, A.M. and M.A. Tolbert. Draft of *Understanding Global Changes: Earth Science and Human Impacts – Stratospheric Ozone Depletion*. UCAR: Boulder, CO, **1996**.

Mills, A., S. K. Lee and A. Lepre. "Photodecomposition of Ozone Sensitized by a Film of Titanium Dioxide on Glass." *J. Photochem. Photobiol. A: Chem.* 155 (**2003a**): 199-205.

Mills, A., G. Hill, S. Bhopal, I.V. Parkin, and S.A. O'Neill. "Thick Titanium Dioxide Films for Semiconductor Photocatalysis." *J. Photochem. Photobiol. A: Chem.* 160 (**2003b**): 185-194.

Nardi, B., W Bellon, LD Oolman, and T Deshler. "Spring 1996 and 1997 Ozonesonde Measurements Over McMurdo Station, Antarctica." *Geophys. Res. Lett*. 26 (**1999**): 723-726.

National Park Service – U.S. Department of Interior. "2001-2003 Average of the Annual 4th Highest Daily Maximum 8-hr Ozone Concentration." Accessed 10 July 2005. <http://www2.nature.nps.gov/air/Monitoring/exceed2.htm> (1st Nov. **2004**).

Neufeld, H.S., J.R. Renfro, W.D. Hacker, and D. Silsbee. "Ozone in Great Smoky Mountains National Park: Dynamics and Effects on Plants." *Proceedings of Air and Waste Management Association Symposium on Tropospheric Ozone and the Environment II - Effects, Modeling and Control, Atlanta, G.A.* Pittsburgh, PA: Air & Waste Management Association; **1992**. 594-617.

New York Public Library. "The Disappearing Ozone?" *Science Desk Reference*, Ed. P. Barnes-Svarney. Stonesong Press Inc.: New York, **1995**. 482-483.

Obee, T.N. and R.T. Brown. "TiO_2 Photocatalysis for Indoor Air Applications. Effects of Humidity and Trace Contaminant Levels on the Oxidation Rates of Formaldehyde, Toluene, and 1,3-Butadiene." *Env. Sci. Tech.* 29 (**1995**): 1223-1231.

Ohmi, T., T. Isagawa, T. Imaoka, and I. Suciyama. "Ozone Decomposition in Ultrapure Water and Continuous Ozone Sterilization for a Semiconductor Ultrapure Water System." *J. Electrochem. Soc.* 139 (**1992**): 3336-3345.

Ohtani, B., S.-W. Zhang, S. Nishimoto and T. Kagiya. "Catalytic and Photocatalytic Decomposition of Ozone at Room Temperature Over Titanium(IV) Oxide." *J. Chem. Soc. Faraday Trans.* 88.7 (**1992**): 1049-1053.

Ollison, W.M., T.E. Kleindienst and C.D. McIver. "A Study of Interferences in Ambient Ozone Monitors." *Proceedings of Air and Waste Management Association International Symposium on Measurements of Toxics and Related Air Pollutants, Research Triangle Park, N.C.* Pittsburgh: Air & Waste Management Assoc., **1997.** 215-217.

Parish, D.D. and F.C. Fehsenfeld. "Methods for Gas-phase Measurements of Ozone, Ozone Precursors and Aerosol Precursors." *Atmos. Enviro.* 34, (**2000**): 1921-1957.

Park, D.R., M. Anpo, J. Zhang, K. Ikeue and H. Yamashita. "Photocatalytic Oxidation of ethylene to CO_2 and H_2O on Ultrafine Powdered TiO_2 Photocatalysts in the Presence of O_2 and H_2O." *J. Catal.* 185 (**1999**): 114-119.

Peral, J. and D. Ollis. "Heterogeneous Photocatalytic Oxidation of Gas-phase Organics for Air Purification: Acetone, 1-Butanol, Butyraldehyde, Formaldehyde, and *m*-Xylene Oxidation." *J. Catal.* 136 (**1992**): 554-565.

Peral, J. and D.F. Ollis. "TiO_2 Photocatalyst Deactivation by Gas-phase Oxidation of Heteroatom Organics." *J. Mol. Catal. A: Chem* 115 (**1997**): 347-354.

Perma Pure LLC. "Our Technology." Accessed 4 July 2005. <http://www.permapure.com/OurTechnology.htm> (**2004**).

Phillips, L.A. and G.B. Raupp. "Infrared Spectroscopic Investigation of Gas-solid Heterogeneous Photocatalytic Oxidation of Trichloroethylene." *J. Mol. Catal.* 77 (**1992**): 297-311.

Piera, E., J. Peral, J.A. Ayllón and X. Doménech. "TiO_2 Deactivation During Gas-phase Photocatalytic Oxidation of Ethanol." *Catal. Today* 76 (**2002**): 259-270.

Robinson, J.K. "Luminol-Hydrogen Peroxide Detector for the Analysis of Nitric Oxide in Exhaled Breath." Ph.D. Thesis, University of Colorado, Boulder, Colorado (**1999**).

Roncero, M.B., M.A. Queral, J.F. Colom, T. Vidal. "Why Acid pH Increases the Selectivity of the Ozone Bleaching Processes." *Ozone–Sci. & Engin.* 25 (**2003**): 523-534.

Sandvik Materials Technology AB. "Product Information: Titanium Grades." Accessed 5 July 2005. <http://www2.sandvik.com/sandvik/0140/internet/se01974.nsf/GenerateFrameset1?readForm&url=http://www2.sandvik.com/sandvik/0140/internet/se01974.nsf/1ab734b4713311544125653d002eb28b/a09783b3907e8b02c1256b0a003bfd18?OpenDocument> (**2000**).

Sauer, M.L. and D.F. Ollis. "Acetone Oxidation in a Photocatalytic Monolith Reactor." *J. Catal.* 149 (**1994**): 81-91.

Sauer, M.L. and D.F. Ollis. "Catalyst Deactivation in Gas–Solid Photocatalysis." *J. Catal.* 163 (**1996**): 215-217.

Schalekamp, M. "A Comparison of Two Ozone Water-Treatment Plants –One with Low and the Other with Medium High Frequency." *Ozone–Sci. & Engin.* 1 (**1979**): 107-117.

Schulz, A., M. Rex, N.R.P. Harris, G.O. Braathern, E. Reimer, R. Alfier, I. Kilbane-Dawe, S. Eckermann, M. Allaart, M. Alpers, B. Bojkov, J. Cisneros, H. Claude, E. Cuevas, J. Davies, H. DeBacker, H. Dier, V. Dorokhov, H.. Fast, S. Godin, B. Johnson, B. Kois, Y. Kondo, E. Kosmidis, E. Kyro, Z. Litynska, I.S. Mikkelsen, M.J. Molyneux, G. Murphy, T. Nagai, H. Nakane, F. O'Connor, C. Parrondo, F.J. Schmidlin, P. Skrivankova, C. Varotsos, C. Vialle, P. Viatte, V. Yushkov, C. Zerefos, P. von der Gathen. "Arctic Ozone Loss in Threshold Conditions: Match Observations in 1997/1998 and 1998/1999." *J. Geophys. Res. – Atmos.* 107 (**2001**): 7495-7503.

Schulz, K.J. "Measurements of Landscape-Scale Fluxes of Carbon Dioxide at Two AmeriFlux Sites Using a New Vertical Profiling Technique." Ph.D. Thesis, University of Colorado, Boulder, Colorado (**2003**).

Schulz, K.J., M.L. Jensen, B.B. Balsley, K. Davis, and J.W. Birks. "Tedlar Bag Sampling Technique for Vertical Profiling of Carbon Dioxide Through the Atmospheric Boundary Layer with High Precision and Accuracy." *Environ. Sci. & Tech.* 38, (**2004**): 3683-3688.

Sedin, D.L. and K.L. Rowlen. "Adhesion Forces Measured by Atomic Force Microscopy in Humid Air." *Anal. Chem.* 72 (**2000**): 2183-2189.

Seinfeld, J. H., and S. N. Pandis. *Atmospheric Chemistry and Physics From Air Pollution to Climate Change*. John Wiley: New York, **1998**. 28.

Serpone, N., D. Lawless, J. Disdier, and J.M. Hermann. "Spectroscopic, Photoconductivity, and Photocatalytic Studies of TiO_2 Colloids: Naked and with the Lattice Doped with Cr^{3+}, Fe^{3+}, and V^{5+} Cations." *Langmuir* 10 (**1994**): 643-652.

Singer, S.F. and R.C. Wentworth. "A Method for the Determination of the Vertical Ozone Distribution from a Satellite." *J. Geophys. Res.* 62 (**1957**): 299-308.

Skubal, L.R. and N.K. Meshkov. "Reduction and Removal of Mercury from Water Using Arginine-Modified TiO_2." *J. Photochem. Photobiol. A: Chem.* 148 (**2002**): 211-214.

Soria, J., J.C. Conesa, V. Augugliaro, L. Palmisano, M. Sciavello and A. Scalfani. "Dinitrogen Photoreduction to Ammonia Over Titanium Dioxide Powders Doped with Ferric Ions." *J. Phys. Chem.* 95 (**1991**): 274-282.

Stephens, G.L. *Remote Sensing of the Lower Atmosphere*. Oxford University Press: New York, **1994**.

Takeuchi, M., H. Yamashita, M. Matsuoka, M. Anpo, T. Hirao, N. Itoh and N. Iwamoto. "Photocatalytic Decomposition of NO Under Visible Light Irradiation on the Cr-ion-implanted TiO_2 Thin Film Photocatalyst." *Catal. Lett.* 67 (**2000**): 135-137.

Turco, R.P. "The Stratospheric Ozone Layer." *Earth Under Siege*. Oxford University Press: New York, **1997a**. 411.

Turco, R.P. "Smog: The Urban Syndrome." *Earth Under Siege*. Oxford University Press: New York, **1997b**. 157.

Turco, R.P. "Smog: The Urban Syndrome." *Earth Under Siege*. Oxford University Press: New York, **1997c**. 23.

U.S. EPA Office of Air and Radiation. *Ozone and Your Health – EPA-452/F-99-003*. Washington, DC: US Environmental Protection Agency, **1999a**.

U.S. EPA Office of Air and Radiation. *Smog – Who Does It Hurt? – EPA-452/F-99-001*. Washington, DC: US Environmental Protection Agency, **1999b**.

U.S. EPA Office of Air and Radiation. *Ozone: Good Up High, Bad Nearby – EPA-451/K-03-001*. Washington, DC: US Environmental Protection Agency, **2003**.

U.S. EPA Office of Air and Radiation. "Clean Air Ozone Rules of 2004: Final Rule Designating and Classifying Areas Not Meeting the National Air Quality Standard for 8-Hour Ozone." Accessed 10 July 2005. <http://www.epa.gov/ozonedesignations/finrulefs.htm > (20th May **2005**).

U.S. EPA Office of Air Quality Planning and Standards. *Quality Assurance Handbook for Air pollution Measurement Systems - EPA-454/R-98-004*. Research Triangle Park, N.C.: U.S. Environmental Protection Agency, **1998**.

U.S. EPA Office of Air Quality Planning and Standards. *The Ozone Report: Measuring Progress Through 2003 – EPA-454/K-04-001*. Research Triangle Park, N.C.: U.S. Environmental Protection Agency, **2004**.

Vichi, F.M., M.A. Anderson, and M.I. Tejedor-Tejedor. "Effect of Pore-wall Chemistry on Proton Conductivity in Mesoporous Titanium Dioxide." *Chem. Mater.* 12 (**2000**): 1762-1770.

Wang, R., K. Hashimoto, A. Fujishima, M. Chikuni, E. Kojima, A. Kitamura, M. Shimohigoshi, and T, Watanabe. "Photogeneration of Highly Amphiphilic TiO_2 Surfaces." *Adv. Materials* 10 (**1998**): 135-138.

Wilke, K. and H.D. Breuer. "The Influence of Transition Metal Doping on the Physical and Photocatalytic Properties of Titania." *J. Photochem. Photobiol. A: Chem.* 121 (**1999**): 49-53.

Wu, J. and C. Yu. "Aligned TiO_2 Nanorods and Nanowalls." *J. Phys. Chem. B* 108 (**2004**): 3377-3379.

Worsley, D., A. Mills, K. Smith, and M.G. Hutchings. "Acid Enhancement Effect in the Clean Oxidation of Toluenes Photocatalyzed by TiO_2." *J Chem Soc, Chem Comm.* (**1995**): 1119-1120.

Yu, J.C., Y. Xiea, H.Y. Tanga, L. Zhanga, H.C. Chanb and J. Zhao. "Visible Light-Assisted Bactericidal Effect of Metalphthalocyanine-Sensitized Titanium Dioxide Films." *J. Photochem. Photobiol. A: Chem.* 156 (**2003**): 235-241.

Zhao, G., T. Yoko, H. Kozuka, H. Lin and M. Takahashi. "Preparation and Photoelectrochemical Properties of $Ti_{1-x}V_xO_2$ Solid Solution Thin Film Photoelectrodes with Gradient Bandgap." *Thin Solid Films* 340 (**1999**): 125-131.

Zorn, M.E., D.T. Tompkins, W.A. Zeltner and M.A. Anderson,. "Catalytic and Photocatalytic Oxidation of Ethylene on Titania-Based Thin-Films." *Env. Sci. Tech.* 34 (**2000**): 5206-5210.

Zorn, M.E. "Photocatalytic Oxidation of Gas Phase Compounds in Confined Areas: Investigation of Multiple Component Systems." *Proceedings of the 13th Annual Wisconsin Space Conference*. August 14-15, 2003. Green Bay: Wisconsin Space Grant Consortium, **2003**.